



Using Sensor Data from Building Automation Systems in Digital Twins
Nutzung von Sensordaten der Gebäudeautomation in Digitalen Zwillingen

by

Rehan Ahmad Khan

from

Noida, India

Master Thesis submitted to the Faculty of Civil Engineering, Institute of Construction Informatics,
University of Technology Dresden in partial fulfilment of the requirements for the degree of

Master of Science

Responsible Professor: Prof. Dr.-Ing. habil. Karsten Menzel

Second Examiner: Prof. Dr.-Ing. John Grunewald

Scientific Supervisor: Dipl.-Ing. Adrian Schubert

Dresden, 16th November 2020

Declaration

I confirm that this assignment is my own work and that I have not sought or used the inadmissible help of third parties to produce this work. I have fully referenced and used inverted commas for all text directly quoted from a source. Any indirect quotations have been duly marked as such.

This work has not yet been submitted to another examination institution – neither in Germany nor outside Germany – neither in the same nor in a similar way and has not yet been published.

Dresden,

Place, Date

Signature

Acknowledgment

First and foremost, I feel a sense of obligation in conveying my sincere gratitude to Prof. Dr.-Ing habil. Karsten Menzel, Chair of the “Institute of Construction Informatics” and Prof. Dr.-Ing John Grunewald, Chair of the “Institute of Building Physics” for providing me the opportunity to work on my master thesis and having faith in my work.

Furthermore, I am honestly indebted to Dipl.-Ing. Adrian Schubert for his constant backing and supervision during the course of the work. Alongside this, I would also like to acknowledge the necessary help provided by all the staff at the “Institute of Construction Informatics” for their invaluable assistance.

Finally, I am thankful to my family- my parents and my siblings for their relentless support and continuous encouragement throughout my career. Without your endless support and love, I cannot comprehend reaching this stage.

Abstract

A Digital Twin, as a means to link digital models and simulations with real-world data, establishes new possibilities for improved creativity, competitive leverage, and human-centered design. Digital Twins can help deliver on the imposing challenges facing society, including achieving the United Nations Sustainable Development Goals and addressing rapid urbanization, population growth, and escalating infrastructure costs.

On the technological front, three major advancements have enabled the concept of Digital Twin; namely computing capability, sensors, and visualization. Recent computing advancements have enabled us to process, store, and communicate a massive amount of information used to operate modern buildings. The second technological improvement is through sensors, which have enabled the rise of smart buildings. Buildings can now be made to sense and communicate their precise status to permit us to know and manipulate exactly what is occurring within, simply by examining their Digital Twin. The third technology amelioration has been visualization, thus enabling us to render geometric designs virtually, in breath-taking constancy. With 3D visualization, we can merge the Digital Twin with its corresponding physical building, in order to see how the building is performing and rectify failures beforehand.

In the research study, sensed and metered data recorded from the building automation system installed at the Institute of Construction Informatics (NUR31) at TU Dresden, is used as a reference for the calibration of the Energy Simulation model in IESVE software. Subsequently, the output from the calibrated IES model is used to visualize the energy data in the Unity3D model, in order to establish a “proof of concept” for a Digital Twin of the Institute of Construction Informatics. Thus the creation of a Digital Twin bridges the gap between the physical and digital worlds through sensors that collect real-time data within the physical environment. Thus providing a real-time understanding of how a building is performing – enabling immediate adjustment to optimize efficiency and to provide data to improve the design of future buildings.

Table of Contents

Declaration.....	I
Acknowledgment.....	II
Abstract	III
Table of Contents.....	IV
List of Figures	VII
List of Tables	XIV
List of Abbreviations	XV
1 Introduction	1
1.1 Motivation	1
1.2 Objective of the thesis	2
1.3 Problem statement	3
1.4 Organization of the thesis	3
2 Background and related work.....	4
2.1 Digital Twins	4
2.1.1 Building Information Modelling	6
2.1.2 Comparison of BIM and Digital Twin of building.....	7
2.1.3 Digital Twins in the AEC industry	8
2.1.4 Digital Twins usability in the FM industry.....	11
2.1.5 Digital Twin for a smarter built environment	13
2.2 Building Energy Simulations.....	15
2.2.1 Classification of Energy Simulation Models	17
2.3 Building Automation Systems	20
2.3.1 The framework of Building Automation Systems.....	22
2.3.2 IoT based Building Automation Systems.....	23
2.4 Integration of sensor data	25

2.4.1	Strategies for real-time data integration.....	26
2.4.2	Challenges to data analytics	29
2.5	Case studies	31
2.5.1	ARUP Tokyo	31
2.5.2	NTU Singapore	36
3	Framework for Digital Twin	40
3.1	Data from sensors.....	40
3.1.1	Wireless room sensor SR04.....	44
3.1.2	Brightness and motion sensor MDS	47
3.1.3	Homematic IP Weather Station	49
3.2	IES VE model	53
3.2.1	Solar	54
3.2.2	ApacheSim and VistaPro	55
3.2.3	Daylighting.....	59
3.2.4	MicroFlo (CFD).....	61
3.3	REVIT-BIM model	65
3.4	Unity VR model	70
4	Methodology for Digital Twin environment.....	73
4.1	Analysis of data.....	73
4.2	Calibration 1.0 of the IES model.....	76
4.3	Calibration 2.0 of the IES model.....	79
4.4	Visualization of data	83
4.4.1	Visualization of simulation data	84
4.4.2	Visualization of sensor data.....	90
4.5	Digital Twin environment	97
5	Conclusions and Future work.....	99
5.1	Conclusions.....	99

5.2 Future work.....	102
Bibliography	103
Appendices	106
Appendix A: Sensor data from BAS	106
Appendix B: Existing IES VE model	108
Appendix C: Calibration of simulation and sensor data	124

List of Figures

Figure 1: Essential components to create a digital twin of building and difference with BIM (Khajavi et al., 2019).	1
Figure 2: The Digital Twin paradigm (Boje et al., 2020).	5
Figure 3: Description of BIM Levels (Sacks et al., 2018).	7
Figure 4 Facilities management enhancement by DT's (Martynova, 2020).	11
Figure 5: Representation of an intelligent building (Martynova, 2020).	13
Figure 6: Outlay of a smart city workflow in Rotterdam.	14
Figure 7: Spatiotemporal Flux and Reality-Virtuality integration: Digital Twin City of Atlanta (Mohammadi and Taylor, 2018).	15
Figure 8: General data flow of simulation engines (Maile, Fischer and Bazjanac, 2007).	16
Figure 9: Heat processes through a building (Wasmi and Salih, 2019).	18
Figure 10: Smart Home network prototype (Fabi, Spiglientini and Corgnati, 2017).	22
Figure 11: Hierarchical levels for BAS (Kastner et al., 2005).	22
Figure 12: The prospective architecture for IoT BAS (Bode et al., 2019).	25
Figure 13: Real-time sensor data flow diagram of the designed WSN (Khajavi et al., 2019).	25
Figure 14: Cloud-based cyber-physical system architecture (Alam and El Saddik, 2017).	27
Figure 15: Multi-view real-time synchronisation in equipment-level simulation (Liu et al., 2019).	29
Figure 16: Layout of the Arup office in Tokyo with installed sensors (ARUP, 2019).	31
Figure 17: Sensors concealed as 'penguins' (ARUP, 2019).	32
Figure 18: Free-address area in the ARUP Tokyo office.	33
Figure 19: Monitor showing processed data at the entrance Arup Tokyo office (ARUP, 2019).	33
Figure 20: Digital Twin illustrating real-time performance data, CO2 level, and people count (ARUP, 2019).	34
Figure 21: Correlation between measured variables in the conference room (ARUP, 2019).	34

Figure 22: Target vs. measured CO ₂ concentrations in the conference room (ARUP, 2019).	35
Figure 23: Master-planning for NTU Singapore (Woods and Freas, 2019).	36
Figure 24: Results after phase 1 testbed (Woods and Freas, 2019).	37
Figure 25: Measured temperature and CO ₂ levels (Woods and Freas, 2019).	38
Figure 26: Virtual model of one of the 21 buildings at NTU campus (Woods and Freas, 2019).	38
Figure 27: Results from phase 2 of testbed (Woods and Freas, 2019).	39
Figure 28: NUR 31 building at TU Dresden's campus (Dresden, 2020). (PC: March Mosch)	40
Figure 29: Floor plan for the Institute of Construction Informatics.	41
Figure 30: The sr04 room sensor in room 210 showing temperature (left) and relative humidity (right) recordings.	45
Figure 31: Temperature levels measured on the wireless room sensor from May to July.	46
Figure 32: Relative humidity levels measured on the wireless room sensor from May to July.	46
Figure 33: CO ₂ levels measured on the wireless room sensor from May to July.	47
Figure 34: Top-view of placed mds-sensors in room 210 w.r.t windows.	48
Figure 35: The real position of mds-sensors in room 210 is shown by arrows.	48
Figure 36: Illuminance (brightness) levels measured by mds_5 and mds_6 in room 210.	49
Figure 37: Ground view of the weather station installed outside the Institute of Building Informatics.	50
Figure 38: Close-up view of the weather station in close proximity to room 214.	50
Figure 39: Humidity levels measured on the weather station from May to July.	51
Figure 40: Rainfall levels measured on the weather station from May to July.	51
Figure 41: Temperature levels measured on the weather station from May to July.	52
Figure 42: Wind speed measured on the weather station from May to July.	52
Figure 43: IESVE model for the NUR31 building with sun path on 15 th June at 08:00.	53
Figure 44: Solar Energy Analysis (North Façade)	55

Figure 45: Solar Exposure Analysis (North Façade)	55
Figure 46: Selected rooms library (left) and student help (right) for analysis.....	56
Figure 47: Selected laboratory room for analysis.....	57
Figure 48: Correlation between air temperature and CO ₂ concentration (library).	58
Figure 49: Correlation between air temperature and relative humidity (library). 58	
Figure 50: Correlation between solar gain and conduction gain (external and internal) (library).....	59
Figure 51: Illuminance in room 210 (laboratory).	60
Figure 52: Daylight simulation in the room (laboratory) with respect to the window openings.	61
Figure 53: The initiation of the wind velocity slice for CFD analysis across the room.	62
Figure 54: CFD (velocity filled contour) in the library room (201).....	63
Figure 55: The initiation of the temperature field slice for CFD analysis across the room.....	64
Figure 56: CFD (temperature filled contour) in the library room (201).....	64
Figure 57: Floor plan at level 2 NUR31 building.	65
Figure 58: The rendered image of the student help room (202) using Lumion 3D rendering software.	68
Figure 59: The rendered image of the laboratory room (210) using Lumion 3D rendering software.	69
Figure 60: The rendered image of the library/meeting room (201) using Lumion 3D rendering software.	69
Figure 61: Unity3D model of the BIM Institute.....	70
Figure 62: Room 210 in the BIM institute with the modeled BAS in light green colour.	71
Figure 63: The individual modelled components such as temperature sensor and thermostat in the Unity3D model.	71
Figure 64: CO ₂ concentration levels from the IES simulations and from the sensors in room 201.	74
Figure 65: Temperature levels from the IES simulations and from the sensors in room 201.....	75

Figure 66: Relative humidity levels from the IES simulations and from the sensors in room 201.	75
Figure 67: Calibration of CO ₂ concentration levels in IES using data measured by the sensors as a reference for room 202.	77
Figure 68: Calibration of temperature levels in IES using data measured by the sensors as a reference for room 202.....	77
Figure 69: Calibration of relative humidity levels in IES using data measured by the sensors as a reference for room 202.....	78
Figure 70: Calibration 2.0 of temperature levels on IES for room 201(library).....	80
Figure 71: Calibration 2.0 of relative humidity levels on IES for room 201(library).	81
Figure 72: Calibration 2.0 of CO ₂ concentration levels on IES for room 201(library).	82
Figure 73: Flowchart of the CFD visualization (Berger and Cristie, 2015).....	85
Figure 74: MicroFlo CFD viewer showing CFD grid all three Cartesian directions.	86
Figure 75: Results of CFD simulation visualized on VR in room 201.....	87
Figure 76: Results of CFD simulation moving in Z-axis direction visualized on VR in room 201.....	87
Figure 77: Interactive 3D visualization of daylighting simulation of room 204 on VR.....	88
Figure 78: Interactive 3D visualization of daylighting simulation of room 213 (view 1) on VR.	88
Figure 79: Interactive 3D visualization of daylighting simulation of room 213 (view 2) on VR.	89
Figure 80: Display of device (sr04-2) information in room 202.	91
Figure 81: Display of device (mds-3) information in room 202.	91
Figure 82: Particle effect switched off when above the threshold temperature. .	92
Figure 83: Particle effect switched on when below the threshold temperature. .	93
Figure 84: Color transformation (blue and green) based on temperature from room sensors.....	94
Figure 85: Color transformation (yellow and red) based on temperature from room sensors.....	95
Figure 86: Particle system as visualization on VR for room 202.....	95

Figure 87: The airflow direction for both particle systems in room 210.	96
Figure 88: Illuminance (brightness) levels measured by mds-sensor in room 201.	106
Figure 89: Illuminance (brightness) levels measured by mds-sensor in room 202.	106
Figure 90: Illuminance (brightness) levels measured by mds-sensors in room 210.	107
Figure 91: Illuminance (brightness) levels measured by mds-sensors in room 213.	107
Figure 92: Ground floor construction details (U-value: 0.2200 W/m ² K).	108
Figure 93: Internal 300 mm floor construction details (U-value: 0.7873 W/m ² K).	108
Figure 94: Internal 282.5 mm floor construction details (U-value: 1.0866 W/m ² K).	108
Figure 95: External 1 mm aluminium wall construction details (U-value: 5.8821 W/m ² K).	108
Figure 96: External 208.9 mm wall construction details (U-value: 0.2599 W/m ² K).	108
Figure 97: External 1 mm steel wall construction details (U-value: 5.8817 W/m ² K).	109
Figure 98: External 340 mm wall construction details (U-value: 1.5766 W/m ² K).	109
Figure 99: Internal 155 mm wall construction details (U-value: 1.7157 W/m ² K).	109
Figure 100: External 75 mm wall construction details (U-value: 1.7888 W/m ² K).	109
Figure 101: Door construction details (U-value: 2.1977 W/m ² K).	109
Figure 102: Window construction details (U-value: 1.600 W/m ² K).	109
Figure 103: Window construction details (U-value: 1.600 W/m ² K).	110
Figure 104: Window construction details (U-value: 3.8462 W/m ² K).	110
Figure 105: Window construction details (U-value: 2.300 W/m ² K).	110
Figure 106: Roof 300 mm construction details (U-value: 3.6977 W/m ² K).	110
Figure 107: Roof 317 mm construction details (U-value: 1.1800 W/m ² K).	110
Figure 108: Location selection and corresponding weather parameters.	111
Figure 109: Nearest to site weather file.	111

Figure 110: Thermal template for various space systems.	112
Figure 111: Thermal template for space conditions.....	112
Figure 112: Thermal template for space internal gains.	113
Figure 113: Correlation between air temperature and CO2 concentration (student help).....	114
Figure 114: Correlation between air temperature and relative humidity (student help).....	114
Figure 115: Correlation between solar gain and conduction gain (external and internal) (student help).....	115
Figure 116: Correlation between air temperature and CO2 concentration (laboratory).	115
Figure 117: Correlation between air temperature and relative humidity (laboratory).	116
Figure 118: Correlation between solar gain and conduction gain (external and internal) (laboratory).....	116
Figure 119: Selected Annual Sunlight Exposure (ASE) for the daylighting simulation.	117
Figure 120: Generated dynamic results for ASE simulation.	117
Figure 121: The target of 750 Lux for 50 hours in the ASE simulation.	117
Figure 122: Template for the Radiance IES simulation.....	118
Figure 123: Template parameters selected for Radiance IES simulation.....	118
Figure 124: Illuminance in room 201 (library).	119
Figure 125: The ASE simulation with a target of 750 Lux for at least 50 hours in room 201 (library)	119
Figure 126: Illuminance in room 213 (VR cave).	120
Figure 127: The ASE simulation with a target of 750 Lux for at least 50 hours in room 213 (VR cave).	120
Figure 128: Template for running a CFD analysis.	121
Figure 129: Template for importing boundary conditions to run a MicroFlo (CFD) analysis at a particular instance of time.	121
Figure 130: Defining the iteration level (500 iterations) for CFD analysis.	122
Figure 131: CFD (velocity filled contour) in the 210 room.....	122
Figure 132: CFD (temperature filled contour) in the 210 room.....	123

Figure 133: CO ₂ concentration levels from the IES simulations and from the sensors in room 202.	124
Figure 134: Temperature levels from the IES simulations and the sensors in room 202.	124
Figure 135: Relative humidity levels from the IES simulations and the sensors in room 202.....	125
Figure 136: CO ₂ concentration levels from the IES simulations and the sensors in room 210.....	125
Figure 137: Temperature levels from the IES simulations and the sensors in room 210.	126
Figure 138: Relative humidity levels from the IES simulations and the sensors in room 210.....	126
Figure 139: Calibrating dry-bulb temperature according to data from sensors.	127
Figure 140: Setting the minimum and maximum saturation levels according to data from sensors.....	127
Figure 141: Enhancement of occupancy profile.....	128
Figure 142: Addition of missing insulation layer in the external wall.	128
Figure 143: Calibration of CO ₂ concentration levels in IES using data measured by the sensors as a reference for room 201.	129
Figure 144: Calibration of temperature levels in IES using data measured by the sensors as a reference for room 201.....	129
Figure 145: Calibration of relative humidity levels in IES using data measured by the sensors as a reference for room 201.	130
Figure 146: Edited weather file for Dresden using Elements software.	130

List of Tables

Table 1: A detailed comparison of BIM and digital twin of a building (Khajavi et al., 2019).....	8
Table 2: Stratification of Energy simulation models (Menzel, 2018).....	17
Table 3: Control system characteristics over four generations (Li and Zhang, 2013).	20
Table 4: Functionality of rooms and influences.	41
Table 5: Component list for sensors.	42
Table 6: Component list for actuators.	43
Table 7: Installed BAS at the NUR31 building.....	43
Table 8: Room details in the IESVE model.	53
Table 9: Room details in the REVIT-BIM model.	66
Table 10: Construction details and Thermal Properties of Building Elements in the Revit-BIM model.	66
Table 11: All the components of the BAS modelled in Unity3D.	71
Table 12: Daily occupancy profile according to sensor data.	81
Table 13: Color spectrum assigned for temperature based metamorphism.	94

List of Abbreviations

AEC	Architecture, Engineering, and Construction
AI	Artificial Intelligence
ASHRAE	American Society of Heating, Refrigerating and Air-Conditioning Engineers
BAS	Building Automation Systems
BES	Building Energy Simulation
BIM	Building Information Model
C2PS	Cloud-Bases Cyber-Physical System
CIBSE	Chartered Institution of Building Services Engineers
CFD	Computational Fluid Dynamics
DT	Digital Twin
FM	Facilities Management
HVAC	Heating, Ventilation, and Air-Conditioning
IESVE	Integrated Environmental Solutions Virtual Engineering
IoT	Internet of Things
VR	Virtual Reality

1 Introduction

1.1 Motivation

The expression “if these walls could talk” is taking on an entirely new meaning with the emerging opportunity to create Digital Twins (DT) for buildings. With the emanation of the Internet of Things (IoT) which to some degrees can be attributed to Moore’s law allowing powerful semiconductor chips to be manufactured at very low prices can influence every facet of our economy. Progressions such as cars that are connected and autonomous to flying robots and smart houses are all examples of either IoT being merged into legacy systems or IoT facilitating the creation of entirely new concepts (Khajavi *et al.*, 2019). For instance, the concept of smart cities is emerging in multiple continents where enhanced street lighting controls, infrastructure monitoring, public safety and surveillance, physical security, and transportation analysis and optimization systems are being implemented on a city-wide scale. A related and cost-effective user-level IoT application is the sustenance of IoT-enabled smart buildings.

Digital Twin a known concept in the field of manufacturing in simplest term is a digital representation of a real-world asset. Existing buildings can consequently benefit from the execution of a DT for the enrichment of building operating and maintenance. Figure 1 metaphorically explains the use of a 3D CAD model extracted from Building Information Modelling (BIM) along with various sensor networks to create a real-time view of the asset. This holistic view provides for real-time analytics, informed decision making, building efficiency, and comfort enhancement.

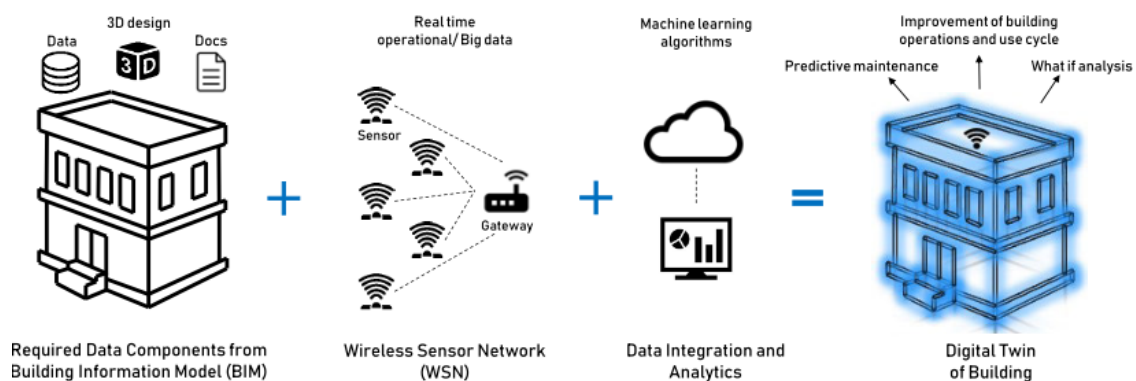


Figure 1: Essential components to create a digital twin of building and difference with BIM (Khajavi *et al.*, 2019).

1.2 Objective of the thesis

Digitalization in construction leads to the creation of an increasing number of digital building models. Furthermore, these digital building models contribute to both, an increase in efficiency during the planning and execution stages of the building and a thriving potential for improved process management during the operational aspects of a building. Digital Twins of buildings can contribute as an example so as to reduce the costs of facility management. Thus the building NUR31 at the campus Technische Universität Dresden campus is chosen as the test case for establishing a proof of concept for the Digital Twin. The two main objectives of the study are as follows:

1. Calibration of existing Energy Simulation Model

The first aim of the thesis is to use sensed and metered data for the calibration of Energy Simulation Models. The data gathered from the sensors installed at the institute is foremost analysed from the period of May 2020 to July 2020 and then conclusions are drawn for the plausible causes of the results obtained for various parameters governing a room's conditioning. Based on the results obtained from the sensed and measured data, the existing energy simulation model on the IES software is calibrated. Firstly, some discrepancies in the IES model are rectified and then the calibration is done to correlate the real-time data from the sensors to resemble the real room conditions as far as possible.

2. Visualization of data from sensors and simulation results

In the second objective, the output from simulation runs are forwarded to 3D-modelling and simulation tools in order to visualize the current or past status of the building. The visualization is carried out on the game development engine Unity3D. Possible immersive, innovative, and interactive visualization techniques are developed to create a virtual environment of the physical building. The main aim is to keep the visualization needs as clear and specific in consonance with the user's needs and to support collaboration and coordination from a functional as well as from an ergonomic perspective.

1.3 Problem statement

This research study concentrates on the following questions:

1. The concept behind Digital Twins in regards to the construction industry.
2. What parts are needed to create a framework for Digital Twin.
3. Calibration of existing energy simulation with sensor data.
4. How to integrate real-time sensor data into a Digital Twin environment.
5. How to visualize sensed data and simulation results on Unity3D.

1.4 Organization of the thesis

The thesis is categorized into five sections. In the very first section, a brief introduction includes the motivation behind the selection of the exact research field. The second section dwells into the theoretical background of the research which is subdivided into five parts covering the various concepts and literature for this research, further validated by case studies. Whereas, the third section corresponds to the analysis of the various models thus including the sensor data from the Building Automation System (BAS), the energy simulation IES model, the BIM-Model (Revit), and the Virtual Reality (VR)-Model (Unity). The methodology adopted for creating the DT constituents the fourth section in regards to the feasibility of proof of a concept to create a DT. The last section contemplates the outcomes obtained from this research work and the future work that can be considered for the improvement of DT's framework for the current work and numerous alternate applications.

2 Background and related work

2.1 Digital Twins

Digital twin (DT) is an old term, which was coined almost 2 decades ago, resurfacing now as the world becomes interconnected. The notion of a virtual, digital equivalent to a physical product or the Digital Twin was introduced in 2003 at the University of Michigan Executive Course on Product Lifecycle Management (PLM) (Grieves, 2014). The DT concept was at the outset published in the aerospace field and was defined as *"a reengineering of structural life prediction and management"*, later appearing in manufacturing.

Smart manufacturing in essence is the cardinal requirement shared by all large-scale manufacturing initiatives such as Industry 4.0 and Industrial Internet. Digital twins are one of the most propitious propositions for this realization, which is symbolized by the cyber-physical integration (Tao *et al.*, 2019). Therefore, smart manufacturing entices the industry with vital challenges in relation to the connection between physical and virtual spaces. With the ongoing brisk development of simulation, data acquisition, data communication, and other advanced technologies have set in motion greater synergism between the physical and virtual spaces. The significance of a DT, which inherently values cyber-physical integration, is vehemently advocated by both academia and industry. The data from the physical world is siphoned onto the virtual models through the sensors to complete the simulation, validation, and dynamic alteration. Furthermore, the simulation data are fed back to the physical world to act on the changes, with aim of enhancing the performance of the product/process in the physical space (Qi and Tao, 2018).

For the purpose of research, we adopt the approach provided by Grieves (Grieves, 2014), allocating a holistic view of the complex system representing a DT. Thus, the main DT components (as shown in Figure 2) considered here are:

- a) The Physical components
- b) The Virtual models and
- c) The Data that connects them

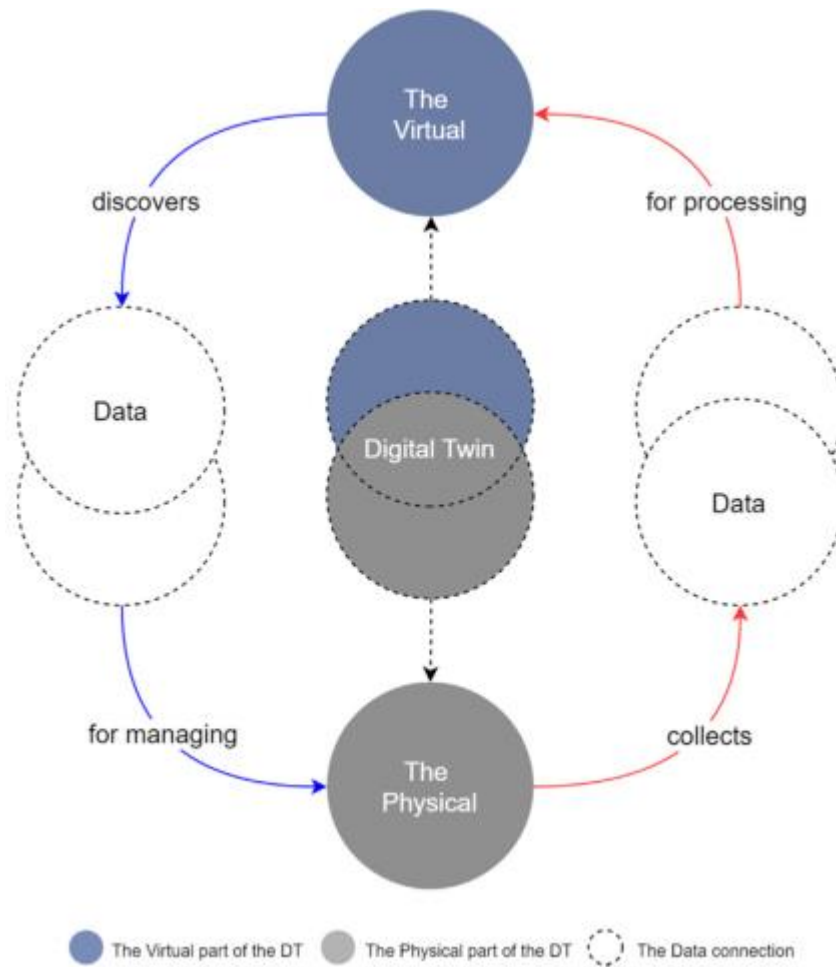


Figure 2: The Digital Twin paradigm (Boje et al., 2020).

The linkage loop between the “Virtual-Physical” duality of the system is provided by the “Data” in its many forms. For instance, Grieves (Grieves, 2014) considers the data from the “Physical to the “Virtual” to be raw and thus needing processing, while the data on the contra is subject to numerous transformations, which can be processed information and stored knowledge athwart digital modes. In a nutshell, the “Physical” part gathers data that is proceeded for processing. In return, the “virtual” part applies its embedded engineering models and AI to discover statistics which is utilized for supervising the day-to-day usage of the “Physical” (Boje et al., 2020).

2.1.1 Building Information Modelling

In accordance with the US National Building Information Model Standard Project Committee, BIM (Azhar, Khalfan and Maqsood, 2012) is said to be “a digital representation of physical and functional characteristics of a facility. A BIM is a shared knowledge repository for science about a facility thus providing a reliable basis for decisions during its life cycle; construed as existing from earliest conception to demolition.” In the meantime, Ghaffarianhoseini et al. defined BIM as “an overarching term to describe a range of activities in object-oriented Computer-Aided Design (CAD), which provisions the representation of building elements in terms of 3D geometric and non-geometric (functional) facets and relationships.” Although, BIM is different from 3D CAD modelling its main priority relies on embedded information (e.g., specification, material type, installation method, time, cost) in the design model and further on the interoperability of this all-inclusive information-rich model for enhanced alliance in the AEC/FM industry (Ghaffarianhoseini *et al.*, 2017).

BIM has been evolving over the years (see Figure 3). According to the BIM maturity model presented in (Sacks *et al.*, 2018), Level 0 BIM in the 1990s benefited from early CAD modeling software, hence information was scattered and data sharing was mostly limited to paper drawings. During the 2000s, Level 1 BIM became prevalent; companies began to use 3D CAD modeling and a common data environment (CDE) for digital sharing. Nevertheless, Level 1 BIM did not support the project team members to share the models with each other. Level 2 BIM gained significance during the 2010s when collaboration and digital file-sharing facilitated the evolution process through the use of common file formats and the introduction of Industry Foundation Class (IFC) and Construction Operation Building Information Exchange (COBie). The majority of the companies are presently at Level 1 or Level 2 however; Level 3 BIM is being developed with an emphasis on stakeholder collaboration (i.e., through the use of the same design model). The aim of Level 3 is to store in a centralized cloud-based repository to safeguard collusion through the building life cycle.

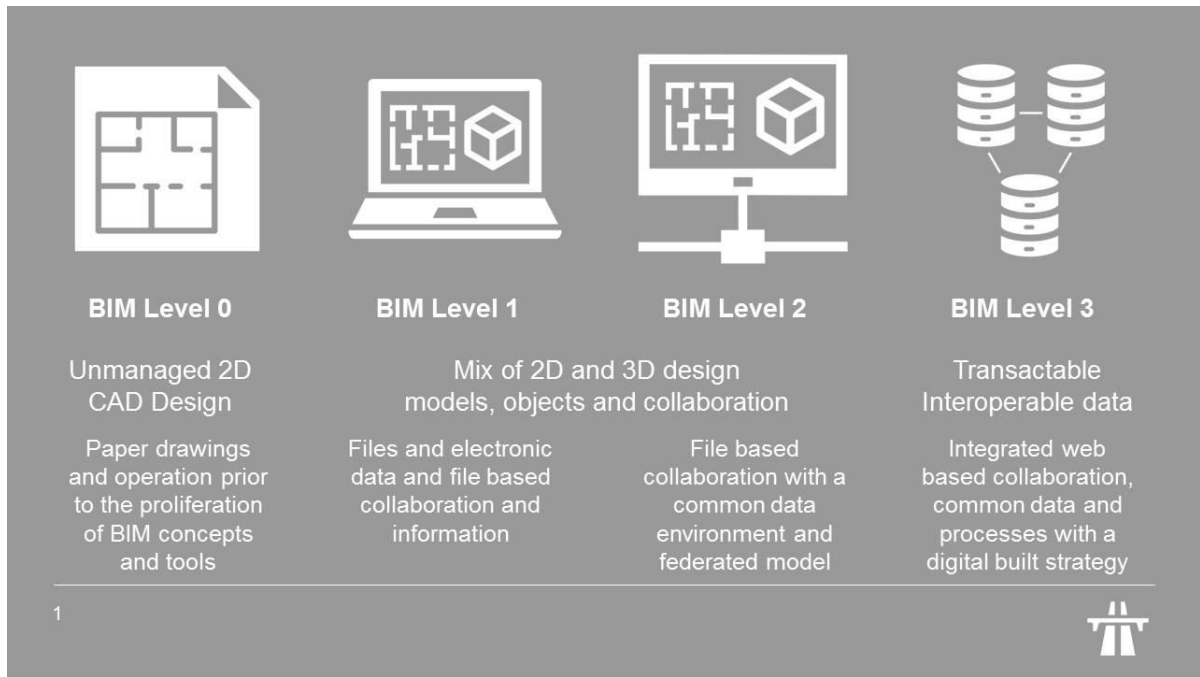


Figure 3: Description of BIM Levels (Sacks et al., 2018).

2.1.2 Comparison of BIM and Digital Twin of building

BIM and Digital Twin of a building can be compared in detail based on the following features; application focus, users, supporting technology, software, stages of a life cycle, and origin (see Table 1). BIM is primarily used to prevent errors during the design of a building, facilitate communication between stakeholders, improve construction efficiency, and monitor the construction project's time and cost. Whilst, the DT of a building can be used for predictive maintenance, resource efficiency improvement, enhancement of tenant's comfort, what-if analysis for optimization of the building design, and enabling the closed-loop design to transfer learnings from a building to the future ones. The handlers of BIM are architects, engineers, and constructors who employ it during the design and construction stage. Notably, BIM is used by facility managers for maintenance planning through the building life cycle. Meanwhile, DT's are applied by facility managers in the use phase of the building life cycle to augment its operation. Furthermore, DT's also offers architects valuable input for the design of future buildings based on the detected flaws and enhancement zones uncovered during the use phase of a building.

Table 1: A detailed comparison of BIM and digital twin of a building (Khajavi et al., 2019).

Differentiator	Concept	
	BIM	Digital Twin
Application focus	Design visualization and consistency, Clash detection, Lean Construction, Time and cost estimation, Stakeholders interoperability	Predictive maintenance, Tenant comfort enhancement, Resource consumption efficiency, What-if analysis, Closed-loop design
Users	AEC, Facility manager	Architect, Facility manager
Supporting Technology	Detailed 3D model, Common data environment (CDE), Industry Foundation Class (IFC), Construction Operations Building Information Exchange (COBie)	3D model, WSN, Data analytics, Machine learning, Automation, and control systems
Software	Revit, MicroStation, ArchiCAD, Open source BIM server, Grevit	Examples are Predix, Dasher 360, Ecodomus
Stage of a life cycle	Design, Construction, Use (maintenance), Demolition	Use (operation)

With regards to adaptability, although some buildings are still constructed using pre-BIM conventional methods, they can still enhance from Digital Twin by being retrofitted with sensors and by taking advantage of cloud-based analytics tools (Khajavi et al., 2019). Digital Twin methodology is one way to aid uplift BIM beyond CAD display. IoT and DT's endows BIM models to track, store, and display complex data, and efficiently turn models into "living" documents that update automatically.

2.1.3 Digital Twins in the AEC industry

The Architecture, Engineering, and Construction (AEC) industry has already made momentous strides since the conception of BIM and has gained adequate recognition and momentum to enable a shift from static, closed information to a dynamic, web-based one embracing IoT integration and a higher degree of AI implementation fuels Digital Twin in AEC. The concept of construction DT conveys a more holistic socio-technical approach with the following probable applications.

Automated progress monitoring

Progress monitoring substantiates that the completed work is consistent with plans and schedules. By recreating as-built of a building or infrastructure we can compare it to as-planned execution in BIM and take necessary actions to rectify any anomalies. For as-designed models to match the as-built reality, companies need to invest considerable time and labor in the construction project's early phase. For instance, the contractor's detailers had a different starting point each time in terms of different stakeholders: different owners, designers, and subcontractors (Tetik *et al.*, 2019). The use of technological advancements like photogrammetry and laser scanning to track site progress to an already developed model is a potential solution. On the contrary, some studies also considered the interior spaces of a building under construction to establish a methodology to improve the automatic updating of 4D models using computer vision.

Hence, having automated means of data collection and comparison by incorporation of Digital Twins enables the resulting model in comparison to an as-designed BIM model to be less liable to human error and subsequently reflect this in terms of quality assessment and cost reductions long term.

Safety monitoring

The construction industry is one of the most hazardous sectors in the world. According to the Bureau of Labour Statistics in the United States, more than four thousand construction workers died on-site between 2008 and 2012. Nevertheless, the process of applying safety management following systematic and purposeful workflows with transparency is still deficient. The fact that many subcontracting companies work for a temporary period on-site with large temporary workforce safety management issues is often undervalued.

(Rwamamara *et al.*, 2010) advocate the use of three-dimensional (3D) and four-dimensional (4D) visualization techniques to serve as an extensive safety net to avoid health and safety risks. Taking into consideration the design process where clash detection, work tasks sequence, workspace congestion can be identified by project stakeholders who in turn are able to plan for alternate solutions to reduce rework, heavy material handling, and repetitive and awkward postures for workers susceptible to musculoskeletal injury risks. Recently, tech giants Microsoft

also pressed for use of AI through already installed cameras or people equipped with portable cameras for making construction sites safer (Jones, 2017).

Therefore, with modern site monitoring equipment, DT has the potential to spearhead site safety prediction, thus providing a more automatic way to gather and classify safety events, making safety management more reliable.

Holistic web-based integration

A fully semantic data environment reaps proportionate benefits, such as allowing the design and construction supply chain to leverage web-based linked data. Disturbances in construction phase deviations from designed BIMs can occur due to change in specified equipment for a particular manufacturer during purchase orders, optimization of costs, or unavailability with the timeframe of the project. Linked data over the web with project supplier databases, products, and order changes can help condense aftermaths of such disruptions on productivity. Conversely, building components themselves can have a DT from a manufacturing domain as DT is quite prevalent in manufacturing. Suppliers of a DT will also benefit by having, by monitoring and collecting data about their product use and customer feedback. Thus, web-based integration would propel a knowledge base for construction efficiency (Boje *et al.*, 2020).

Life cycle management

A DT should incorporate the entire lifecycle of the physical asset, with long-term cost reduction contemplated as the fundamental added benefit. Planning for the entire lifecycle will consistently generate profound differences, depending on the application territory. Manufactured assets with DT applications generally have shorter lifespans, with high predictability of design-manufacturing-operation processes. However, when taken into account for the AEC industry the considered buildings, infrastructures, or city districts, this is observed as an ongoing process of optimising running costs, structural integrity, and safety (Boje *et al.*, 2020).

2.1.4 Digital Twins usability in the FM industry

Technological advancements are aiding a paradigm shift in facilities management (FM), changing occupant's expectations of building capabilities and comfort. Modern buildings are highly automated and comprise versatile control systems to help facility managers ensure efficient resource utilization and effectively operate their infrastructures. The widely accepted use of DTs in manufacturing, automotive, and logistic industries has enabled increased reliability, improved productivity and safety, and enhanced cost-efficiency. All of these sectors are already profiting from the technology's advantages, such as increased reliability, improved productivity and safety, and enhanced cost-efficiency. From the perspective of facilities management, Digital Twins have the potential to replicate an entire built ecosystem rather than a single asset. As seen in Figure 4 a DT of a building informed by real-time sensor data unravels the hidden data points that can transform the way facilities are controlled and managed.

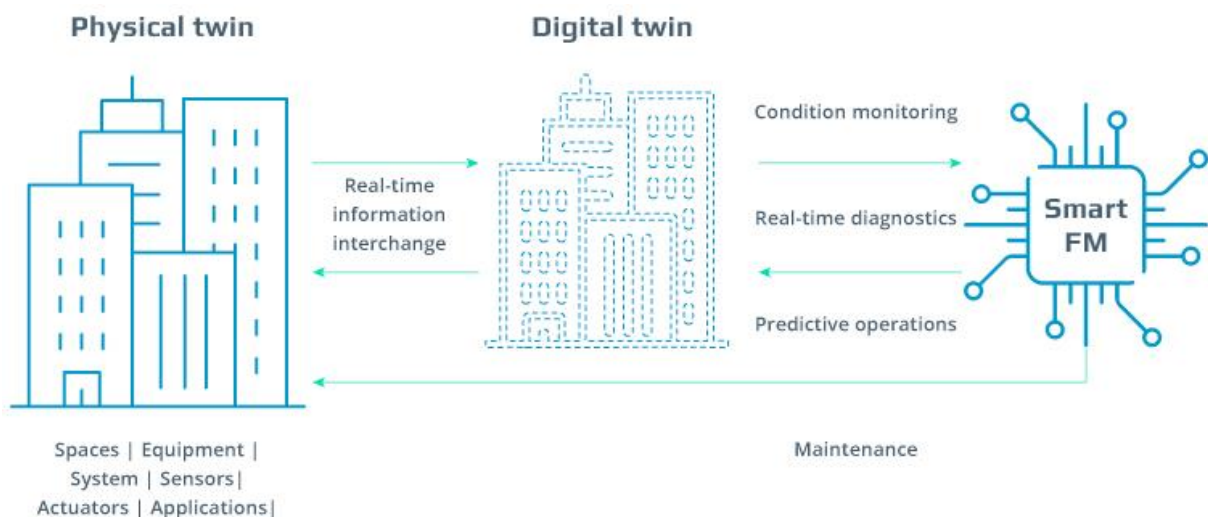


Figure 4 Facilities management enhancement by DT's (Martynova, 2020).

Dynamic condition monitoring

A digital twin model sustains on information gathered in real-time from fire detectors, HVAC equipment, lighting fixtures, consumption meters, indoor sensors, and other systems installed on the premises. Continuously powered by dynamic data, they accurately recreate every single metric within all facility systems, adding to collective facility intelligence that mirrors exact on-site

conditions and enables immediate action when, for example, a leaking valve or a faulty sensor is detected.

Insights driven predictive maintenance

Predictive maintenance is the frontrunner in terms of the application of DT's in Industry 4.0. The expansive use of this concept in FM is predicted to generate up to a 20% reduction in building maintenance and energy costs. Digital twin based predictive software accumulates real-time records from every physical asset within a facility and evaluates them against historical readings. Through continuous learning, digital replicas can immediately recognize that a given component is wearing down and requires attention, and signal the issue to the facility manager. Armed with this knowledge, facility operators know when to take action, and may run simulations to predict how an object will behave under different conditions. The opportunity to test various maintenance approaches allows them to anticipate every possible outcome before dispatching a maintenance team on-site. As a result, they can enhance the overall asset lifecycle, avoiding over-servicing and over-maintaining assets, and keeping maintenance costs in check (Martynova, 2020).

Autonomous facility operations

Digital Twin draws together dynamic and static data from numerous sources in 3D models, thus contributing invaluable comprehension of energy and water consumption patterns, room occupancy, HVAC utilization, and other aspects of facility operations. This knowledge equips facility managers to adapt the facility systems to enrich occupant comfort. With further improvement in facilities management software and IoT sensors could be the cornerstone in creating self-maintaining facilities capable of operating autonomously without support from public services. Intelligent buildings (Figure 5) will constantly observe tenant behavioral patterns (such as room occupancy throughout the day, room lighting and temperature pretenses, etc.), enhance their understanding of human needs and tailor the ecosystem to meet these.

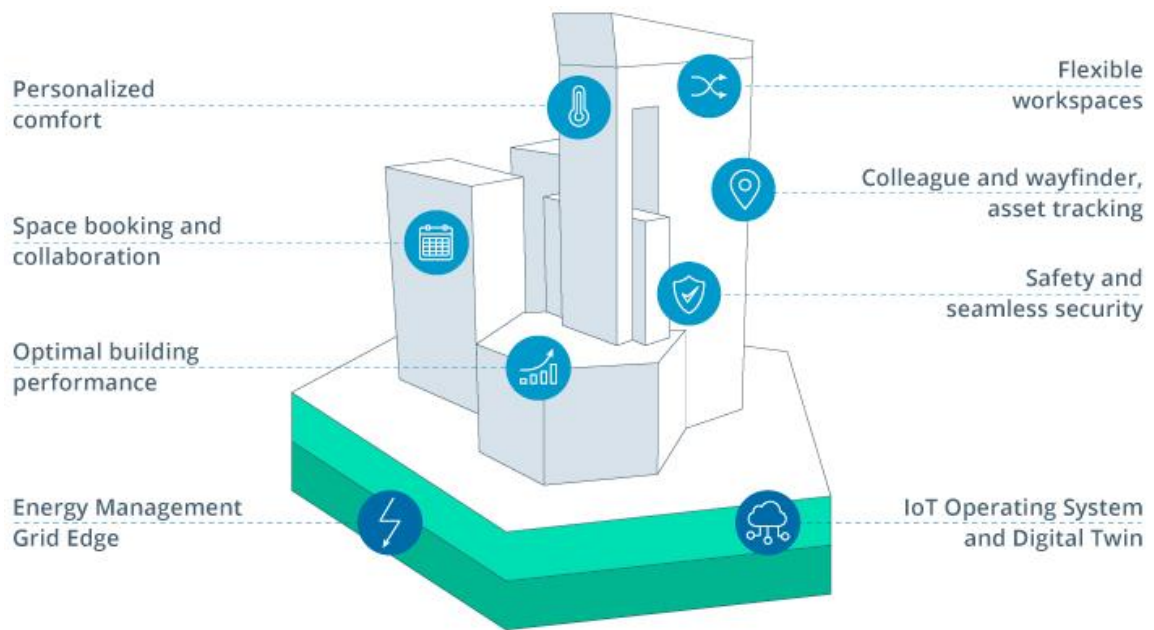


Figure 5: Representation of an intelligent building (Martynova, 2020).

2.1.5 Digital Twin for a smarter built environment

Cities are accountable for much of the globe's total resource consumption and are flourishing briskly in terms of size and population, thus having a significant impact on the economic, environmental, and social future. In order to handle such complexities, along with global sustainability burdens, many cities are consciously enforcing technological advancements in their operations for smarter performance, thus transforming cities into smart cities.

Smart Cities, as a concept, can be traced back to the conception of wired cities in the 1980s and digital cities in the early 1990s, followed by the smart growth movement (Mohammadi and Taylor, 2018). At the forefront of a smart city is the Dutch city of Rotterdam. The historic port city has been developing and applying a wide range of smart solutions to urban conundrums in recent years. As is depicted in Figure 6 a smart thermal grid is being constructed, for instance, that will expedite heat exchange between buildings and make the entire neighbourhood more energy efficient. Smart parking and intelligent (electric) mobility are aiding better traffic flow, and an array of other benefits in order to make life better for inhabitants of the city. At the moment, Rotterdam is going a step further by shaping a "Digital Twin" for the city, which will act as a platform for a new era of digital city applications. A DT which is a smart 3D model would

precisely represent the streets, buildings, public spaces, and so on of the physical city. Sensors and data streams around the city feed into the virtual model to give real-time updates such as the movement of people or vehicles, which can be assimilated into the system (Editorial, 2019).

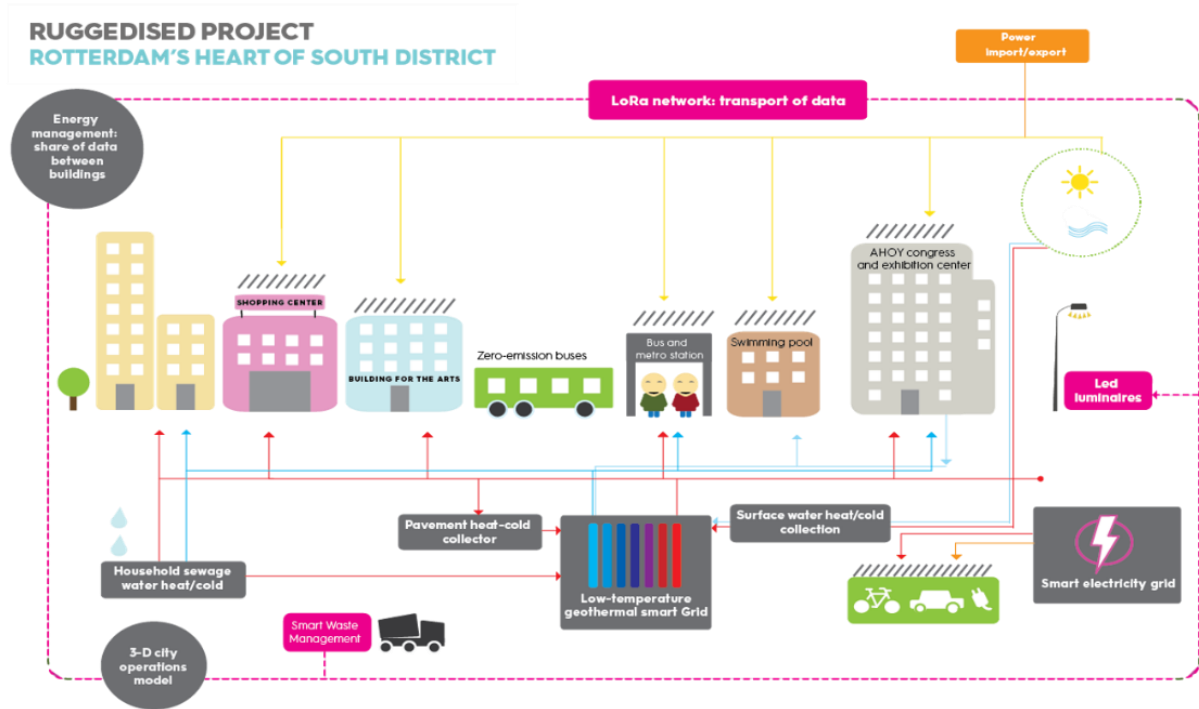


Figure 6: Outlay of a smart city workflow in Rotterdam.

The emergence of Digital Twins, an effort to create intelligent adaptive machines by generation a parallel virtual version of the system alongside connectivity and analytical competence facilitated by IoT constitutes the foundation for the cognitive development of Smart City Digital Twins. As illustrated in Figure 7 the digital clone of the city (Figure 7 (b1) and (b2)), is progressively informed by the real physical city (Figure 7 (a1) and (a2)), via real-time spatiotemporal data from infrastructure and human systems.

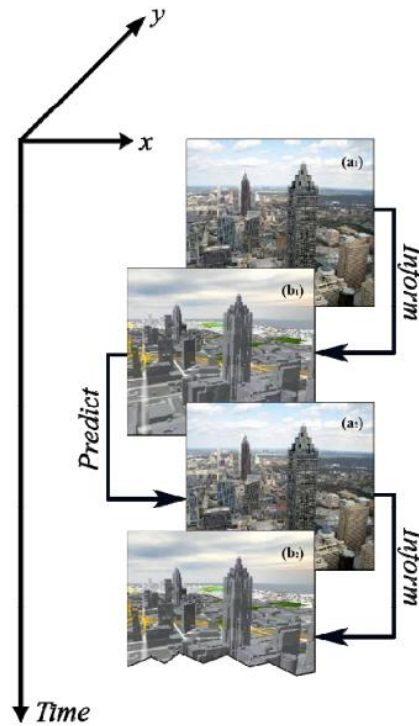


Figure 7: Spatiotemporal Flux and Reality-Virtuality integration: Digital Twin City of Atlanta (Mohammadi and Taylor, 2018).

Thus, a Digital Twin cognizant of the city's infrastructure performance, human dynamics, their interdependencies and interoperability, and their variations in time and space, is progressively able to foresee changes of state in the systems and envisage future behaviors. The predictive nature of the Digital Twin city banks on the real-time and aggregated historical performance of the human-infrastructure systems. Moreover, regardless of the current state of the city, a DT can simulate what-if situations in the system and predict emergent action. Such insight is decisive in evaluating whether or not smart growth strategies are effective, reducing the gap between smart utopia and smart reality (Anthopoulos, 2017).

2.2 Building Energy Simulations

The fundamental function of Building Energy Simulation (BES) is to predict the energy performance of a given building and thermal comfort for its occupants. Furthermore, decisions on how to dimension, layout, and operate buildings services systems are based on the outcome of such simulations. The nitty-gritty of BES involves knowledge in relation to thermal comfort, ventilation, and indoor air quality, additional lighting system, HVAC efficiency, etc. Henceforth, energy

simulation programs are powerful tools to study energy performance and thermal comfort during the building's life cycle. Today, plenty of such tools are accessible and differ in several aspects; in their thermodynamic models, their graphical user interfaces, their intended use, their life-cycle use, and their ability to exchange data with other software applications.

At the onset, any simulation result is as accurate as the input data for the simulation. As depicted in Figure 8 below, the input mainly consists of building geometry, internal loads, HVAC systems and components, weather data, operating strategies and schedules, and simulation explicit framework. Each simulation engine is based on thermodynamic equations, principles, and assumptions. Since thermal processes in a building are complicated and not easy to comprehend, energy simulation programs approximate their results with quantified equations and approaches (Maile, Fischer and Bazjanac, 2007).

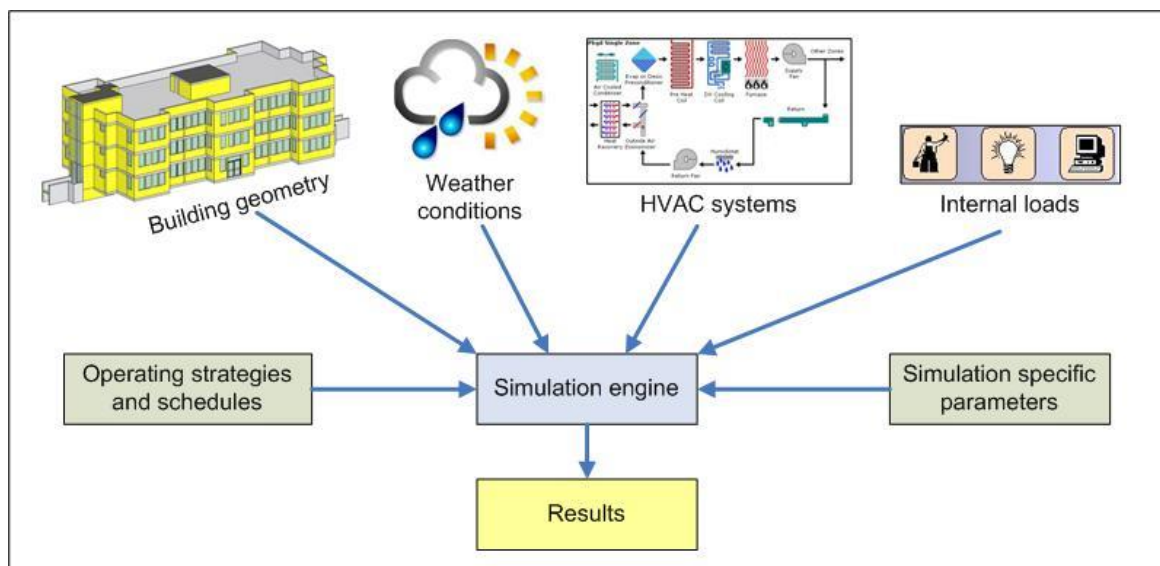


Figure 8: General data flow of simulation engines (Maile, Fischer and Bazjanac, 2007).

Universally, energy simulations could be applied in every stage of the building's life, since the notions considered are equally valid independent of the stage of a building's life. The design-oriented tools can help in shaping the components of a building's fabrics (wall, window, roof, etc.) and form the heating and air-conditioning perspective as well. While in contrast, the simulation tools use more generic concepts and hence can be used during the operation stage. Also, the latter, produce more data (typically over a 1-year period) that can be compared to

the actual building performance and, thus, they are also valuable for commissioning and operations life stages.

2.2.1 Classification of Energy Simulation Models

Based on the calculations and concepts to get building energy performance, the various energy simulation models can be categorized according to three fundamental criteria's as follows:

- a) Physical principles of energy (heat) transfer.
- b) Levels of abstraction.
- c) Time-dependency of input variables.

This categorization is represented in Table 2 according to the above principles.

Table 2: Stratification of Energy simulation models (Menzel, 2018).

Physical Principles	Levels of Abstraction	Time-dependency
Thermal Radiation	Mono-Zone Models	Steady-state models
Conduction	Multi-Zone Models	Dynamic Models
Convection/Advection	Zonal Models	
	CFD-Models	

According to Physical Principles

The thermal performance of the building material is in concordance with three mechanisms of heat transfer.

- **Thermal radiation:** It is defined as the emission of electromagnetic waves from elements that have a higher temperature than absolute zero caused due to the thermal motion of charged particles. It represents the transfer of thermal energy into electromagnetic energy. Solar radiation is absorbed and emitted through opaque and transparent building elements. Figure 9 illustrates the physical principles of energy (heat) transfer (Menzel, 2018).

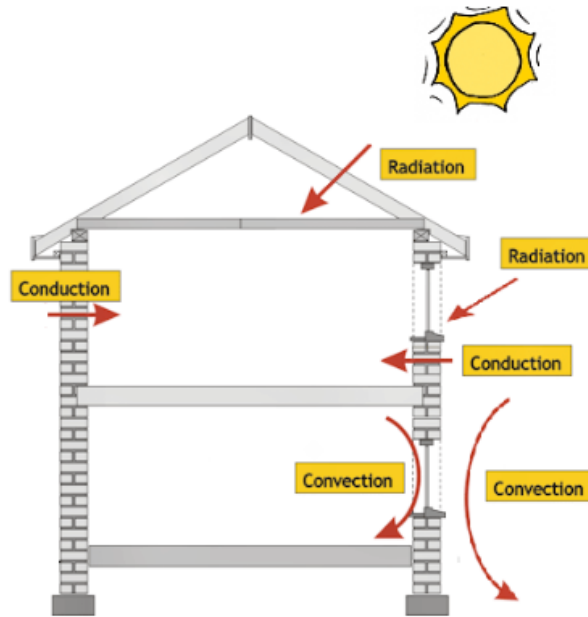


Figure 9: Heat processes through a building (Wasmi and Salih, 2019).

- **Conduction:** Conduction or thermal transmittance (U-value) signifies the transfer of heat within the material due to microscopic diffusion and collision of particles. The heat transfer is from higher to lower temperatures of the body. Hence, it is the main form of heat transfer mechanism influencing the energy consumption of the building. The inverse of conductivity is known as resistivity (R-value) (Menzel, 2018).
- **Convection:** The principle of heat transfer caused due to movement of molecules via a material carrier (air or liquid). The energy transfer occurs because of the buoyancy forces of the carrier due to variation in density.

According to the levels of abstraction

As there is a necessity for input data for energy simulation on the design phase of the building lifecycle. Such as if the simulation is at the early stage of the design, then the required data is governed by the outer dimension of the building and its orientation. The following level of abstraction describes the data required for different models.

- **Mono-zone models:** Mono-zone models signify the highest level of abstraction and hence are used in early design stages. This approach considers the building as an individual block with a single zone of operation for facilities. The selection of building material and HVAC-system must be specified. The simulation time steps are generally in order of hours.

- **Multi-zone models:** Multi-zone models decomposes the building space into different functional zones with leverage to operate under different constraints. The selection for components of shell and indoor building components must be specified along with parameters for room conditioning and ventilation must be ensured. The simulation time steps are typically in the order of minutes (Menzel, 2018).
- **Zonal models:** In this method the space being operated under a single set of constraints is bifurcated into multiple modeling zones, for instance modeling a select number of windows for opening but not all the windows. The simulation time steps are characteristically in order of minutes.
- **CFD models:** CFD models impart the modeling of space with a fine level of granularity. They apply numerical methods for problems concerning the flow of fluids and their interactions with surfaces as per the boundary conditions. For energy simulations in building they model micro-environments such as an individual workspace or a single room. If required, the simulation time steps can be reduced in the order of seconds (Menzel, 2018).

According to time-dependency

The basic differences between steady-state and dynamic simulations are the input parameters. For steady-state simulations, they remain constant throughout the year while for dynamic simulations they vary over time.

- **Steady-state simulation model:** In this elementary method the input parameters are averaged over a dedicated time period and internal gains are simplified. For example, the weather details at allocation are averaged to the peak heating and cooling loads to be used for simulations. Generally used for heating systems (to increase the temperature of a room) during the coldest weather as a heating load from occupants, lighting, and equipment's won't affect the heating system.
- **Dynamic simulation model:** In this simulation method the parameters are provided over a much shorter time period (e.g. hourly). The dynamic simulations are typically used for cooling load calculations (amount of load required to cool down the room or space temperature). For cooling load calculations, the complex effects of heat transfer (conduction, convection,

and radiation), heat storage long with heat gains from occupants, lighting, and equipment's are always considered. Hence, the dynamic simulation ensures optimized systems (Menzel, 2018).

2.3 Building Automation Systems

Since the first intelligent building came into view in Hartford U.S in 1984, intelligent building matured rapidly with the backing of computer technology. Intelligent building attributes to buildings granting people "a safe, efficient, energy-saving and health building environment" by optimization of the building structure, equipment, services, and management in accordance with the user's needs (Li and Zhang, 2013). With decades of advancement, BAS so far has experienced four generations of control systems document in Table 3; in the first generation it is CCMS (central center monitoring system), the second generation involves DCS (distributed control systems), the third is FCS (field-bus control system) and the current generation is network integration systems.

Table 3: Control system characteristics over four generations (Li and Zhang, 2013).

Period	System	Characteristics
1970's	CCMS	3 levels control system: computer central station, DGP substations, and field devices such as sensors and actuators. Central station completely controlled all equipment's according to the field device information uploaded by DGP sub-stations.
1980's	DCS	Distributed intelligent management system with four levels of control, management system, central station, sub-station, field devices. DGP sub-station with microprocessor developed into direct digital controller (DDC) which can do the processing work independently. Central station will control all sub-stations if needed.
1990's	FCS	3 levels control system: management level of central station, automation

21 st Century	Network system integration	level of sub-station, field-bus network level. System using a web browser as a human-machine interface. People get information through a network. Real-time database is applied.
--------------------------	----------------------------------	---

A building automation system (BAS) is intended at implementing and preserving safety, security, energy reduction, cost optimization, and comfort in commercial and residential buildings. At the onset, assurance of compliance with the comfort necessities of building users, followed by energy reduction in buildings as they contribute largely to total energy consumption. Over the preceding decades, a three-level architecture, which entails of field, automation, and management level, has ripened in Building Automation (BA). The wide range of BA technologies encompasses different disciplines like heating, ventilation, and air conditioning (HVAC), lighting, or security, on differential levels of hierarchical architecture. Hence, interoperability is a vital aspect of this diverse environment with the intention of realizing efficient monitoring and control in terms of building management systems (Schachinger and Kastner, 2016).

In the residential sector building automation is often referred to as “Smart Home System”. In other words, a smart home is a home-like environment that maintains ambient intelligence and automation control, thus enabling it to cater to the behavior of residents and provide them with necessary facilities. The typical method for building smart homes is to computerize them. A set of sensors gather different types of data, with reference to the residents and utility consumption of the home. Subsequently, devices with computing power (e.g., micro-controllers) analyze that data to recognize the actions of residents or events and then react to those actions by controlling certain mechanisms built into that home. Hence, the most vital aspect of the Smart Home system is the network itself (Figure 10), which enables real-time exchange of information from and to the buildings and residents by connecting and managing all the technological devices installed in the network system.

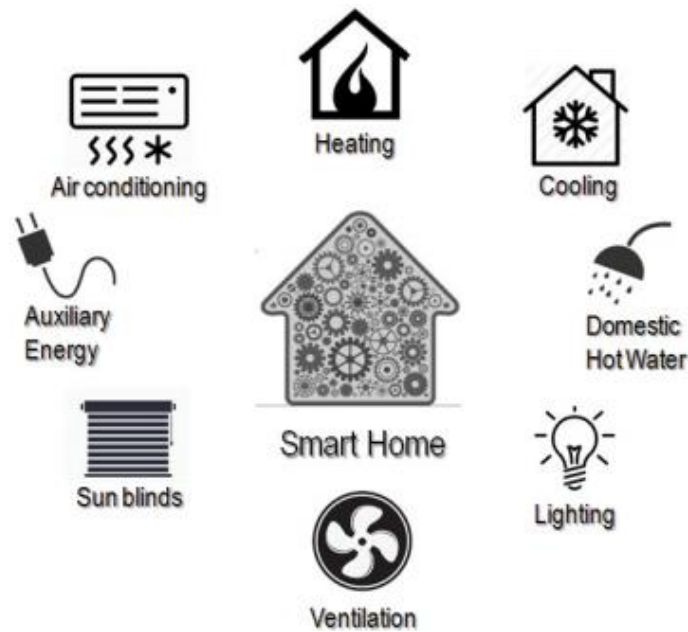


Figure 10: Smart Home network prototype (Fabi, Spigiantini and Corngati, 2017).

2.3.1 The framework of Building Automation Systems

A centralized BAS must have a modular structure (Figure 11) to take into account the networks of hardware and software which monitor and control the environment in industrial, institutional, and residential facilities.

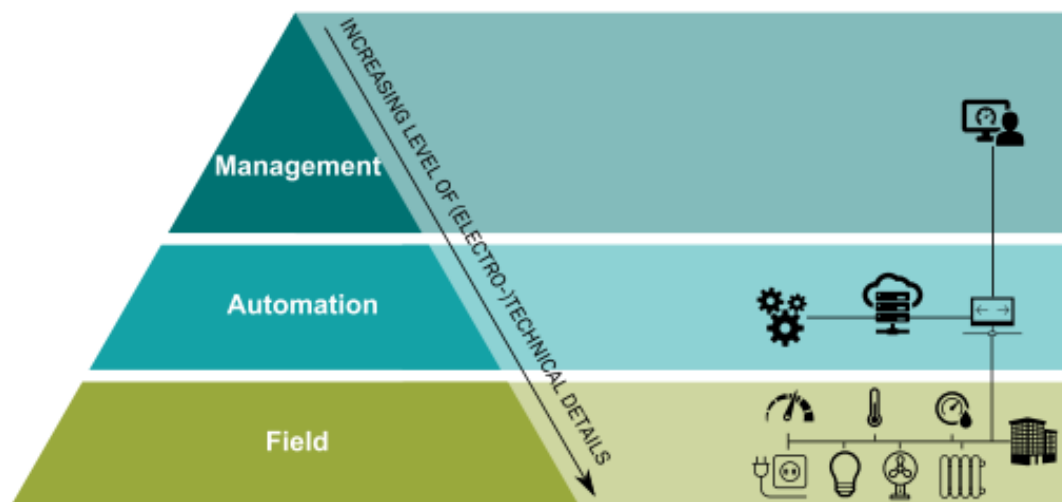


Figure 11: Hierarchical levels for BAS (Kastner et al., 2005).

The components for setting up a building automation system are:

- Field Level: Here the interaction with the physical world takes place. Environmental data (CO₂ output, temperature, humidity, daylight, or even

room occupancy) is collected through sensors and transformed into a form suitable for transmission and processing. To boot, with the help of actuators and relays environmental parameters can be physically controlled (switching, setting, positioning) in response to commands received from the system (Kastner *et al.*, 2005).

- Automation Level: Includes all kinds of autonomously executed sequences. It functions on data generated by the field level, establishing logical conditions and loops. The most commonly used options are BACnet and Modbus. Processing entities may also interconnect the value of more global interest to each other, for instance, the outside temperature or whether night purge is to be activated. This sort of data exchange is referred to as horizontal communication. Additionally, the automation level prepares (possible aggregate) values for vertical access by management level.
- Management Level: At the management level, information acquired through the entire system is accessible. A consolidated user interface or dashboard is presented to the operator for manual intervention. Alerts are generated for uncommon situations like technical faults or critical conditions. Moreover, long-term historical data is stored on the cloud capable of developing reports and statistics for the collected parameters (Kastner *et al.*, 2005).

2.3.2 IoT based Building Automation Systems

In this passage, we discuss the need for transition from classical to IoT-based BAS. In the past decades, buildings have become highly monitored data sources, comprising of thousands of sensors, actuators, and configuration information. However, the data still sources function in a hierarchical way governed by standards and protocols, thus presenting a major challenge to be set up during construction and also increasing the building life-cycle costs. The recent trend and potential of IoT and cloud computing provide easy installation, reduced configuration effort, high availability, and direct cloud integration.

IoT encompasses stakeholders and players across various spheres, each having a different point of view on the problem with perception and concepts oriented towards their field. Hence, IoT represents a synergy of three different versions (Bode *et al.*, 2019):

- The thing-oriented vision: Focussing on the single sensor or component, that is now considered as an individual object rather than part of a major device.
- The internet-oriented vision: Where the network and interconnectivity, and subsequently the middleware, of things are the starting point of the design.
- The semantic-oriented vision: Taking into account the problem of identifying, representing, storing, and exchanging exclusive information.

An IoT-BAS contains, although non-exclusive, devices that can communicate via the internet with servers situated outside the building. The communication path for a contemporary BAS outlined in Figure 12 can have interesting ramifications. Where each field device i.e. sensors and actuators in the BAS should be either Internet Protocol (IP)-enabled or connected to a gateway. The gateways can possibly be installed in close proximity to the field devices, reducing wiring labor or the damping in case of wireless communications. The IP-enabled devices have a fixed identifier such as the MAC address. Also, additional information such as a string containing the position and function of the device can be stored on the device itself. The communication of the devices can be enabled via a cloud platform featuring a light-weight protocol such as MQTT. The platform itself should also support basic modeling of the physical and functional relations of the data points provided by the devices. The cloud platform should also permit the user to implement various kinds of control algorithms such as rule-based and model-predictive control (MPC). One of the key aspects of cloud-based control is that data can be utilized for training the data-driven model, which can be further used for MPC, load predictions, and error detections. It should also be possible to send control decisions back to the device, giving a bi-directional communication (Bode *et al.*, 2019).

Lastly, IT security is one of the foremost concerns of IoT-BAS. The stipulations for Internet-connected devices are quite complex and ensuring secure systems are arduous even for domain experts.

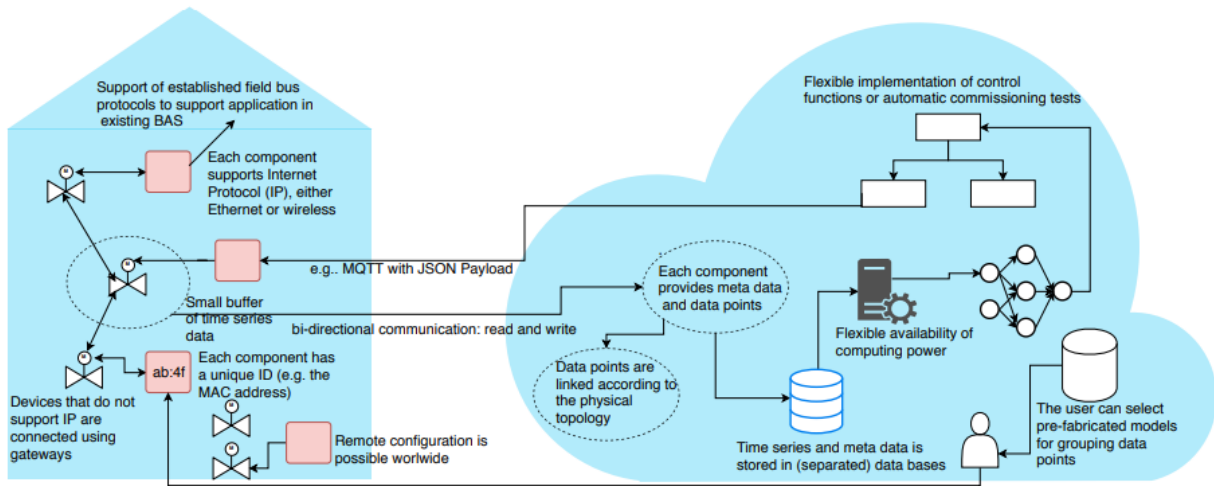


Figure 12: The prospective architecture for IoT BAS (Bode *et al.*, 2019).

2.4 Integration of sensor data

At the onset, the task of real-time sensor data integration and information fusion to build “Digital Twins” is highly challenging to emulate accurately. Digital Twin works specifically with real-time sensor data fed by the sensor systems to record and analyze the real-time structural and environmental parameters of a physical asset with the aim of performing highly accurate DT simulation and data analytics (Khajavi *et al.*, 2019). For the establishment of a methodology for Wireless Sensor Network (WSN) for DT an example of sensors installed on the building’s façade of an office building at the Aalto University in Finland is given. The aim was to collect light, ambient temperature, and relative humidity measurement data of the environment. Figure 13 illustrates the data flow of real-time sensor data into the proposed Digital Twin environment.

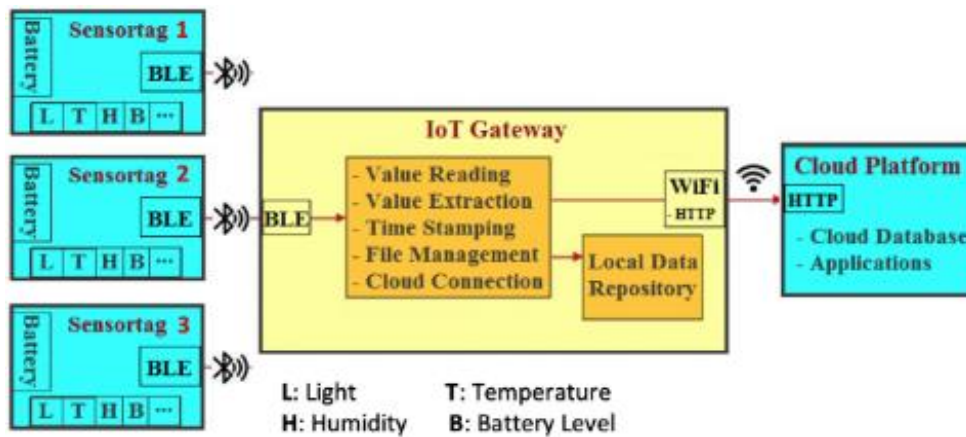


Figure 13: Real-time sensor data flow diagram of the designed WSN (Khajavi *et al.*, 2019).

2.4.1 Strategies for real-time data integration

To enable real-time data collection from a physical twin, in reality, a system of managing sensor nodes is required. Thus, this section presents a brief review of a few possible approaches which facilitate the integration of real-time sensor data with their digital representation to enable advanced simulation, operation, and analysis. Data acquisition and transmission are crucial in DT for real-time information flow and connectivity. The Cyber-Physical System (CPS) which is considered as the next generation of IoT provides us one such sensor data connection path where computation, communication, and control features of the physical system through physical devices provide data sources for computation modules (i.e. Digital Twins). The few possible strategies considered for this literature review include cloud-based CPS and CPS at the equipment level.

Although real-time data acquisition and transmission technology support the interaction between physical space and virtual space, implementing feedback control based on two-way transmission and real-time analysis is still challenging. Based on the foregoing observation, the existing application of DT's is still in an initial stage while the development of product digital twins, process DT's, and operation DT's has great potential for enhancement.

Cloud-based Cyber-Physical System Architecture (C2PS)

Sensors and actuators have become more affordable and available, which ensures the ubiquitous presence of versatile sensors and subsequent data acquisition using computer networks. As a result, data analysis based control of the resources or physical environments is possible than ever before. This phenomenon, however, is addressed as Cyber-Physical Systems (CPS). Here, physical systems collect sensory information from the real world and send them to the Digital Twin computation modules residing in highly capable infrastructures through communication technologies (e.g. wireless). In the proposed C2PS, it is assumed that several independent systems connect together to perform a common goal, where network connections are omnipresent. There prevails a direct one-to-one connection between every twin cyber-physical thing (see Figure 14). Every physical thing and its cyber thing manages a *DataStore*. Every physical or cyber thing is identified by a unique ID (i.e. IPv6, Universal Product Code (UPC), etc.) and is aware of its virtual twin (Alam and El Saddik, 2017).

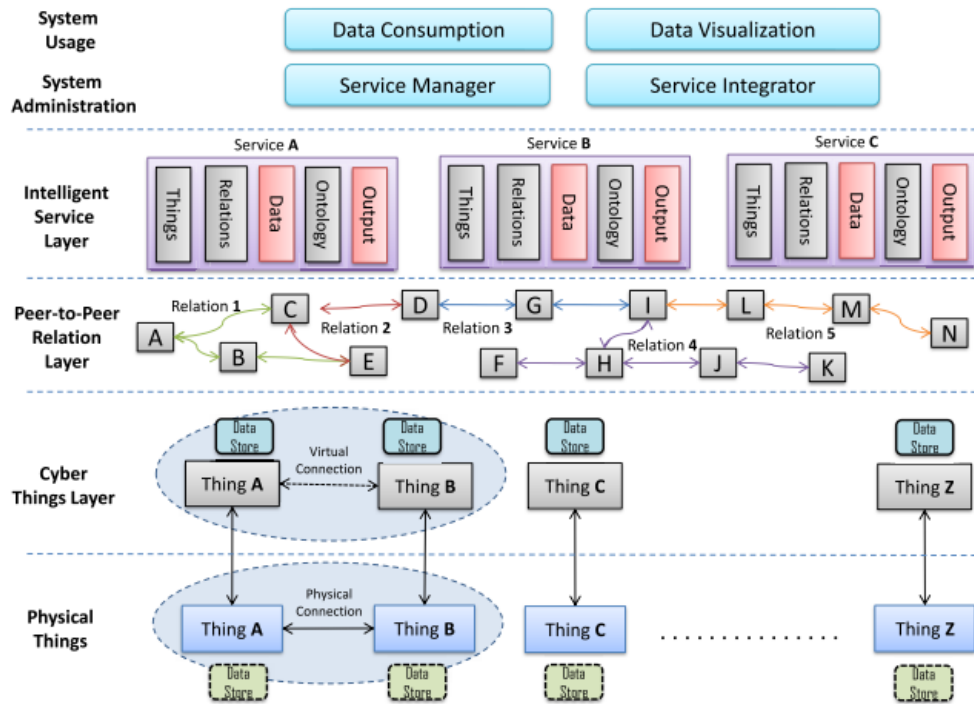


Figure 14: Cloud-based cyber-physical system architecture (Alam and El Saddik, 2017).

Sensor owners have the authority to control sensor privacy by granting access to it through the service middleware layer (Figure 14). Based on networking or communication criteria set by the owner communication groups can be created identified by a *Relation ID*. All the communications in a particular relationship are only transferred to the members of that group. The sensory data from the physical asset is stored in its own cloud storage and also the data store of the cloud-based cyber layer. Furthermore, the interactions among things can occur either through ad-hoc communication (e.g. Vehicular Ad-hoc Networks (VANET)) in the physical layer or through the cloud layer using peer-to-peer communication. Whenever an interaction is received through the cyber later, it is updated to the responsible physical layer and vice-versa.

The *Intelligent Service Layer* acts as the middleware where cyber things, their active relations, and the related ontologies are coupled together. Since network communication is assumed to be omnipresent, hence a hybrid case of sensor-services fusion is also possible in the C2PS architecture. The data center cloud of the C2PS can provide summary related data mining services. Different combinations of services cloud are formed in the C2PS based on the interactions of subsystems (i.e. physical level sensor cloud, cyber level services cloud, and hybrid sensor-services fusion cloud) (Alam and El Saddik, 2017).

Cyber-physical synchronisation in equipment level

The “twinning” between the physical world and a virtual model is a real-time monitoring data synchronisation for the digital copy of a system and can be achieved through (1) building the communication between equipment and system through industrial Ethernet; and (2) conducting a semi-physical simulation of entire Automated Flow-Shop Manufacturing System (AFMS). AFMS is a recent trend in lieu of Industry 4.0 to boost smart manufacturing. AFMS design fundamentally includes finding the optimal number of machines in each manufacturing cell and then devising inventory management strategies, designing the layout, and work process for efficient production. Using a real-time digital copy of AFMS can predict the performance of multiple designs earlier, reduce reliance on expensive and multiple physical testing, optimize for maximum performance, and cut-down design time (Liu *et al.*, 2019).

From the traditional point of view, the design achieves control logic validation with software testing after the mechanical structure design is assembled. However, as depicted in Figure 15, multi-view synchronisation between physical equipment and digital simulation is achieved in a distributed integrating test manner. This multi-view synchronisation is a hybrid technology by incorporating Object linking and embedding for Process Control (OPC) with the database, public protocols, and inside Application Programming Interface (API). By enabling the cyber-physical synchronisation among Manufacturing Execution System (MES), physical equipment, and digital model, it changes the original serial design to a concurrent design. It verifies a Programmable Logic Controller (PLC) of AFMS using a simulation framework consisting of experiments and statistical analysis. Based on the modular encapsulation of the reference model, the input and output interface of each equipment is defined, and then a cyber-physical synchronisation is realized through incorporating multi-view synchronisation technology into PLC. In element, to achieve multi-view synchronisation, the output digital signal and switch variables of simulation should be connected to that of the physical system. With the binding and mapping among I/O point on the simulation model and I/O address on PLC of equipment, it can guarantee the real-time synchronization of DT (Liu *et al.*, 2019).

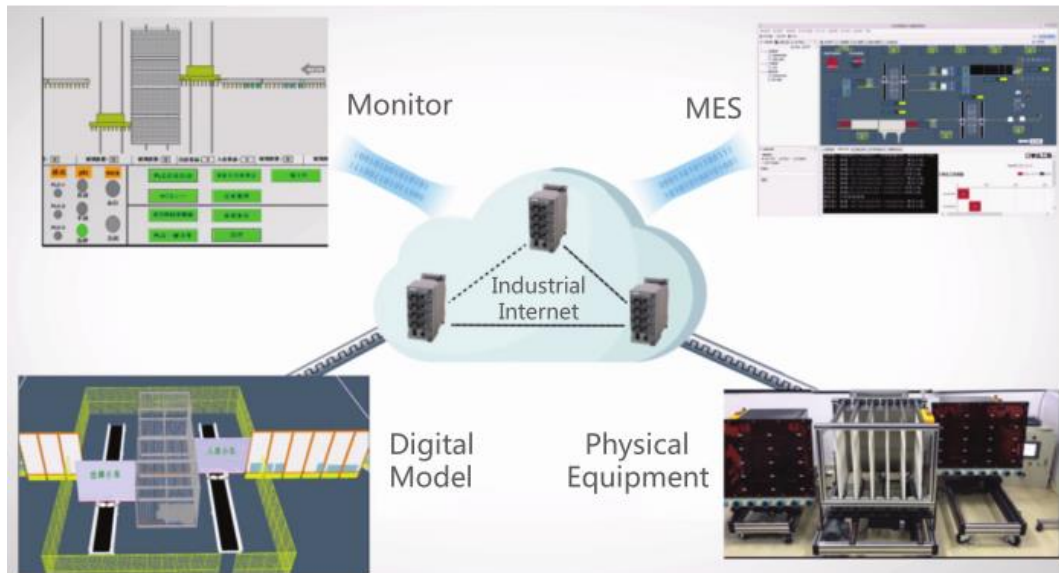


Figure 15: Multi-view real-time synchronisation in equipment-level simulation (Liu et al., 2019).

2.4.2 Challenges to data analytics

It is quite apparent that Digital Twin running in synergy with AI and IoT technology results in shared challenges. Some of the common challenges that can be discovered in both data analytics and the Internet of Things should be identifiable for shared challenges in Digital Twins.

Data analytics challenges

Some of the challenges within the field of machine learning and deep learning are as follows:

- **IT infrastructure:** The first major hurdle is the general IT infrastructure. The rapid growth of AI requires high-performance infrastructure in the shape of hardware and software to execute the algorithms. For instance, the costs of the high-performance graphics processing unit (GPU) to perform machine and deep learning ranges from \$1000 to \$10,000. This challenge can be overcome by using cloud-based data analytics services such as Amazon, Google, and NVIDIA. However, using the cloud for data analytics and Digital Twins still presents challenges in ensuring that cloud analytics gives robust security (Fuller et al., 2020).
- **Privacy and security:** Privacy and security is a very pertinent affair vis-à-vis the computing industry let alone data analytics. Laws and regulations are yet to be legislated fully since the inception of AI. The General Data

Protection Regulation (GDPR) is a recent regulation to ensure privacy and security across the UK and Europe, however, it is just an umbrella regulation for data security as there still remain concerns regarding data handling and development of AI algorithms. The issues pertaining to increased scrutiny, regulation, and measures through legislation is just one step to ensure data is protected while another method is federating learning, a decentralized framework for training models. Hence, this safeguards data in a learning model to stay localized without any data sharing, addressing privacy and security issues when carrying out data analytics within a Digital Twin (Fuller *et al.*, 2020).

- **Trust:** Trust is an additional concern both from the point of view of the user and that of the organization. DT technology needs to be discussed further and explained at the basic level to ensure that the end-user and organization know the benefits of DT. Model validation is a reasonable solution to verify that DT is performing as expected to ensure user trust.

IoT challenges

- **Data, Privacy, Security, and Trust:** The use of IoT increases large volumes of unstructured data. As the data could be sensitive it could of value to the criminal, thereby increasing the threat especially in the context of customer data. Cyber-attacks present challenges with criminals targeting systems and taking them offline, to paralyze an organization's infrastructure. An example of this is the Mirai botnet scandal where nearly 15 million IoT devices worldwide were comprised and used to launch a distributed denial-of-service attack (DDoS). Hence while installing the device, the utmost up-to-date security features are necessary thus preventing a back door entry to infiltrate the IoT environment (Fuller *et al.*, 2020).
- **Connectivity:** Despite the development in IoT use, challenges of connectivity still exist importantly concerning real-time monitoring. Issues with facets like power outages, software errors, or ongoing deployment errors impact connectivity. For example, IoT devices are a single source of feeding data to AI algorithms, this can become an issue if IoT data is missing adversely affecting the running system.

2.5 Case studies

2.5.1 ARUP Tokyo

Reference reason: Enhancing office well-being

Project name: IoT office

Location: Arup Tokyo

Background and motivation

Contemporary advancements in IoT technology have led to the amassment of more detailed and more voluminous data. The Arup Tokyo office, with an area of approximately 700m², has been recently furnished with 12 environmental sensors and 16 human count sensors in order to encompass meeting rooms, private rooms, and open space (see Figure 16).

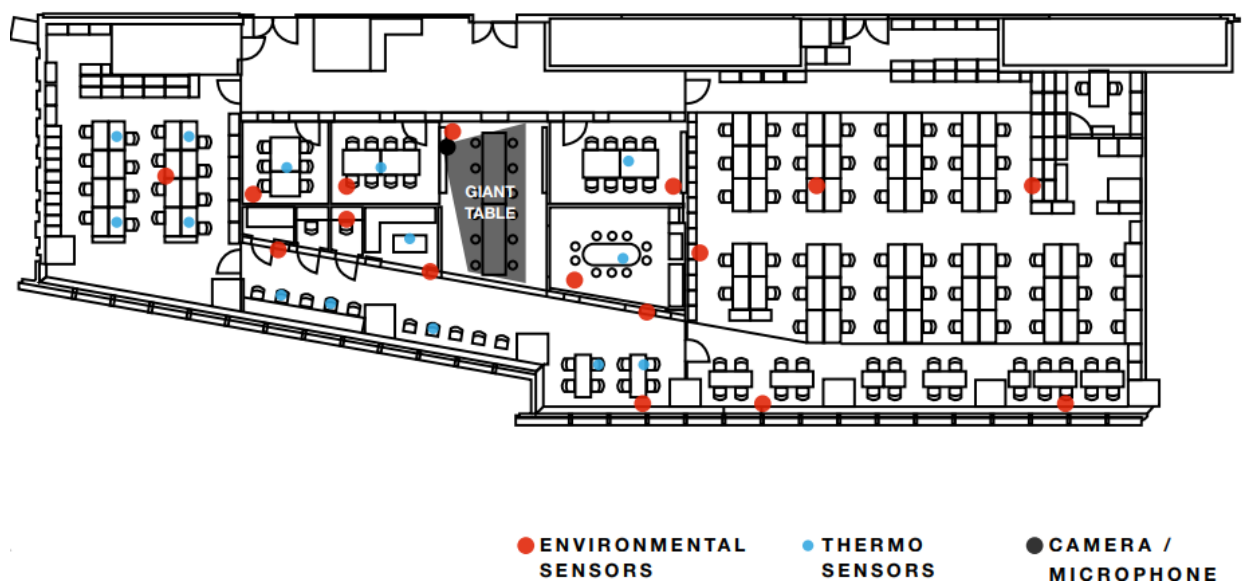


Figure 16: Layout of the Arup office in Tokyo with installed sensors (ARUP, 2019).

Furthermore, an AI camera and emotional analysis device have been installed in an open space used for various gathering events. It is encased in a 3D-printed device termed as the “penguin sensor” (Figure 17). The environmental and penguin sensors take readings every five minutes. In the meantime, another sensor measures people to count every minute. All the sensed data is sent to a single cloud database (InfluxDB) and visualized using a dashboard. This dashboard

is displayed on a monitor equipped at the office entrance (Figure 19 and Figure 20), giving a rapid real-time synopsis of the office status (ARUP, 2019).



Figure 17: Sensors concealed as 'penguins' (ARUP, 2019).

The environmental and penguin sensors take readings every five minutes. In the meantime, another sensor measures people to count every minute. All the sensed data is sent to a single cloud database (InfluxDB) and visualized using a dashboard. This dashboard is displayed on a monitor equipped at the office entrance, giving a rapid real-time synopsis of the office status. The installed commercial environmental sensors measure temperature, humidity, CO₂ concentration, and noise level. Additionally, an infrared camera detects the number of people within the sensing area serving as a movement sensor. The penguin sensor developed in-house includes a Raspberry Pi linked to a camera and microphone. The feed from the camera is used by the onboard neural network to yield a real-time headcount. Concurrently, voice is recorded in the vicinity to be analyzed with a commercial cloud provider, and eventually classified into sections of speech based on their emotional characteristics. Also, about 50% of staff do not have assigned work stations, instead, they can work at a "free-address system" with a large sharing table (see Figure 18). With the solid data of 'user-experience' from IoT sensors under the free-address system, it can be used for the sustainable design of the future office.



Figure 18: Free-address area in the ARUP Tokyo office.

Mining value from data

The data measured demonstrated that temperature and degree of usage between various areas of the office varied widely. In order to depict the current state of the office environment in real-time, the processed data was broadcasted on a monitor fitted at the entrance of the office (Figure 19). This open display enabled staff to more easily identify problems such as malfunctioning air conditioning.



Figure 19: Monitor showing processed data at the entrance Arup Tokyo office (ARUP, 2019).

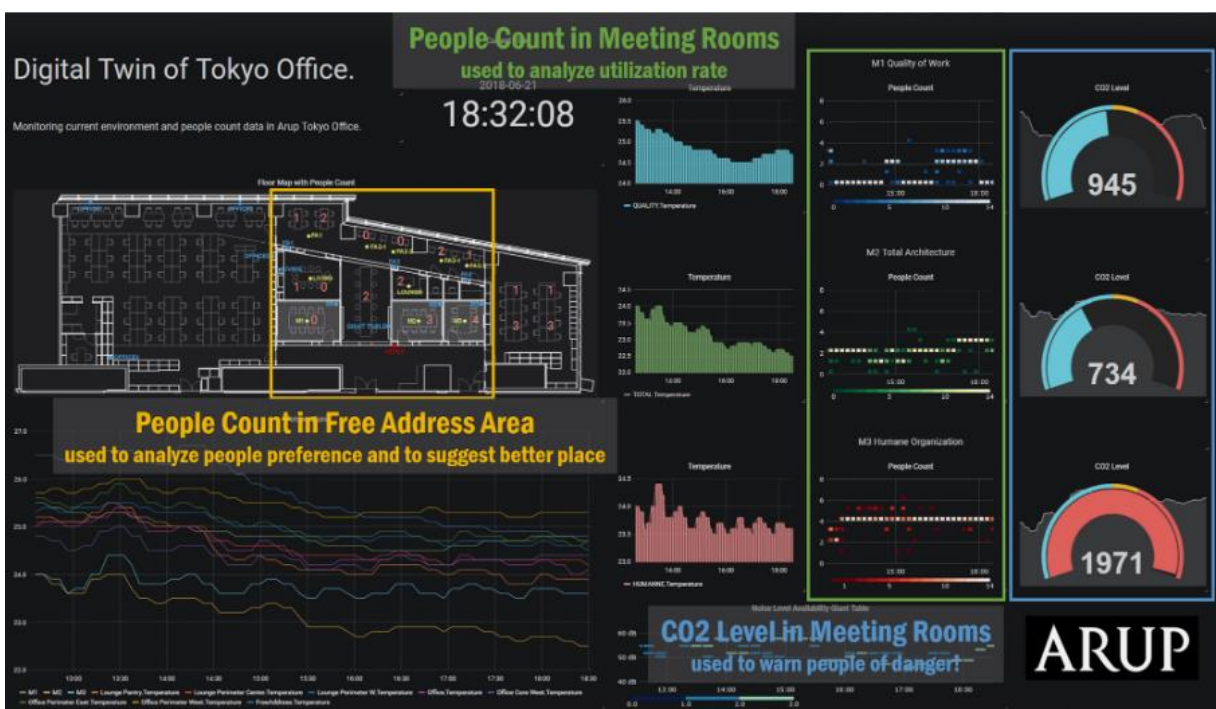


Figure 20: Digital Twin illustrating real-time performance data, CO2 level, and people count (ARUP, 2019).

With the advent of Artificial Intelligence (AI) it plays a key role in the utilization of office data. The measurements of temperature, humidity, CO₂ concentration, and human count in the meeting rooms were taken for further correlation between them (Figure 21).

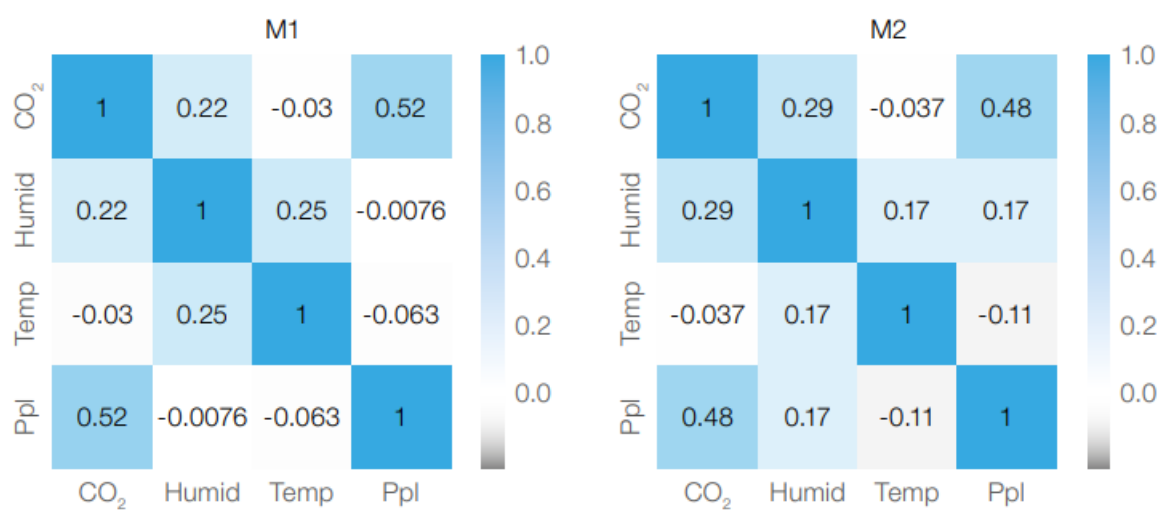


Figure 21: Correlation between measured variables in the conference room (ARUP, 2019).

AI also contemplates that the CO₂ data is highly corresponding to the number of people for each day of the week. At the onset of the week, there is an upward trend in the office hours with two spikes in the afternoon (observed on Monday

and Tuesday). However, the shape of the upward trend changes (see Figure 22) with each day of the week. Nearer to the weekend, CO₂ concentration can be further related to both employees, those who leave the office immediately after working hours, and the rest who work overtime, or stay late to socialize (ARUP, 2019).

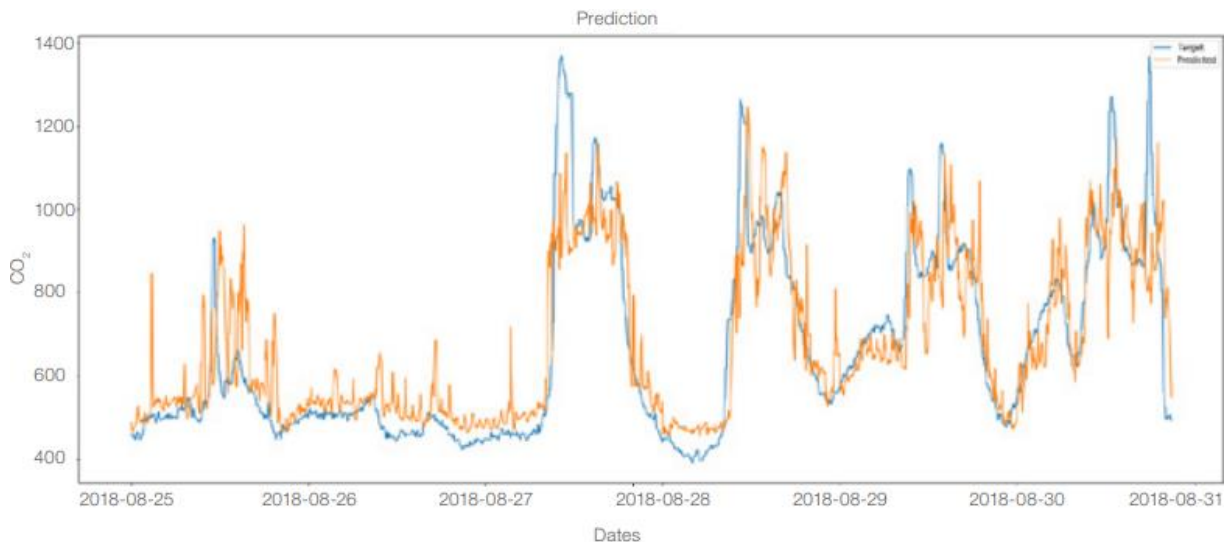


Figure 22: Target vs. measured CO₂ concentrations in the conference room (ARUP, 2019).

Several measurements have been also conducted apart from those focusing on the office environment. As an exemplification, AI is introduced to classify human emotion based on voice data, and subsequently, analyze the results from different events. Lecture-type events showed little emotional change. Whilst, under other conditions such as party-type events, it is observed that positive emotions occur initially followed by a gradual rise in anger. With likely anger not being the elemental source of emotional changes, but rather more passionate communication tones as the night unfolds (ARUP, 2019).

Next steps

The Tokyo office continues to conduct various trials:

- a) Use of pupilometer to gauge employee concentration level to especially during creative meetings and talks.
- b) Stress level from heart rate fluctuations

The process of measuring data through sensors is of vital importance intending to create a workplace environment where staff can work creatively and happily.

2.5.2 NTU Singapore

Reference reason: Reduction in energy consumption

Project name: Creating the Greenest Campus in the World

Location: NTU Singapore

Contributors: IES

Inspiration: Nanyang Technological University (NTU), Singapore, has the vision to be the greenest campus in the world. The university has around 40,000 students and staff and the campus consists of 200 buildings spread over 250 hectares. It undertook a collaborative project with IES to examine how Digital Twin technology could help achieve its goals of reducing energy, water, and waste footprints by 35% for 2020. IES's ICL technology was used to plan, operate, and manage the campus facilities to reduce energy consumption.

Approach: The project was delivered in two phases, using IES's innovative ICL technology to provide high-level visualization and analysis of testbed energy reduction technologies on-site, before probing into detailed simulation and modeling of 21 campus buildings.

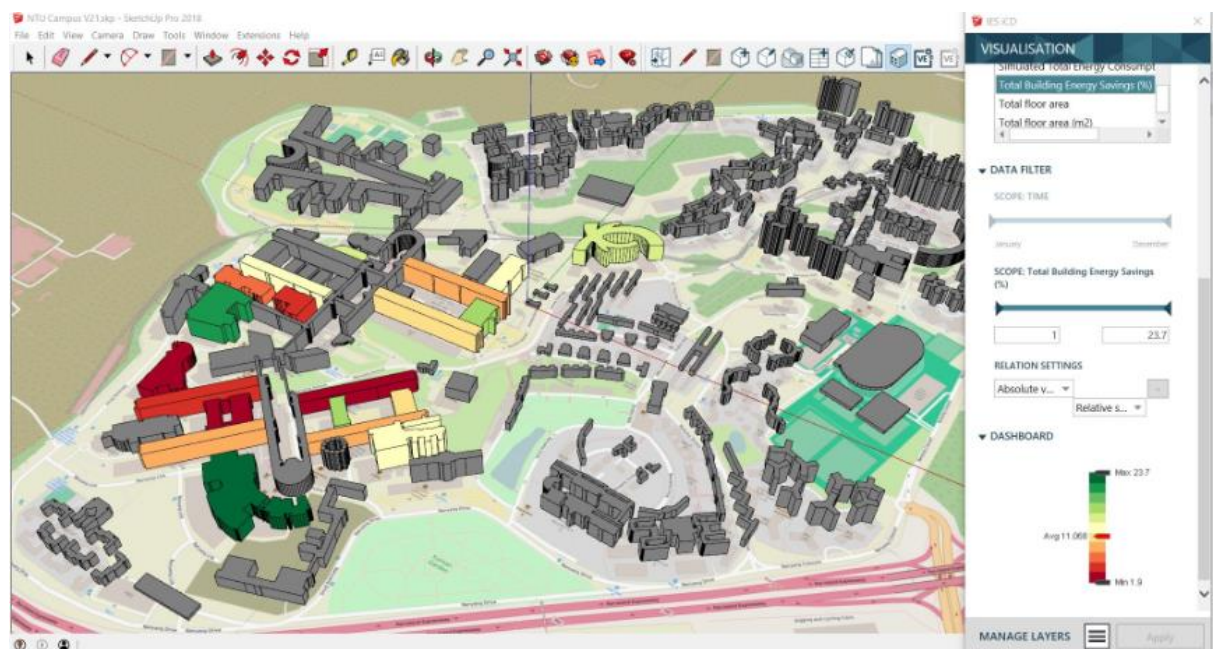


Figure 23: Master-planning for NTU Singapore (Woods and Freas, 2019).

In Phase 1, an overall masterplan was created using an iCD tool to provide an overview of energy consumption across the campus buildings array. The model

was conclusive up to 91% for total energy consumption and 97% for chiller energy consumption. Furthermore, an equivalent online cloud-based Community Information Model (iCIM) for communication and engagement with campus and students were also created and thus connected to the master planning model (see Figure 23) for automatic updates (Woods and Freas, 2019).

Subsequently, the master-planning model was used as a platform to simulate and analyze testbed technologies varying from the thermal performance of the building envelope to lighting sensors, chiller optimization, and smart plugs that turn equipment off out of hours. Noteworthy results obtained after phase 1 are shown in Figure 24.



Figure 24: Results after phase 1 testbed (Woods and Freas, 2019).

Phase 2 then stressed on 21 buildings on the campus for a more articulated investigation using the IES Ci² (Collect, Investigate, Compare and Invest) to establish further savings

- **Collect:** The initial collection of data covered an array of sources including utility bills, automated meter readings, building management systems data, and operational information.
- **Investigate:** Using the ICL iSCAN tool, the collected data constituted of time-series data were integrated and analyzed to discover additional energy savings. This brought to scrutiny issues including low and high CO₂ levels, unstable off-coil temperatures, lower than expected return air temperatures, faulty energy consumption meters, and staff offices and meeting room temperature setting issues (shown in Figure 25).

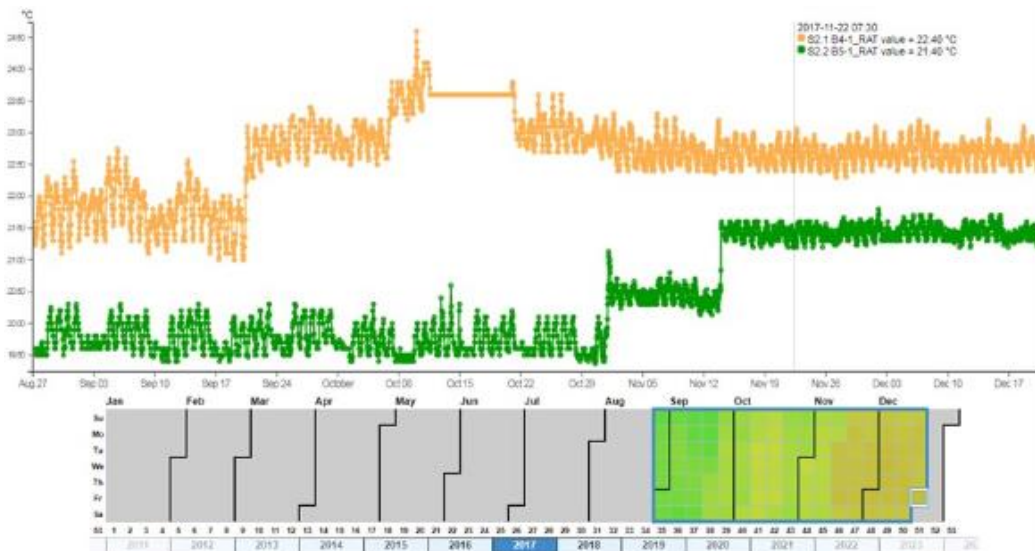


Figure 25: Measured temperature and CO₂ levels (Woods and Freas, 2019).

- Compare: In the next step virtual models (Figure 26) were created for each building in IESVE and calibrate using detailed operational data. These models established a baseline for existing building operations that could be used to regulate savings for a range of prospective technologies in the 'Invest' stage.

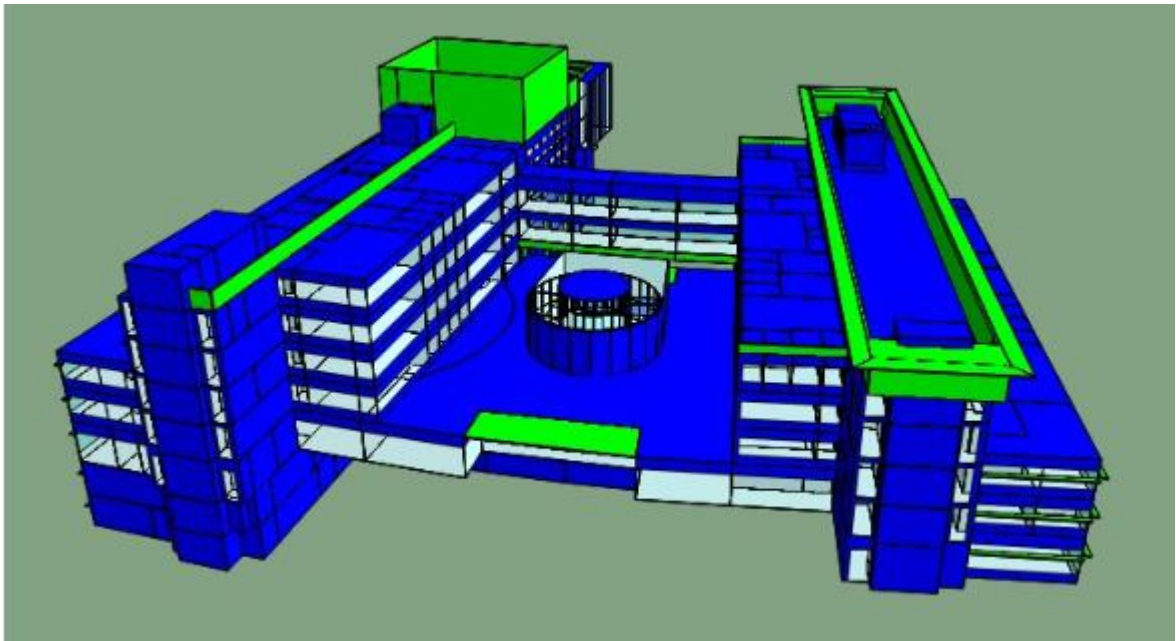


Figure 26: Virtual model of one of the 21 buildings at NTU campus (Woods and Freas, 2019).

- Invest: Five new technologies were simulated using the calibrated models to determine the savings with the likelihood of being installed in the

buildings: high resistance envelope for walls and roofs, high resistance envelope for windows, lighting with occupancy sensors, plug load management, and high performance optimised chillers.

The calibration identified savings in substantial amounts (Figure 27) in terms of energy, money, and carbon footprint. Consequently, the results were uploaded onto the campus masterplan to enrich the management data and to provide a visualisation of the options existing in the campus information model.



Figure 27: Results from phase 2 of testbed (Woods and Freas, 2019).

This can certainly be classified as a good example for a Digital Twin to improve the decision-making of a project to improve the efficiency of campus cooling systems. The aim of the campus management was to determine whether the decentralised cooling systems in each building would be more efficient and cost-effective than a centralized, multi-building system. The campus information model or the DT of the campus enabled the management to assess alternate scenarios based on expected building performance across the campus portfolio. Working out the time series data to show the performance of the different systems throughout the day manifested that a centralized system proved a considerable decrease in carbon emissions all through the operational life cycle (Woods and Freas, 2019).

It is also necessary to understand the current developments taking place in the research, design, and construction sectors related to this research work. Therefore, the above-mentioned two cases study helps in understanding the procedures followed in the implementation of the Digital Twins technology on buildings and the benefits we can reap from it economically as well as ergonomically.

3 Framework for Digital Twin

The main objective of this research work is to define the modeling framework for the Digital Twin. Wherein we have been provided with selected parts of the building NUR 31 at TU Dresden's (see Figure 28) campus based on the repository compiled for the "Digital Design and Operation" laboratory of the Institute of Construction Informatics. Which comprises of an IES-model, a Revit BIM-model, and a Unity3D VR-model. Moreover, a database with data from sensors and actuators assimilated from the building automation system is made available.



Figure 28: NUR 31 building at TU Dresden's campus (Dresden, 2020). (PC: March Mosch)

3.1 Data from sensors

A select number of rooms of the Institute for Construction Informatics were equipped with sensors in order to measure temperature and air quality. Subsequently, based on the measurement automatic control of the window and heating should be attained. Figure 29 shows a layout plan of the Institute of Construction Informatics which is situated on the 2nd floor of the NUR31 building.

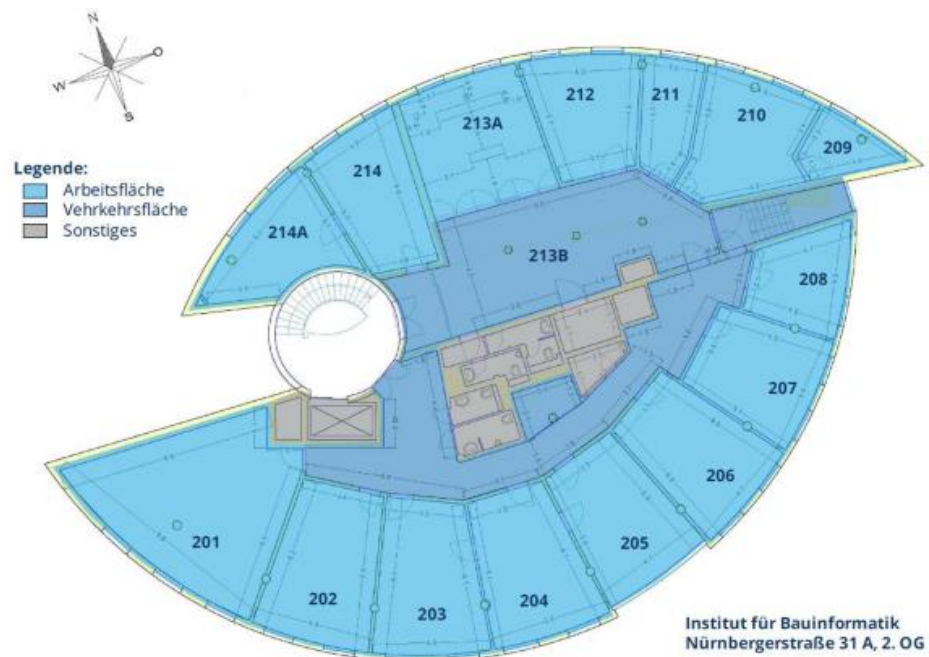


Abbildung 1 Geschossplan

Figure 29: Floor plan for the Institute of Construction Informatics.

Table 4: Functionality of rooms and influences.

Room no. (room function)	Influences
201 (Library, meeting room)	<ul style="list-style-type: none"> Heat production by beamer Stay of up to 15 persons
202 (Laboratory simulation and data analysis)	<ul style="list-style-type: none"> Heat production by PCs Stay of up to 8 persons
204 (Archive, video conference)	<ul style="list-style-type: none"> Heat generation by PCs Low degree of utilization
210 (Digital building and operation laboratory)	<ul style="list-style-type: none"> Heat production by equipment Stay of up to 5 persons Special requirement: test area
213a (VR Cave)	<ul style="list-style-type: none"> Heat production by VR technology Stay of up to 10 persons Windows and heating difficult to access

The sensors were installed in the institute mainly in the four multi-personnel rooms and the possible influences are mentioned in Table 4. Sensors of

HomeMatic and Thermokon were mainly chosen due to their attributes, such as availability of various sensors on each tag, coin-cell power source, and low costs. In addition, a Raspberry Pi was used as the sensor network gateway. Furthermore, a HomeMatic central component was incorporated for local and convenient control of the intelligent home which in turn also provides numerous and individual configurations and control options via the proven WebUI. For the offline part, which was used for the development of this thesis, the data recordings were stored in .db (database) files on the gateways local memory from which .csv files can be obtained through the SQLite tool. The main purpose was to collect temperature, relative humidity, and CO₂ concentration in rooms and flow temperature of radiators measurement data of the environment. Thereby, the measurements which can be used for automatic control of radiators, lighting, and windows. Table 5 and Table 6 document the available sensors and actuators respectively, out of which some components have not still been installed.

Table 5: Component list for sensors.














Components	Photo	Quantity
Sensors		
HomeMatic Room Sensor		1
HomeMatic wireless door/window contact		2
HomeMatic Weather station		1
ThermoKon multisensor for motion detection and brightness detection	 	7
ThermoKon CO ₂ and temperature sensor	 	3
ThermoKon Temperature Sensor		8
Synetica (current meter) Electrical energy meters (3-phase or one phase)		2

Table 6: Component list for actuators.

Components	Photo	Quantity
Actuators		
HomeMatic wireless radiator thermostat		10
HomeMatic IP Switching Measuring Actuator for marker switch (light)		3
HomeMatic IP Wall push button for marker switch 2-fold (window-drive)		3
HomeMatic wireless window operator WinMatic		3

The above-mentioned sensors and actuators were installed in phases at the institute. The data gathered by the sensors in the home automation system were analysed for three months which is from May 2020 to July 2020. However, the data from the first half of May was not available so the actual dates used for analysis are from 14/05/2020 to 31/07/2020.

Table 7: Installed BAS at the NUR31 building.

Room No.	Functionality	Sensors installed (tag) {quantity}	Sensor tags
201	Library, meeting room	<ul style="list-style-type: none"> Thermokon Temperature Sensor (sr) {1} HomeMatic thermostat {2} Thermokon motion and brightness sensor (mds) {2} Thermokon CO2 and temperature sensor (sr-04) {1} 	<ul style="list-style-type: none"> tf_1 tf_9 mds_1 sr04_1
202	Lab for simulation and data analysis	<ul style="list-style-type: none"> (tf) {1} (mds) {1} (sr04) {1} 	<ul style="list-style-type: none"> tf_7 mds_3 sr04_2

204	Archive, video conference	<ul style="list-style-type: none"> • (tf) {1} • (mds) {1} • (sr04) [1] 	<ul style="list-style-type: none"> • tf_6 • mds_4 • sr04_4
210	Digital building and operations lab	<ul style="list-style-type: none"> • (tf) {4} • (mds) {3} • (sr04) {2} 	<ul style="list-style-type: none"> • tf_2 • tf_3 • tf_4 • tf_5 • mds_5 • mds_6 • mds_7 • sr04_3 • sr04_5
213a	VR cave (to be installed)	<ul style="list-style-type: none"> • (mds) {2} 	<ul style="list-style-type: none"> • mds_2 • mds_8

3.1.1 Wireless room sensor SR04

The wireless room sensor SR04 measures CO₂, temperature, and relative humidity in rooms of residential and commercial buildings. It harvests power from a solar cell with optional battery backup. The measuring temperature range is 0 to 51 °C, the measurable humidity ranges from 0 to 100% rH non-condensing, and measurable CO₂ ranges from 0 to 5000 ppm. Figure 30 shows the actual sensors placed in the room for taking room environment measurements.

In total there are five of these room sensors equipped at the Institute of Construction Informatics. Figure 31 visualizes the temperature levels recorded inside the rooms from May to June. It is observable that the sensor (sr04_2) located in room 202 shows higher recorded room temperature in comparison to rooms 201 and 210. Whereas the sudden drop seen in sr04_3 is because of missing data sets between the 15th May and 5th June. Figure 32 expresses the relative humidity which ranged from around 20% to around 50% mostly with peaks of 56% and 77.5% attained by the sensors sr04_2 and sr04_3 respectively. The discrepancy in the graph of sensor sr04_3 is due to missing data.

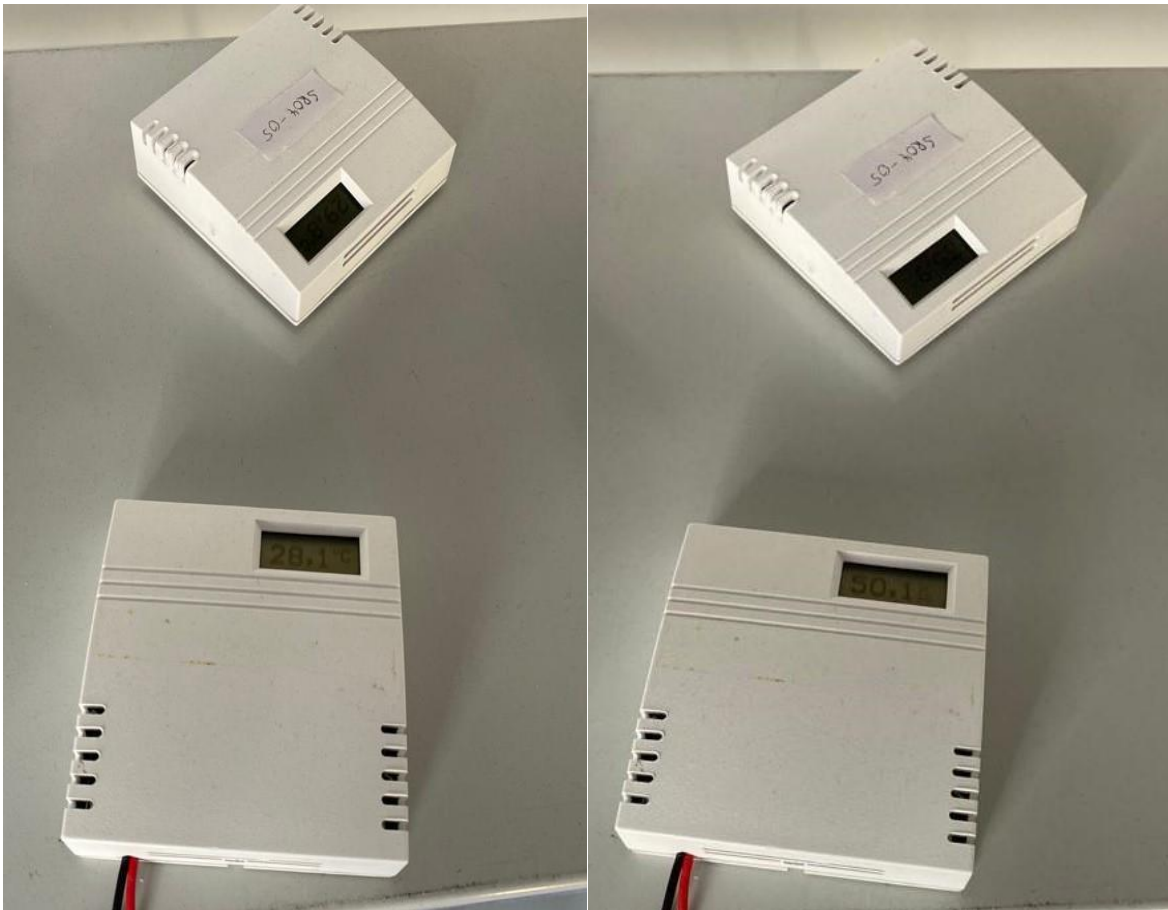


Figure 30: The sr04 room sensor in room 210 showing temperature (left) and relative humidity (right) recordings.

Figure 33 shows the measured CO₂ concentration levels in ppm in all the rooms, where the minimal CO₂ concentration is 400 ppm. The maximum CO₂ concentration recorded is by the sr04_1 sensor placed in the library (room 201), which can be attributed to the online teaching activity in which case the projector is used. The average CO₂ concentrations recorded by the sr04_1 (library) and sr04_2 (simulation lab/student help) sensors from May to July are 555 ppm and 790 ppm respectively. The student help room (202) is more frequently used especially by students and thus has more occupancy in comparison to the library (201) which is less frequently used in the comparison, hence the difference in CO₂ concentrations. Also, more data shows that room 202 was more used up until 15th June 2020, and also for the sr04_1 sensor (digital lab/room 210) CO₂ data is missing till 5th June in the database, resulting in a gap in the graph. Therefore, the measured values of CO₂ concentration are an evident indicator of room quality for the respective rooms at the Institute of Construction Informatics.

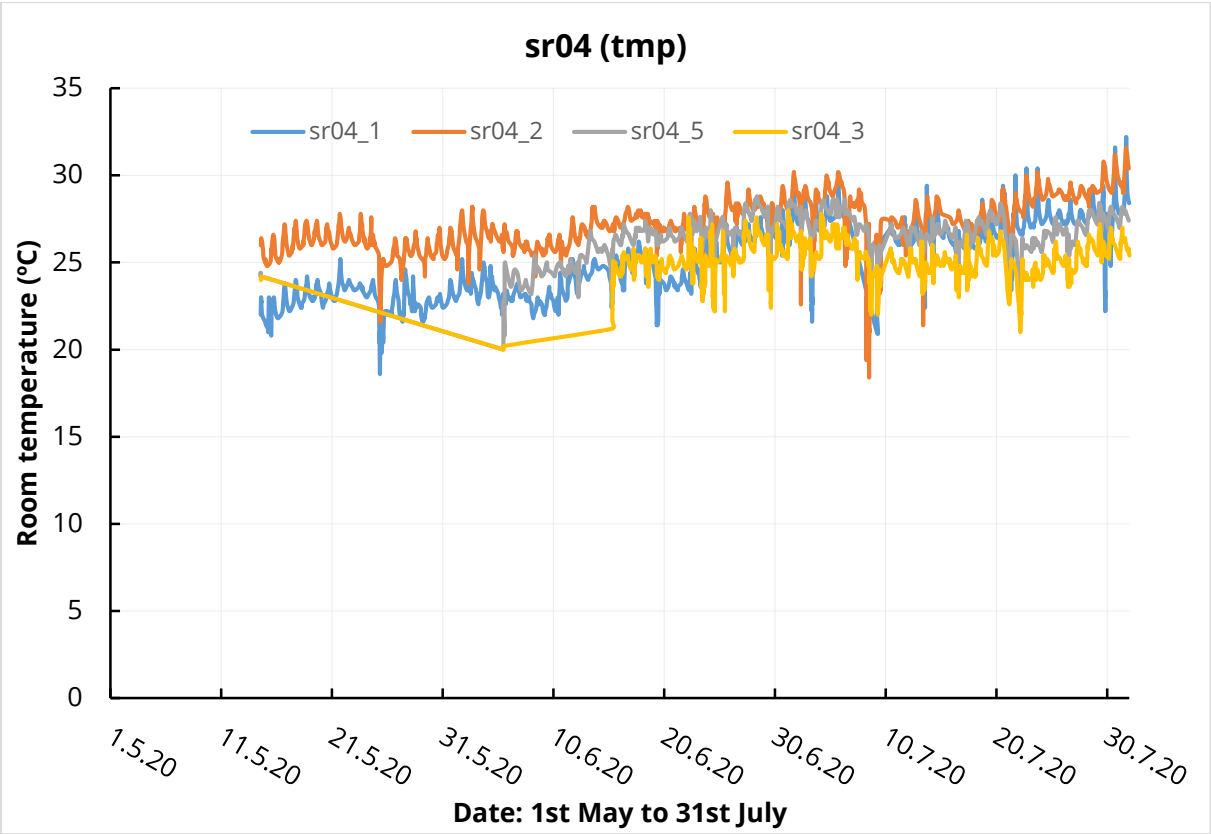


Figure 31: Temperature levels measured on the wireless room sensor from May to July.

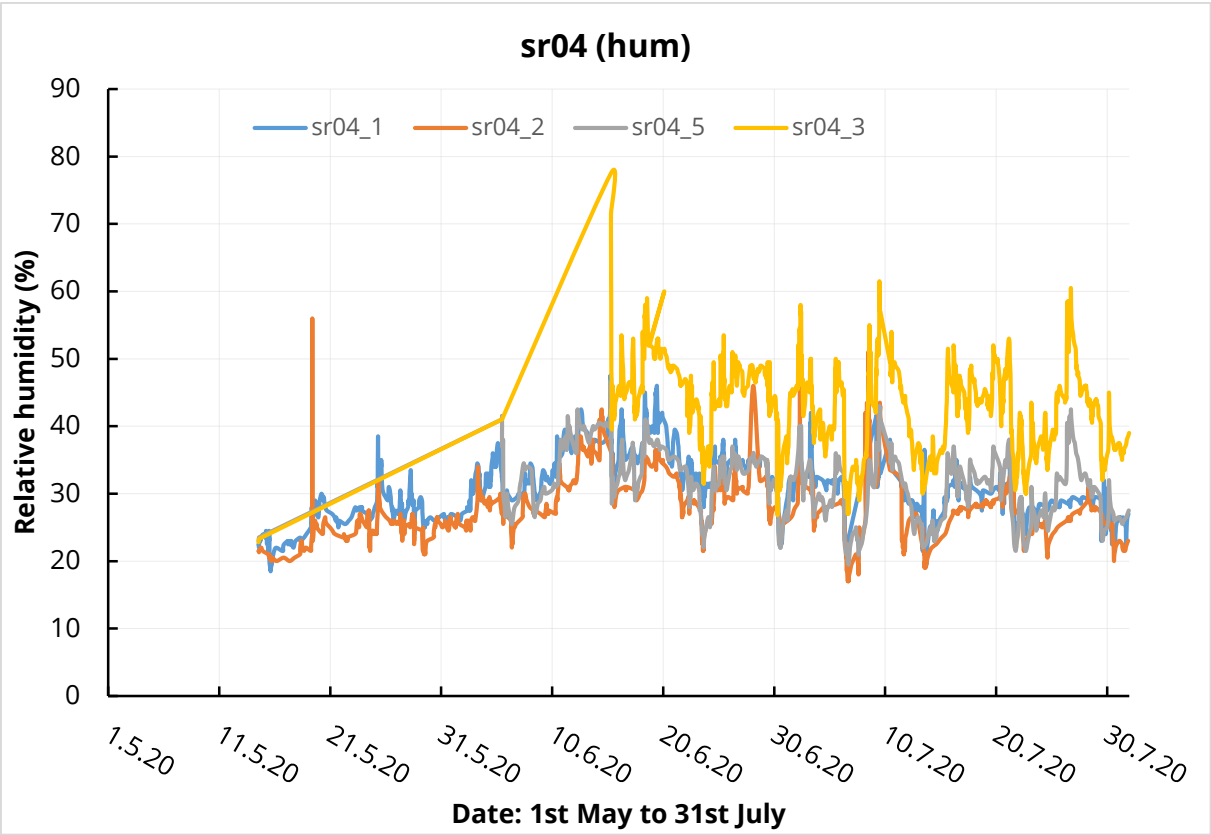


Figure 32: Relative humidity levels measured on the wireless room sensor from May to July.

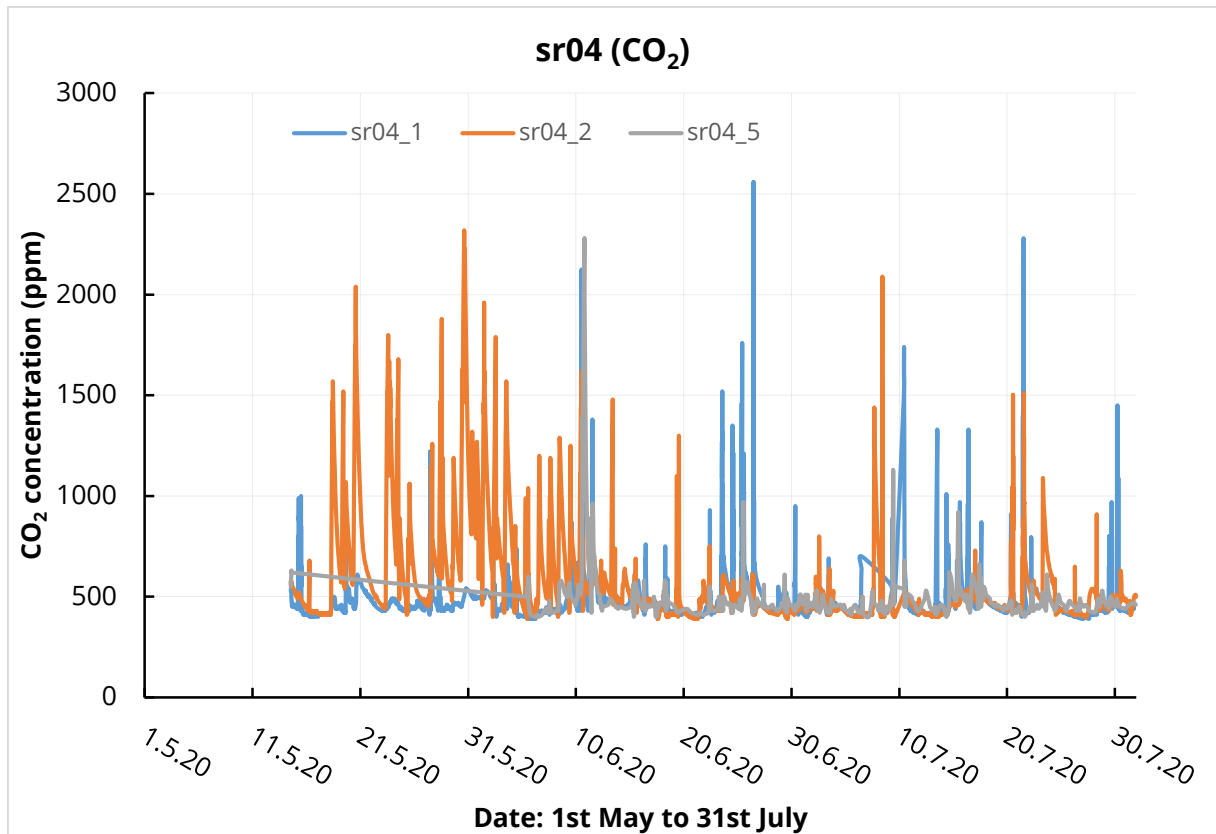


Figure 33: CO₂ levels measured on the wireless room sensor from May to July.

3.1.2 Brightness and motion sensor MDS

There are also brightness and motion sensors included in the BAS installed at the institute. The Thermokon SR-MDS Solar sensor is an energy-harvesting wireless multi-sensor to measure light levels and detect motion. The SR-MDS Solar can be integrated into compatible receiving actuators and gateways and has occupancy detection of 360°. The measuring light range (luminosity) in Lux can be increased up to 1020 Lux by configuring through airConfig. These sensors are supposed to be installed on the ceiling, however in this study there kept on tables as shown in Figure 34 and Figure 35 for room 210, which has three of these sensors at a different location in the room, thus covering the entire spectrum of luminosity measurement in the room. For the brightness measurement data acquired by these sensors in the rest of the multi-personnel rooms refer to Appendix A.1. As can be witnessed in Figure 36 that the mds_5 sensor receives more brightness in comparison to mds_6 due to the close proximity to the window which gives

uninterrupted access to daylight, sensor mds_7 also receives the same amount of brightness as mds_5. The inconsistencies in mds_6 are due to missing data.

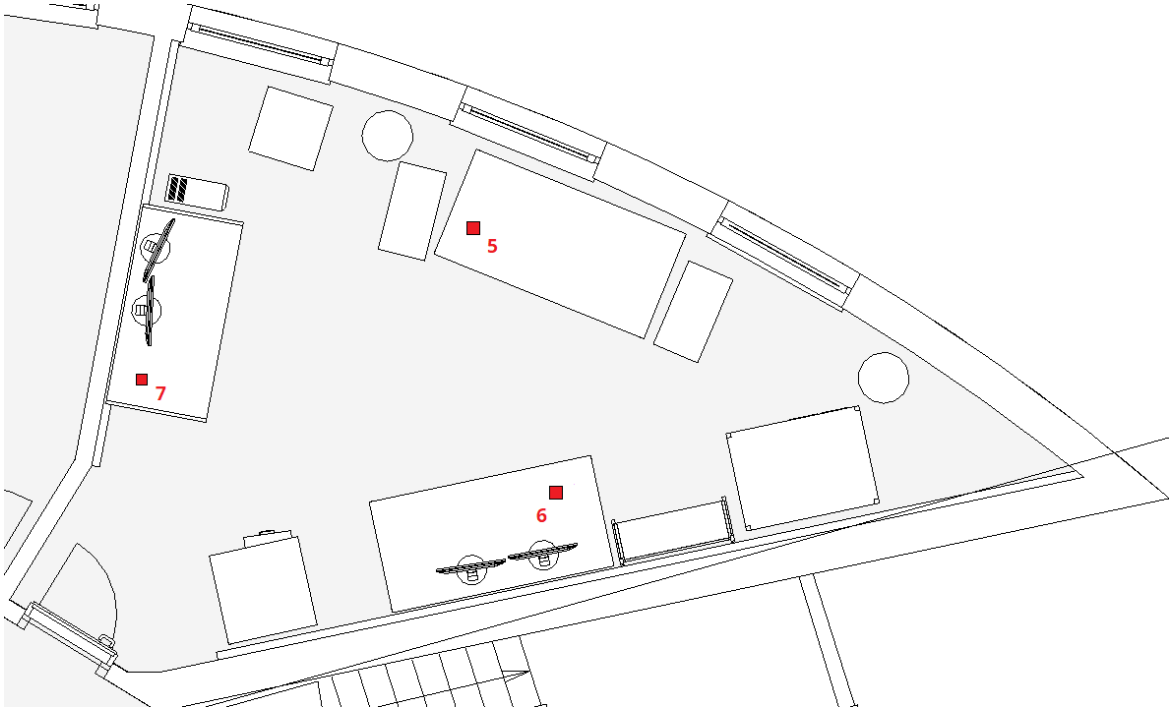


Figure 34: Top-view of placed mds-sensors in room 210 w.r.t windows.



Figure 35: The real position of mds-sensors in room 210 is shown by arrows.

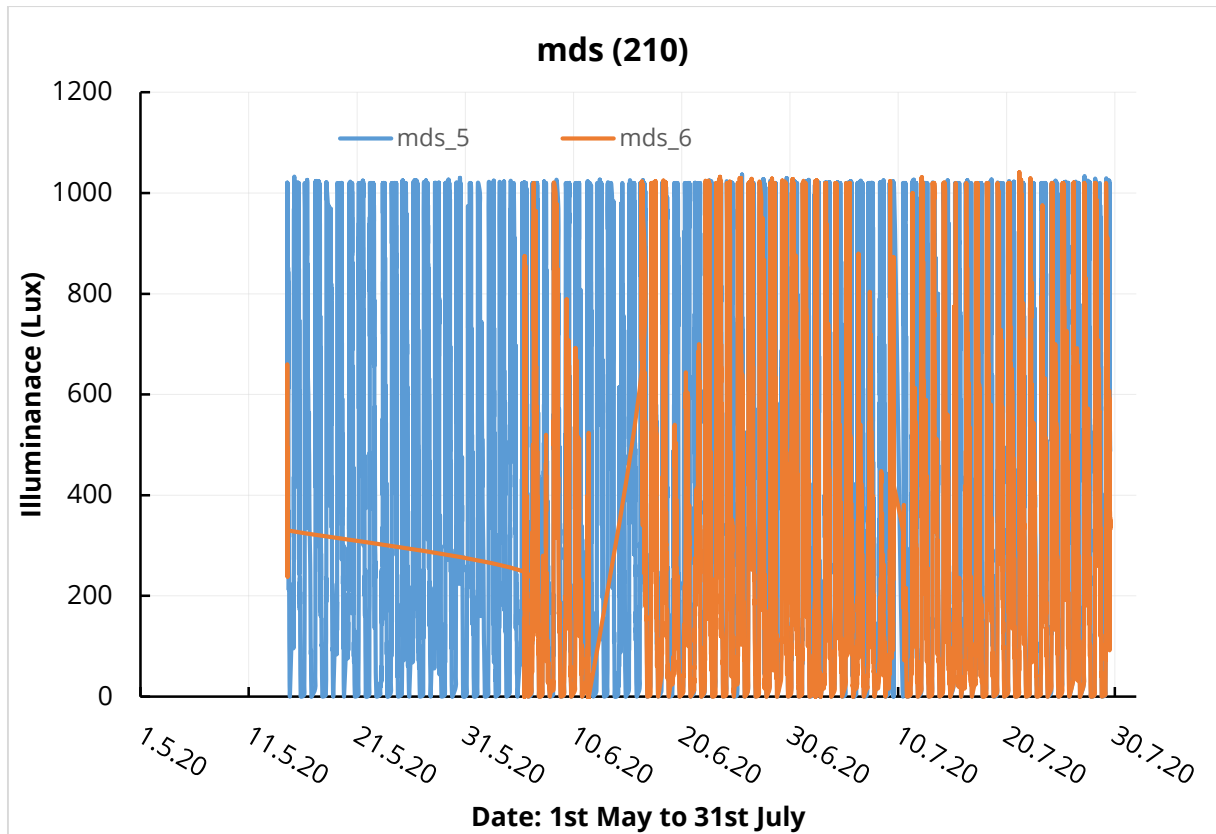


Figure 36: Illuminance (brightness) levels measured by mds_5 and mds_6 in room 210.

3.1.3 Homematic IP Weather Station

The Homematic IP Weather Sensor gives reliable and exact metering of temperature, humidity, wind direction, wind velocity, the onset of rain, rainfall volume, brightness (relative) as well as hours of sunshine. The collected weather data is displayed via the free Homematic IP app. It is easy to install with a durable stainless steel mast and outdoor application is possible due to wireless communication and battery operation. The weather station is located in close proximity to room 214 as captured in Figure 37 and Figure 38 where it gathers the outdoor environmental data. Figure 39 shows that the humidity levels reached a maximum of around 95%. Whereas, (Figure 40) the accumulated rainfall reached around 168 mm by the end of July. In terms of temperature measurements, as can be seen in Figure 41, the temperature level peaked in the month of June with a maximum of around 33 °C, and the average temperature in May was at 15 °C lower than the average temperature in July at 21 °C. Figure 42 displays the wind speeds recorded in km/h during the selected time period with a peak of 33 km/h. This data

can also be probably used to get the actual weather data to calibrate the existing IES model which is also a task to be completed hereafter.

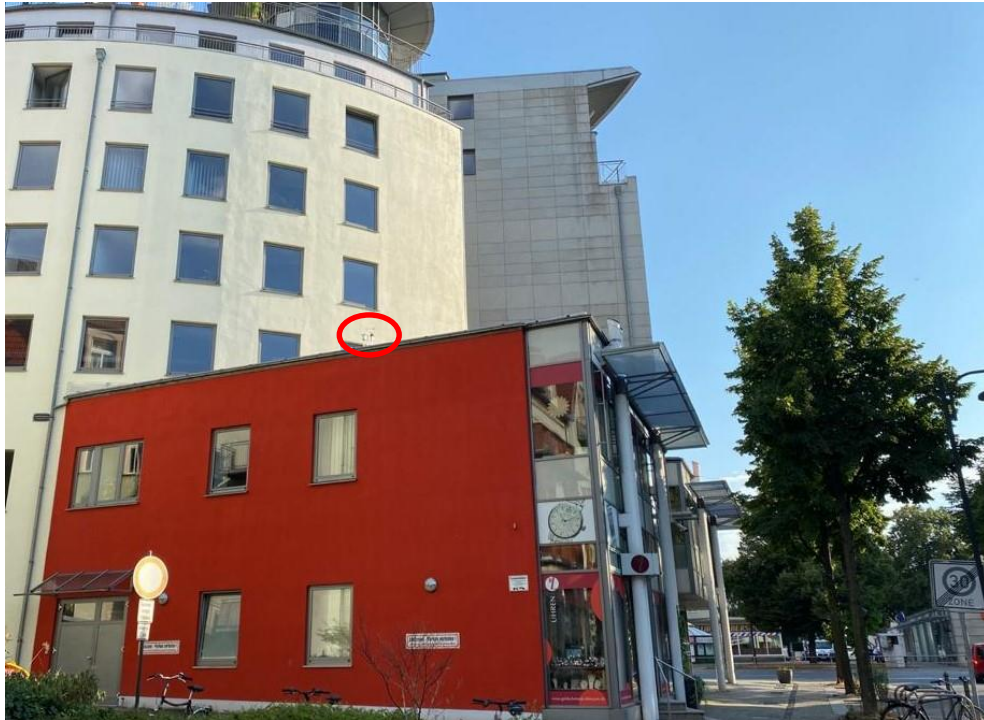


Figure 37: Ground view of the weather station installed outside the Institute of Building Informatics.



Figure 38: Close-up view of the weather station in close proximity to room 214.

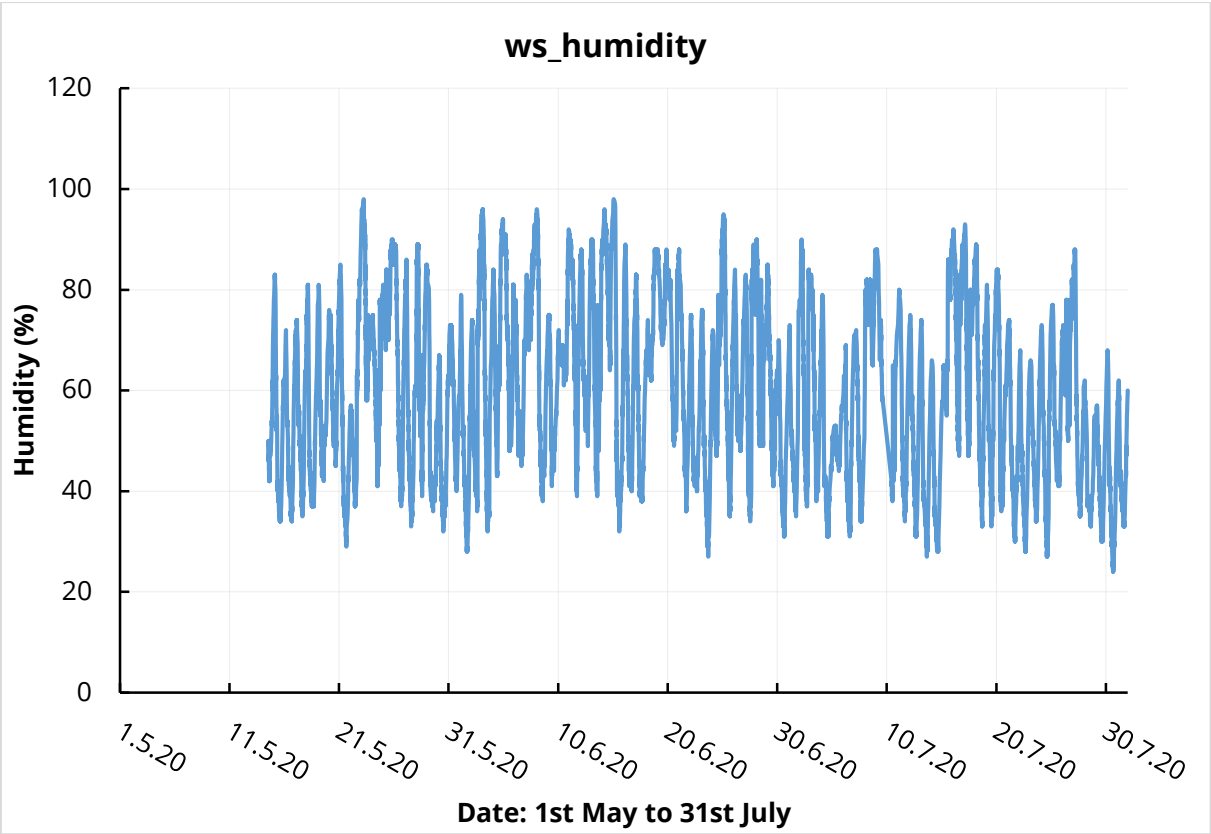


Figure 39: Humidity levels measured on the weather station from May to July.

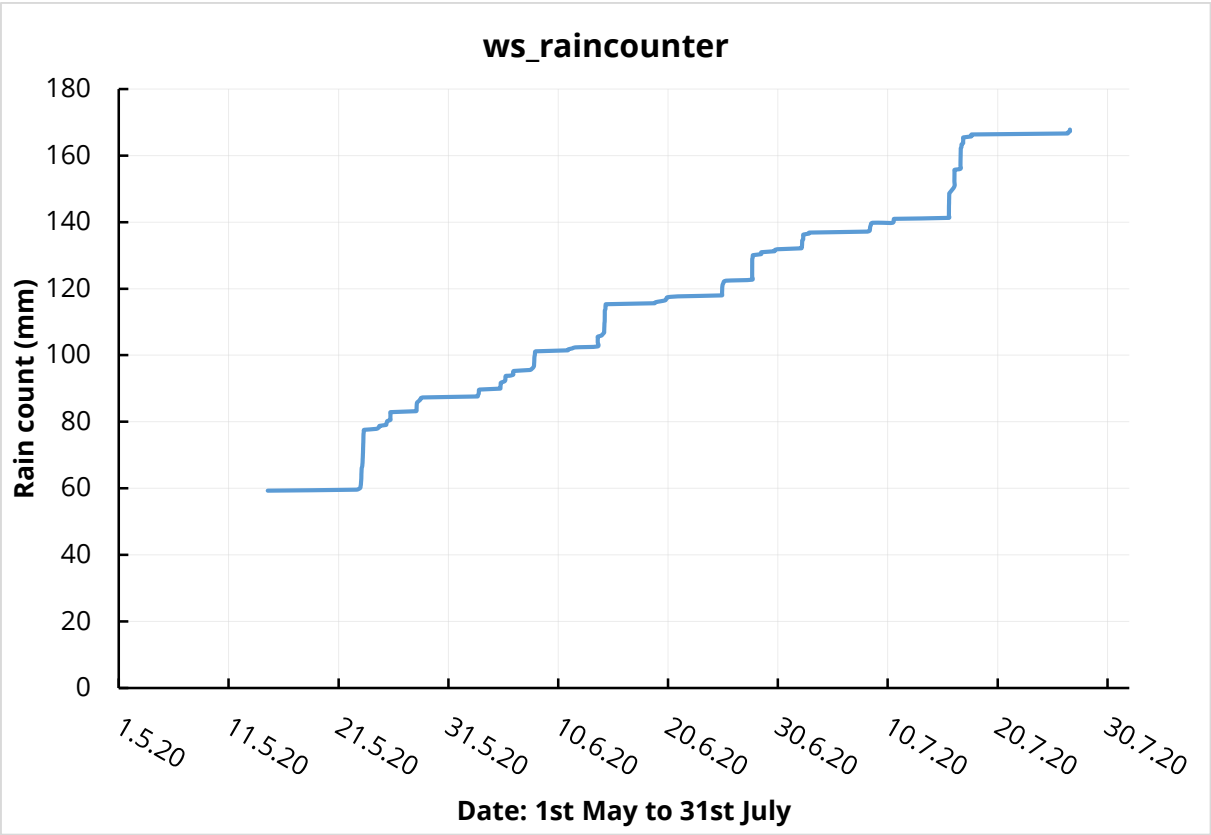


Figure 40: Rainfall levels measured on the weather station from May to July.

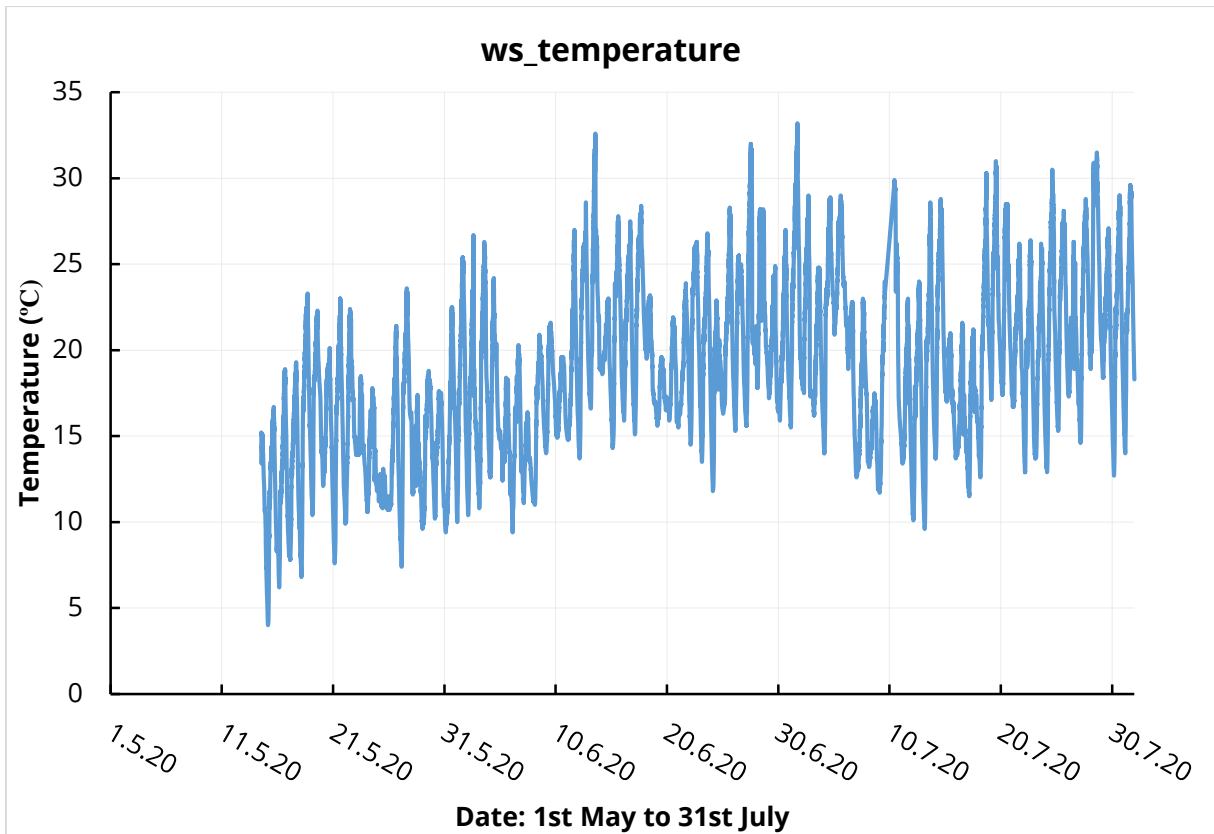


Figure 41: Temperature levels measured on the weather station from May to July.

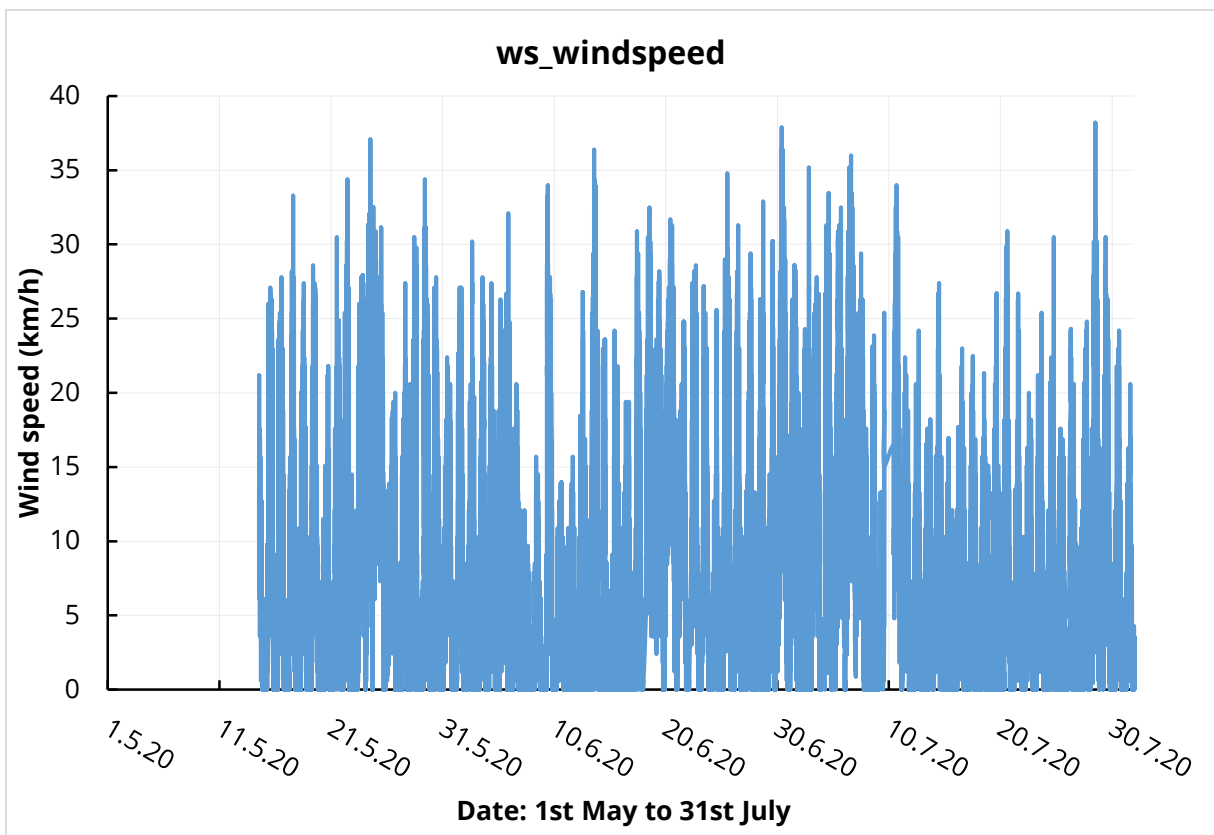


Figure 42: Wind speed measured on the weather station from May to July.

3.2 IES VE model

The IES model provided from the repository “Digital Design and Operation” at the Institute of Construction Informatics is analyzed in this section. IESVE can be defined as a fast, precise, sub-hourly, thermal simulation platform that can model new and existing buildings regardless of size and complexity. The building has a uniform geometry as demonstrated in Figure 43. Since the physical location is to be for assigned Dresden (not available in IES) therefore the weather file is chosen from Berlin although it is 161km away in comparison to Prague which is 111Km away, just to stay inside Germany (refer Appendix A.1). Table 8 below shows the room details of the concerned floor.

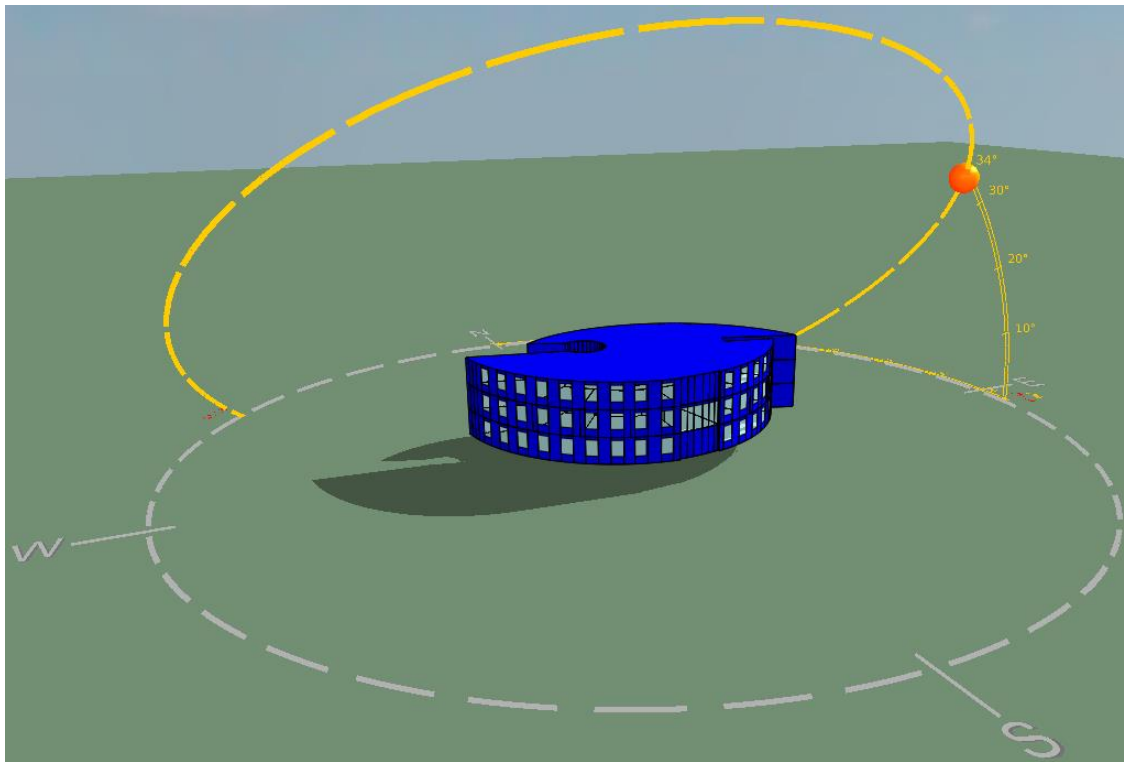


Figure 43: IESVE model for the NUR31 building with sun path on 15th June at 08:00.

Table 8: Room details in the IESVE model.

Room no.	Room term in IESVE	Floor area (m ²)	Volume (m ³)
201	Library	48.30	125.98
202	Student help	26.08	68.01
203	Prathap/ram	24.84	64.78
204	Archive	24.71	64.45
205	Prof. Scherer	23.28	60.72

206	Lin	23.56	61.43
207	Hamdan	20.19	54.64
208	Polter	13.89	36.23
210	Laboratory	28.60	74.60
211	Schubert	10.24	26.70
212	Schüler	19.69	51.38
213	VR Cave	72.13	188.10
214	Professor	39.95	103.92

Energy analysis of the existing IESVE model of the 2nd floor of the NUR31 is done. Herein, we will do the analysis for the model part in ModelIT and the simulation part (SunCast, Radiance, Apache, and CFD). Another noteworthy thing is that the existing IESVE model did not have any HVAC system and artificial lighting incorporated in it, hence all the simulations were run with that consideration.

3.2.1 Solar

SunCast is a tool used to perform shading and solar insulation calculations. Also, it is used to investigate obstruction and shading due to adjacent buildings present, however, in our model, we do not take this aspect into account. Solar Energy and Solar Exposure analysis are carried out for the existing building to understand and analyze where maximum solar radiation is achieved for an efficient design of shading devices to minimize overheating of space and subsequently for the plausible positioning of solar panels. Solar Energy analysis generates hourly solar shading and external incident solar flux data which is then used to produce the energy results in kWh or kWh/m² for the specified period. Solar Exposure analysis generates hourly solar shading data to produce the exposure results in hours and percentage of available hours for the specified period.

As noticed in Figure 45 the north façade and the roof of the building has maximum exposure to solar radiation and thus maximum energy. The exposure varies from 2600 to 4444 hours over the entire year. Hence, providing a prime source of solar energy for the placement of solar panels.

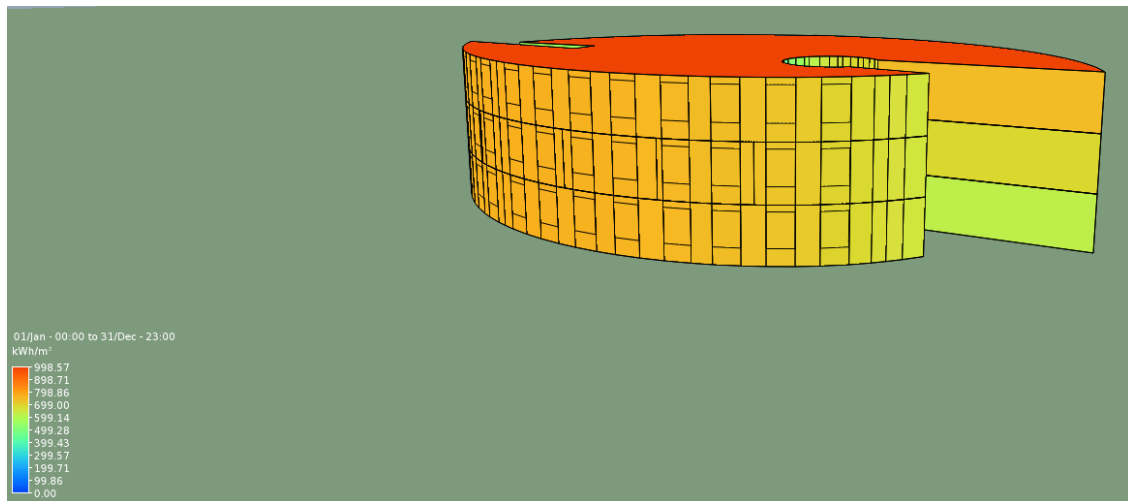


Figure 44: Solar Energy Analysis (North Façade)

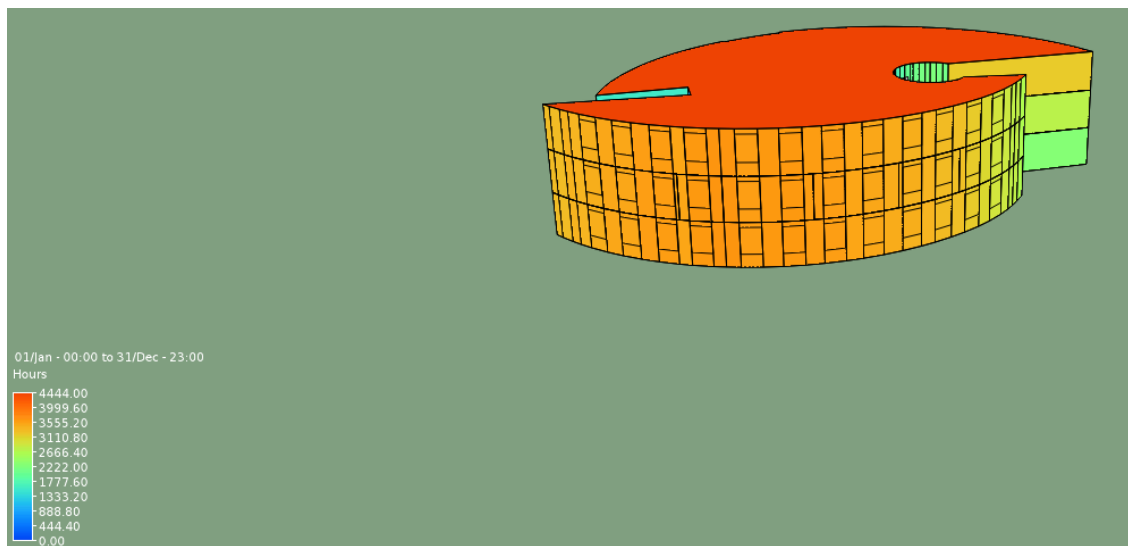


Figure 45: Solar Exposure Analysis (North Façade)

3.2.2 ApacheSim and VistaPro

Apache Simulation is an advanced dynamic thermal simulation tool based on first-principles mathematical modeling of the heat transfer processes occurring within and around the building at sub-hourly time steps for better computation of building components. In this module, several criteria for building energy can be studied, for instance, energy consumption, HVAC loads, room performance indicators such as temperature ventilation, etc.

In this particular study, three different rooms (library, student help, and laboratory) are selected to be analyzed with respect to the following parameters:

- Air temperature: The mean temperature of the air in the room.

- Room CO₂ concentration: The volumetric concentration of carbon dioxide in the room (parts per million).
- Relative humidity: The water vapor pressure of the air is expressed as a percentage of the saturation vapor pressure.
- Solar gain: Solar radiation absorbed on the internal surfaces of the room, plus solar radiation absorbed in glazing and transferred to the room by conduction.
- External conduction gains: Heat conducted into (or if negative, out of) the room through the internal surfaces of the externally exposed elements, including ground floors.
- Internal conduction gains: Heat conducted into (or if negative, out of) the room through the internal surfaces of wall partitions, internal floors/ceilings, and elements with adjacent conditions.
- MacroFlo ext vent: The sum of MacroFlo-calculated air flows entering the room from the external environment.

Figure 46 and Figure 47 symbolize the concerned rooms chosen for Apache Simulation in the plan views, which are highlighted in red colour. The rooms were selected based on the BAS, which is primary installed in the three selected rooms. And in particular, the ThermoKon sensors were installed to collect the data for temperature, CO₂, and relative humidity, hence the above parameters were also chosen.

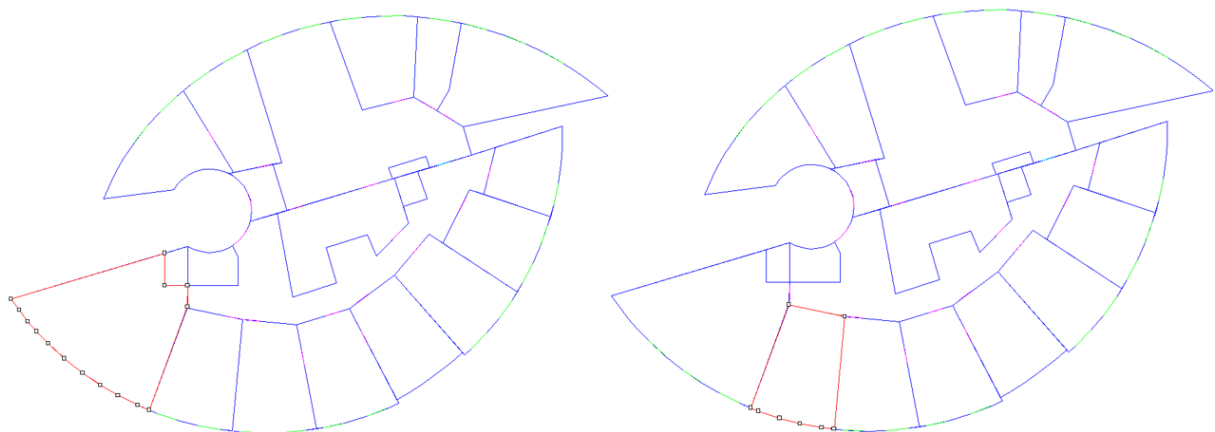


Figure 46: Selected rooms library (left) and student help (right) for analysis.

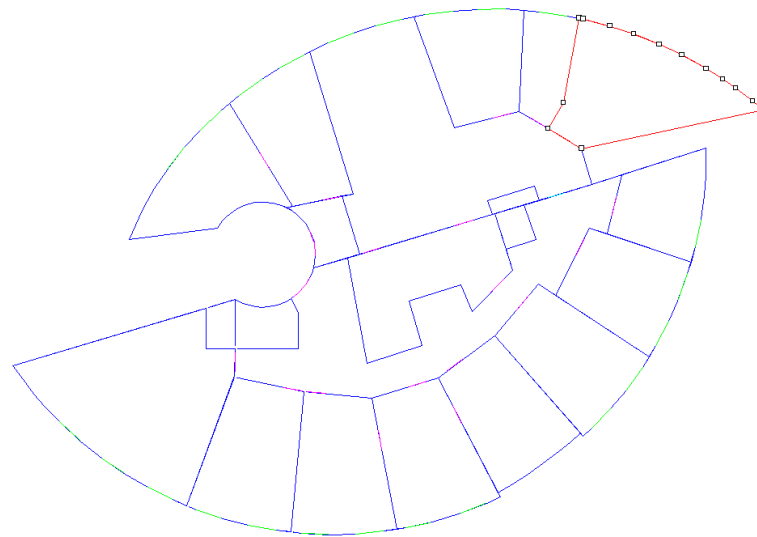


Figure 47: Selected laboratory room for analysis.

As can be ascertained in Figure 48 below, the CO₂ concentration in the room remains the same from January to May and then from mid-October till December in the “library” room. The CO₂ concentration lowers as the air temperature in the room rises above 23.9 °C, the reason for this is that the venting windows are controlled by a threshold temperature (at 23.9 °C) for cooling loads. As seen in Figure 48 the higher CO₂ concentrations always happened on days where outdoor temperatures are lower. The venting windows would only open when the outdoor temperature reaches 23.9 °C, for warmer days the venting would have partially or fully opened so an adequate amount of ventilation would have been achieved, so lowered CO₂ concentrations (i.e. second half of June, July, and August). Due to the temperature difference between indoor and outdoor on warmer days, windows are opened to boost ventilation and subsequently lowering down the CO₂ concentration. Additionally, it is also evident that the CO₂ concentration starts from 400 ppm because the base level for external CO₂ concentration is set as 400 ppm to carry out the simulations (see Appendix B.2). Figure 49 depicts the correlation between the air temperature and the relative humidity for the “library” room, where it is evident that the relative humidity drops in the summer months (June-September) when the room air temperature is above 15 °C due to warmer climate and dryer conditions. Figure 50 demonstrates that the conduction gains correlate to the air temperature, the external conduction gain is lower in the summer months (May to August). Refer to Appendix B.4 for the correlation

between the selected parameters for the other two concerned rooms (laboratory and student help).

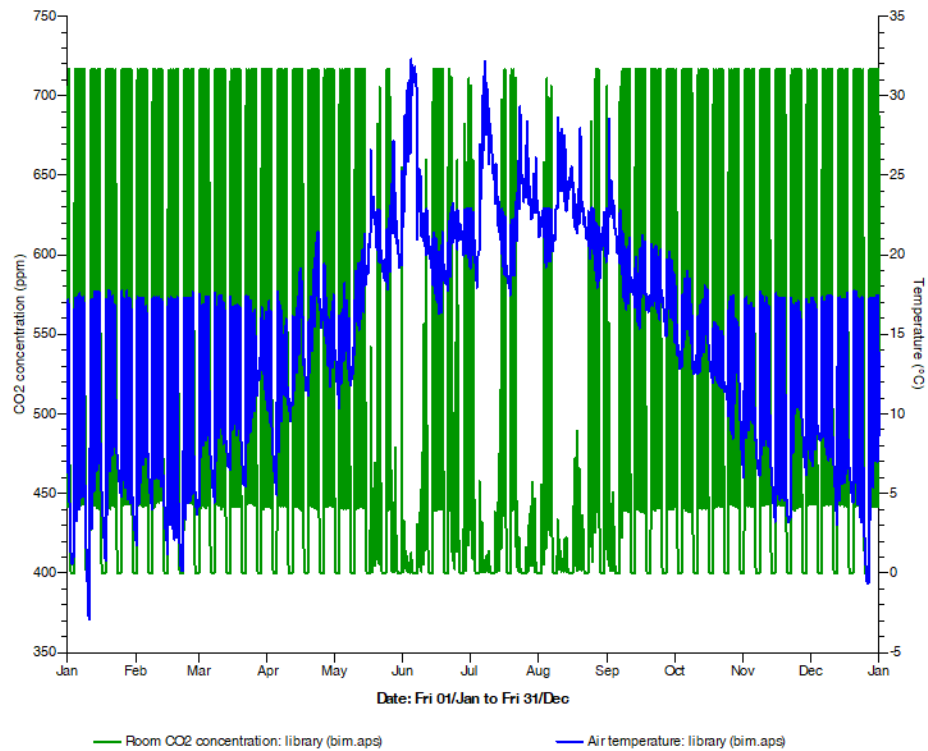


Figure 48: Correlation between air temperature and CO₂ concentration (library).

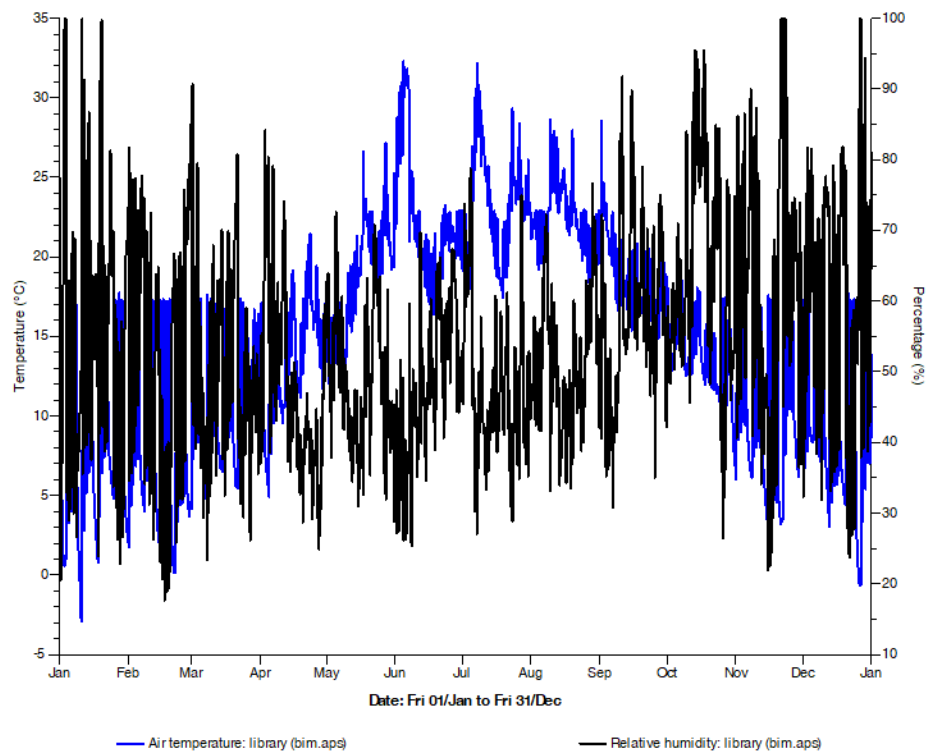


Figure 49: Correlation between air temperature and relative humidity (library).

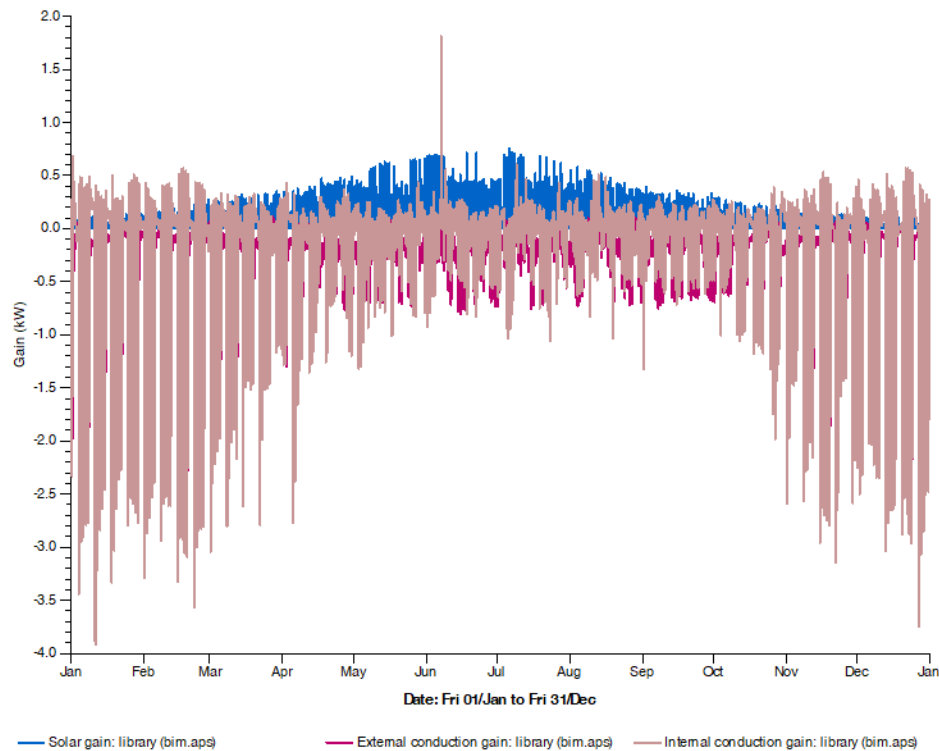


Figure 50: Correlation between solar gain and conduction gain (external and internal) (library).

3.2.3 Daylighting

The RadianceIES simulation tool was used to predict the distribution of visible radiation in illuminated spaces for the concerned rooms. Radiance uses a three-dimensional geometric model of the physical environment, and a default material or map file detailing the spectral radiance value into a “photo-realistic” colour image. It can be used to calculate lighting levels, Daylight Factors, or Glare for daylight and/or artificial lighting.

Annual Sunlight Exposure (ASE) describes the annual potential for visual discomfort in a space. ASE is the percentage of an analysis working plane area that exceeds a specified illuminance level more than a specified number of hours. Hence, ASE is the precursor for the mode of simulation to be done to get the illuminance level. The threshold value in order to run the ASE simulation was set as a target of 750 Lux for 50 hours and the simulation was run for a full period of 365 days. As seen in Figure 51 and Figure 52 the illuminance levels for room 210, were the highest illuminance (3150 Lux) near the window openings due to the direct access of sunlight during the day. Also, since there is no lighting system assigned to this IESVE model, hence artificial lighting component contributes

nothing to the illuminance levels. At least 57 % of the rooms floor area receives light in the range of 500 to 2500 Lux, meeting the minimum requirement of 500-750 Lux required in the laboratory (classroom). Also, room 210 receives the highest amount of daylight in comparison to other rooms (201 and 202) as it is located on the southern façade which receives the highest measure of solar radiation as mentioned previously in the solar analysis section.

The IES simulations can be used to compare the real data measured by mds-sensors (brightness and motion) placed at various locations in the room. In relation to section 3.1.2 where the data collected by the mds brightness sensors in room 210 is presented, it is quite noticeable that the whole room receives daylight illuminance levels in the ambit of 1000 Lux. These observations from the sensors can be correlated to the IES simulations where more than 50% of the room is supposed to receive daylight between 500-2500 Lux (Figure 51). However, in actuality the three widely placed sensors in room 210 covering almost the entire room shows that the majority of the room receives more than sufficient daylight in the range of 750-1000 Lux, thus validating the IES simulation results. The templates and settings used for the Radiance IES simulations in this study are shown in Appendix B.5.1. For daylighting analysis of the rest of the concerned rooms i.e. 201 and 213 refer to Appendix B.5.2.

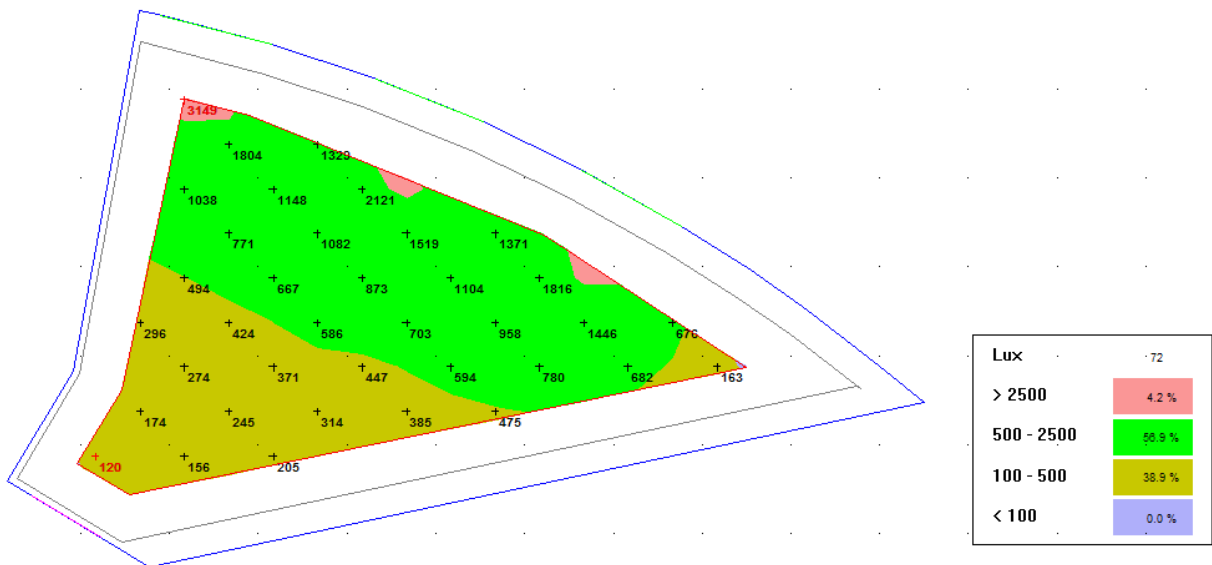


Figure 51: Illuminance in room 210 (laboratory).

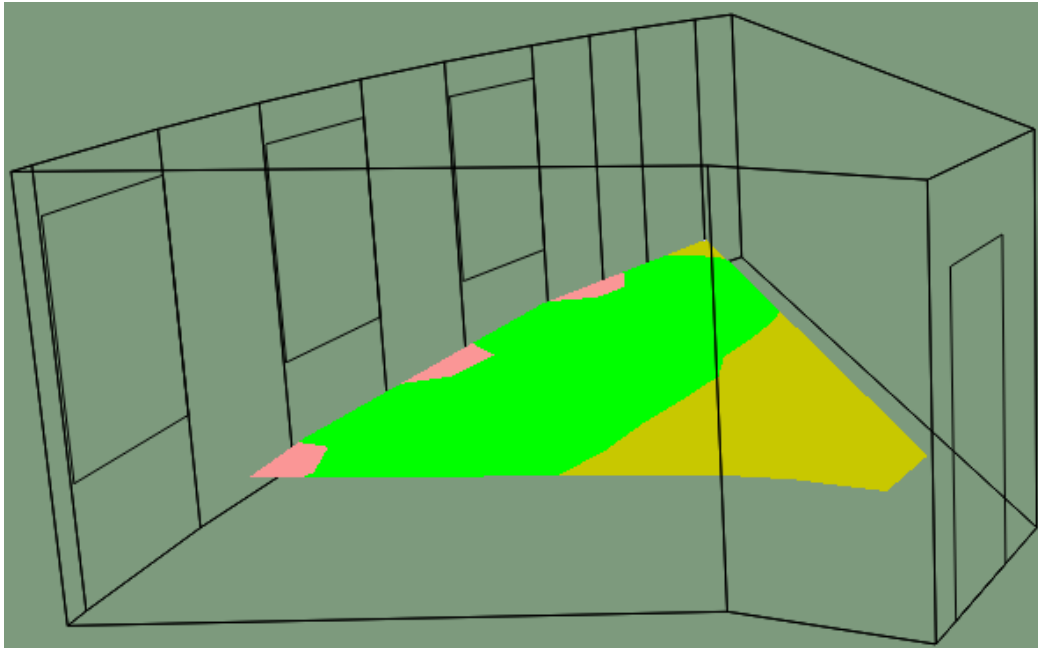


Figure 52: Daylight simulation in the room (laboratory) with respect to the window openings.

3.2.4 MicroFlo (CFD)

A CFD simulation was run for the rooms considered for the analysis. As Computational Fluid Dynamics (CFD) for airflow is calculated for one instance in time it is important for a boundary condition to be defined. This boundary condition was calculated within the VistaPro tool based on the specific criteria, which is that the external ventilation (MacroFlo ext vent) through the selected room should be at its highest value throughout the year (or the particular simulation period selected). This boundary condition is then exported as a file and imported before running the CFD analysis iterations. While the criteria for setting up the simulation starts by selecting the discretization model, which is the Hybrid mode in this case because Hybrid is a combination of both central difference and upward difference, thus the Hybrid schema results in more refined and accurate simulation. Additionally, the turbulence modeling is used to predict the effects of turbulence during the simulation process, where the k-e model was selected which is the most widely accepted turbulence model, calculating turbulent viscosity within each grid cell (IESVE, 2014). For more details and better visual understanding refer to Appendix B.6.

The boundary condition imported was most resourceful in terms of external ventilation for the library room (201) on 03 June at 18:00 and for the student help room (210) was on 03 September at 15:00. Upon looking at Figure 53 and Figure 54, specifying a velocity scale of 0.0 to 0.18 m/s the overall movement of air within the breakout space is at a minimal except for the air near the floor and the ceiling and particularly near the window openings. The overall velocity profile should be read in conjunction with its corresponding temperature profile to determine whether the airflow is acceptable or not. Chartered Institution of Building Services Engineers (CIBSE) guidelines specify that the recommended air velocity within an occupied space should not be greater than 0.3 m/s, so as to not cause discomfort to occupants. Velocities above this recommendation can cause draughts, with the ability to move papers from their place of rest i.e. tables.

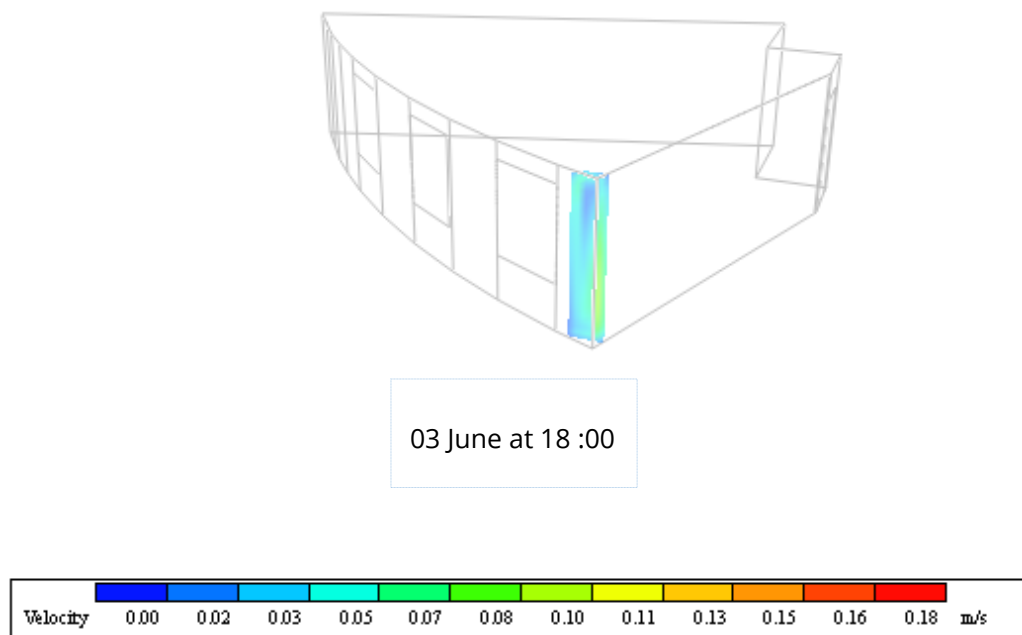


Figure 53: The initiation of the wind velocity slice for CFD analysis across the room.

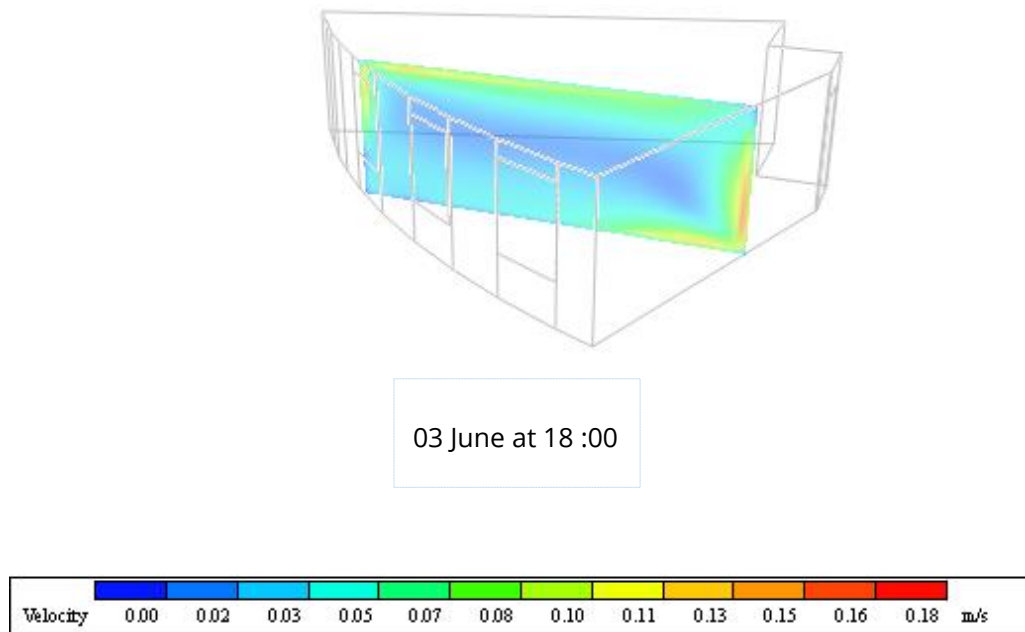


Figure 54: CFD (velocity filled contour) in the library room (201).

The results shown in Figure 56 indicate temperature recordings for the room space at 18:00 on the 3rd of June. It should be noted that temperature readings are that of solar gain and external wind temperature only, as no mechanical heating element was implemented during the analysis. The temperature readings recorded during analysis range between 18°C and 24°C showing a uniform temperature of around 22°C in the majority of the space. The temperature ranges in the CFD between 18°C and 24°C is suitable for human occupancy. However, only above 25°C there might be a requirement for an air condition system, one thing that can possibly be achieved is air-exchange through operable windows without mechanical ventilation. For this, we already have a BAS with operable windows installed at the Institute and thus these can be incorporated to see how the CFD simulations get altered.

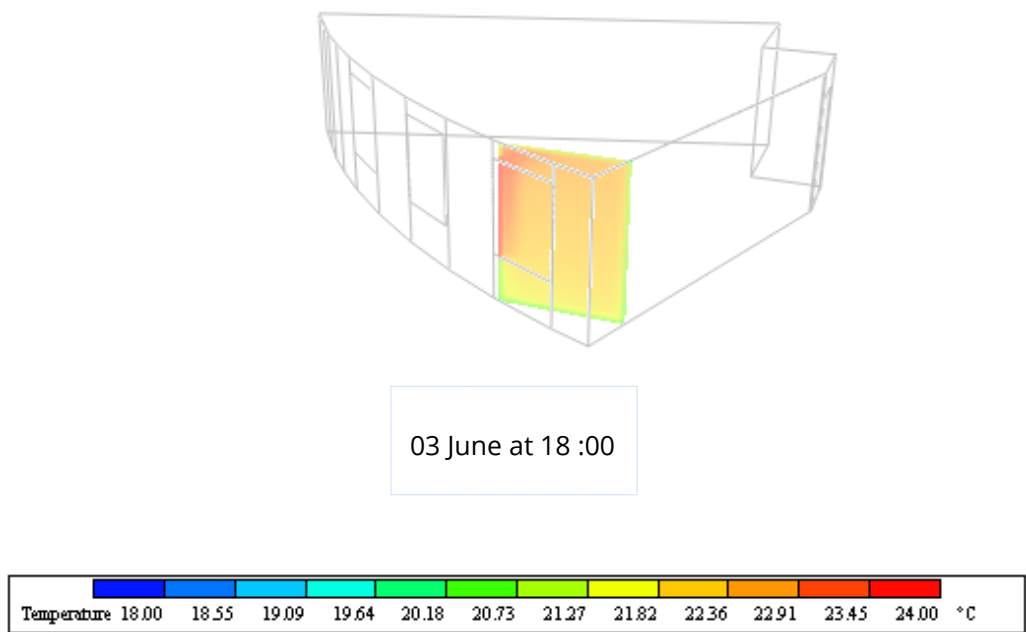


Figure 55: The initiation of the temperature field slice for CFD analysis across the room.

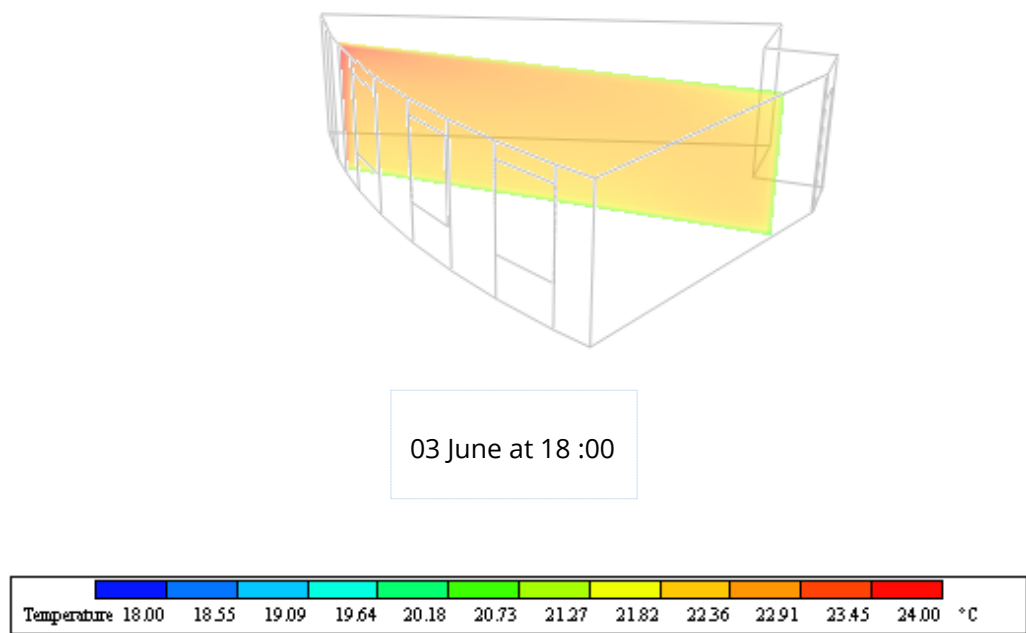


Figure 56: CFD (temperature filled contour) in the library room (201).

3.3 REVIT-BIM model

The structure for the Faculty of Construction Informatics (NUR31) is modeled in Revit. The 2nd floor of the building is modeled in Revit and geometry is assigned to all building elements. Figure 57 shows the floor plan for the Institute of Construction Informatics.

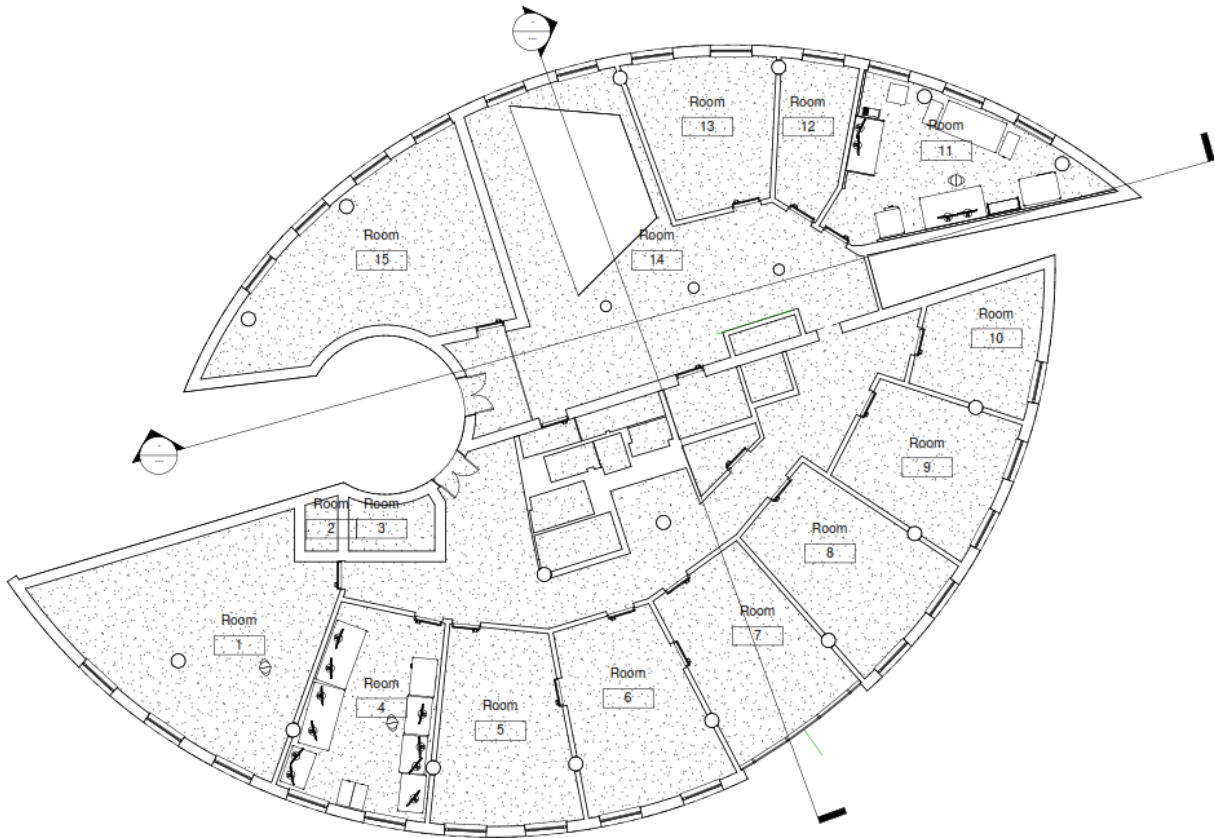


Figure 57: Floor plan at level 2 NUR31 building.

The concerned 2nd floor of the building is divided into separate rooms (refer to Table 9) and every room is designated with different spaces and space types. The model was constructed in Revit by using different Revit families. Suitable and related families are used to construct different building components like walls, roof, floor, etc. Also, all these elements are interconnected in order to restrict air gaps and overlaps. Revit provides a number of default constructions for each building element, however, it allows the user to define its own corresponding style for material, properties, layers, and thickness. Henceforth, these construction details are well summarized in Table 10. One thing to be noted is that in the Revit

model the external wall doesn't have an insulation layer, which is then further adjusted in IESVE (see section 4.2).

Table 9: Room details in the REVIT-BIM model.

Room no. (Revit)	Actual room no.	Area (m ²)
1	201	48
4	202	26
5	203	25
6	204	25
7	205	24
8	206	23
9	207	20
10	208	14
11	210	28
12	211	10
13	212	20
14	213	73
15	214	40

Table 10: Construction details and Thermal Properties of Building Elements in the Revit-BIM model.

Element	Parameters	Value
Exterior Wall Type 1 (KS-Maurwerk)	Thickness	340 mm
	Heat Transfer Coefficient (U)	1.5882 W/m ² .K
	Thermal Resistance (R)	0.6296 m ² .K/W
	Thermal Mass	41.13 kJ/K
	Structural Material	Brick, Sand Lime
Exterior Wall Type 2 (Exterior- Beton)	Thickness	340 mm
	Heat Transfer Coefficient (U)	3.8235 W/m ² .K
	Thermal Resistance (R)	0.2615 m ² .K/W
	Thermal Mass	47.76 kJ/K
	Structural Material	Concrete Masonry Units
Interior Wall Type 1 (Interior- Beton 2)	Thickness	340 mm
	Heat Transfer Coefficient (U)	3.8235 W/m ² .K
	Thermal Resistance (R)	0.2615 m ² .K/W
	Thermal Mass	47.76 kJ/K

	Structural Material	Concrete Masonry Units
Interior Wall Type 2 (Interior- Plaster Board)	Thickness	155 mm
	Heat Transfer Coefficient (U)	3.2903 W/m ² .K
	Thermal Resistance (R)	0.3039 m ² .K/W
	Thermal Mass	15.48 kJ/K
	Structural Material	Plaster
Curtain Wall Interior (Curtain Wall)	Length	3280 mm & 4882 mm
	Area	8 m ² & 12 m ²
Door Type 1 (Institut_Tuer)	Height	2130 mm
	Width	900 mm
	Function	Interior
	Quantity	19
Door Type 2 (Institut_Tuer_Glas)	Height	2130 mm
	Width	900 mm
	Function	Interior
	Quantity	1
Door Type 3 (M_Door- Exterior-Double-Full- Glass-Wood_Clad)	Height	2000 mm
	Width	1200 mm
	Function	Exterior
	Heat Transfer Coefficient (U)	2.9641 W/m ² .K
	Thermal Resistance (R)	0.3374 m ² .K/W
Window (Institutur_Fenster)	Head Height	2585 mm
	Still Height	850 mm
	Width	1330 mm
	Quantity	26
Floor at level 2 (160 mm Concrete with 50 mm Metal Deck)	Area	536 m ²
	Thickness	210 mm
	Heat Transfer Coefficient (U)	4.9810 W/m ² .K
	Thermal Resistance (R)	0.2008 m ² .K/W
	Thermal Mass	29.48 kJ/K
Roof at level 2 (Basic Roof: Generic Roof- 300mm)	Material	Concrete, Cast-in-place
	Area	537 m ²
Roof at level 2 (Basic Roof: Generic Roof- 300mm)	Thickness	230 mm
	Heat Transfer Coefficient (U)	4.5478 W/m ² .K
	Thermal Resistance (R)	0.2199 m ² .K/W
	Thermal Mass	32.39 kJ/K

The Revit-BIM model usually describes the building elements in a very mundane manner for visualization purposes, thus rendering and architectural visualization is a necessary tool for professionals to communicate their project ideas with clients, colleagues, and others. Thus the Lumion 3D rendering software is used to provide an easy and streamlined rendering process of the existing Revit-BIM model so that we obtain a rich, animated, and photorealistic or conceptual view. Figure 58 to Figure 60 epitomises the effect of rendering for the concerned rooms which were focused on in this study.



Figure 58: The rendered image of the student help room (202) using Lumion 3D rendering software.



Figure 59: The rendered image of the laboratory room (210) using Lumion 3D rendering software.



Figure 60: The rendered image of the library/meeting room (201) using Lumion 3D rendering software.

3.4 Unity VR model

Additionally, a Unity3D model was also created by exporting the Revit-BIM model into Unity (see Figure 61). Visualization of digital data in BIM plays a vital role as it provides a primary communication medium to the project participants, where VR can offer a new dimension of experiencing BIM and developing the collaboration of various stakeholders of a project. Unity3D game engine is suitable for visualization of the desired tasks. Unity3D can take BIM models through FBX file format to import geometric, and texture, and other material properties from Autodesk Revit BIM models. Besides the developed models can be deployed in Windows, Mac, and iOS, and Android systems.

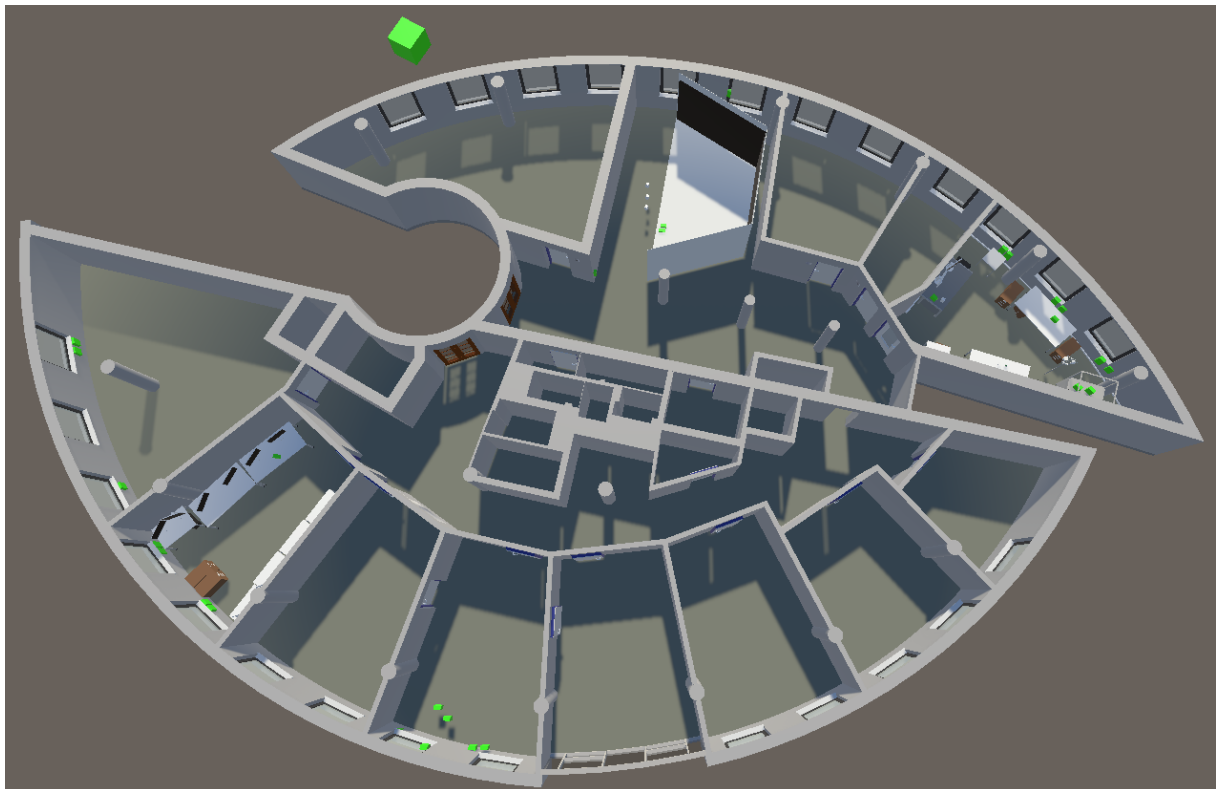


Figure 61: Unity3D model of the BIM Institute.

The BAS mentioned in the Building Automation Systems section previously have all been modelled in the current Unity3D model. Wherein Figure 62 gives an illustration of the installed sensors and actuators in room 210 modelled at their respective locations corresponding to their real locations in the room. The individual components such as the temperate radiator sensor and the thermostat are shown in Figure 63. Furthermore, Table 11 documents all the sensors and

actuators part of the BAS installed at the Institute of Construction Informatics created in the Unity3D model.

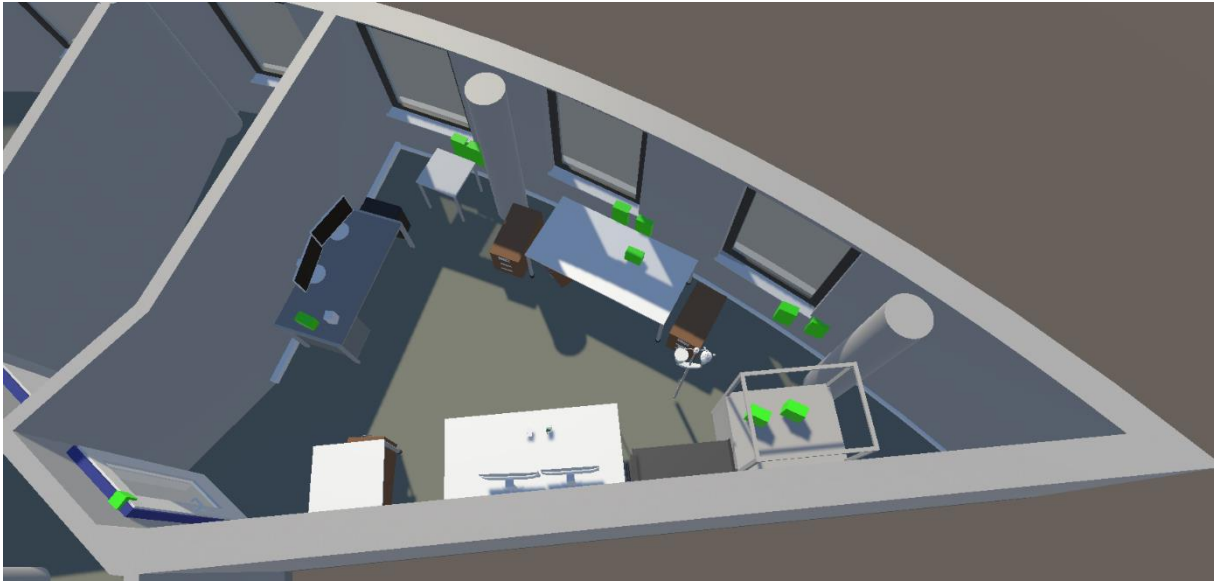


Figure 62: Room 210 in the BIM institute with the modeled BAS in light green colour.

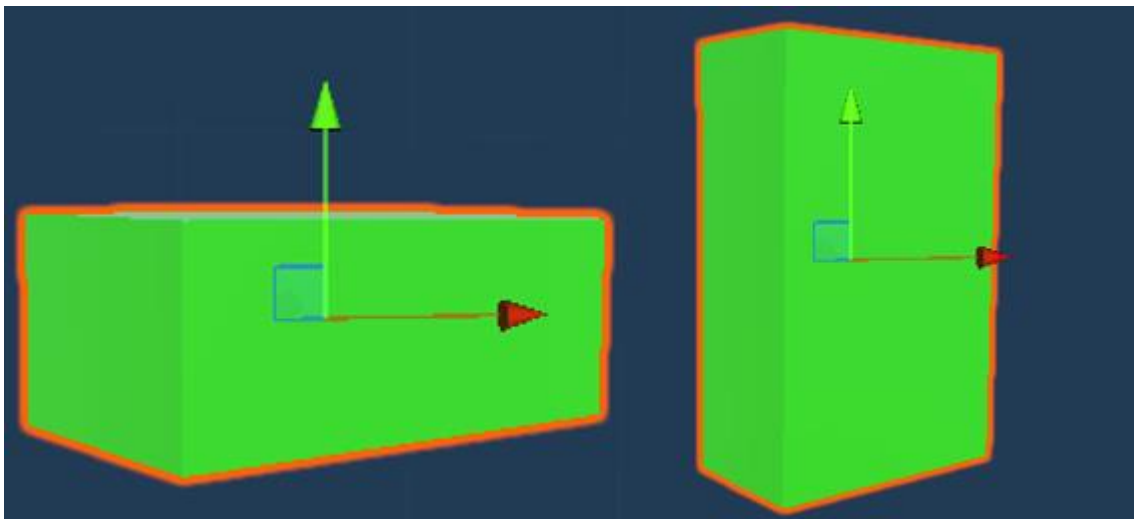


Figure 63: The individual modelled components such as temperature sensor and thermostat in the Unity3D model.

Table 11: All the components of the BAS modelled in Unity3D.

Room no.	IoT device modeled
201	Temperature sensor radiator right
	Thermostat radiator right
	Temperature sensor radiator left
202	Temperature sensor radiator left

	Thermostat radiator left
	Temperature sensor radiator right
	Thermostat radiator right
	Multi-ceilings sensor
	MDS-4
204	Thermostat radiator left
	Temperature sensor radiator left
	SR04-x
	T-204 R
	Window opener right
	Door contact laboratory
	Thermostat radiator left
	Thermostat radiator middle
	Thermostat radiator right
	Temperature sensor radiator left
210	Temperature sensor radiator middle
	Temperature sensor radiator right
	MDS-5
	MDS-7
	Portable measuring device
	Light switch laboratory
	CO ₂ and air humidity sensor
213	Light switch
	Window opener switch
	Window opener
	Actuator window
	Door contact main door
	Multi-ceilings sensor
	Temperature sensor
	MDS-8
214	Weather station

4 Methodology for Digital Twin environment

4.1 Analysis of data

The analysis of the sensor data with respect to the values from the existing IES model followed by the calibration of the existing IES model with actual (real environmental data) values obtained from the sensors is mainly done in two parts which are pre-calibration (pec) and post-calibration (poc). In this section, the pre-calibration analysis is presented. The time period for the simulation was chosen from 15th June to 31st July, thus a shorter period for simulation would help in better interpretation of results.

Figure 64 shows the CO₂ concentration gathered by the (sr04_2) room sensor in room 201 and the data from the IES simulations. It is quite apparent from the graph that there is a vast difference between the CO₂ concentration values and the real data recorded by the sensors. In the case of IES, the base external CO₂ is set at 400 ppm which very similar to the real data recorded from the sensors, however, the occupancy profile is set to 1 although, in reality, more than 1 person were present in the rooms. The considered room 201's main purpose is to serve as a library and also as a meeting room for the Institute of Construction Informatics. As per the Technical University of Dresden directive under the COVID-19 guidelines the teaching of the classes had to be resumed online, hence this room was used to conduct online classes during these times (May to July). Hence, while conduction of the online classes the room had occupancy of around 2 people, also the projector and computer were used to carry out the class. Accordingly, the factors of occupancy and air exchange gains would have primarily contributed to the CO₂ concentration recorded by the sensor placed in the room. The highest value of 2530 ppm recorded on Friday 26th June at 11:39 corresponds to the online teaching schedule of the Institute. Likewise, on 25th June when we obtain a CO₂ of 1760 ppm is due to the defense of a master studies student with occupancy of around 4 people and the equipment gain. The rest of the large value of CO₂ concentration above 1500 ppm on various dates can be correlated to the online teaching schedule being carried out in the library (i.e. room 210).

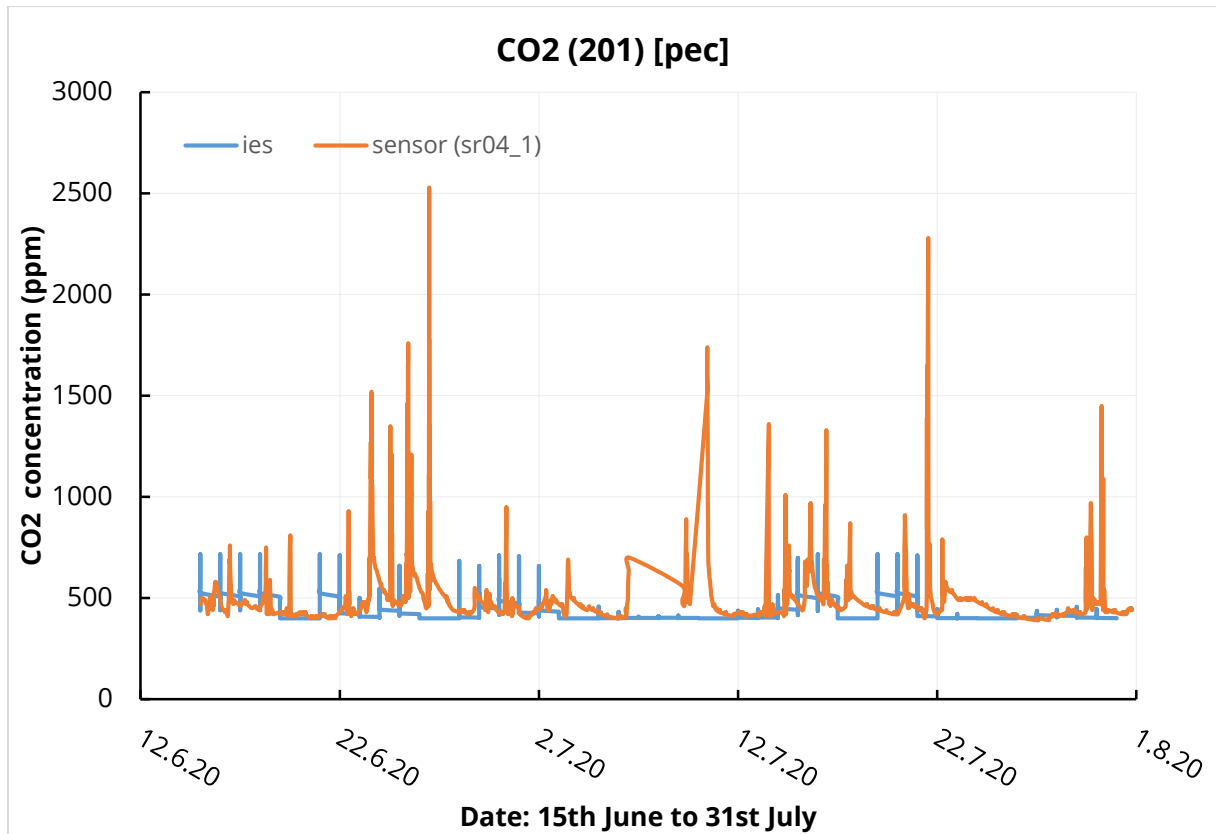


Figure 64: CO₂ concentration levels from the IES simulations and from the sensors in room 201.

Depicted in Figure 65 are the temperature levels for room 201. The average temperature recorded by the sensors in the timespan of mid-June to the end of July is around 26.5 °C, whereas in the IES simulation the variation in temperature is quite significant, as it takes into account the outside maximum and minimum dry-bulb temperature in order to do the calculations of mean air temperature in the room. Therefore, there is a difference between the IES simulation temperature data and the actual temperature recorded by the room sensors and hence the model needs to be calibrated to represent actual conditions. Figure 66 characterizes the relative humidity levels from the IES simulations and the sensor. The average relative humidity in the room is around 31.6% during the time period of June to July. For the IES simulations, the relative humidity is correlated to the room temperature, when the room air temperature is high the relative humidity is low, as in IES the humidity is expressed as a percentage of saturation vapor pressure, hence when the temperature is high comparatively dryer room condition will prevail and in turn less relative humidity level in the room. For the graphs corresponding to rooms 202 and 210 refer to Appendix C.1.

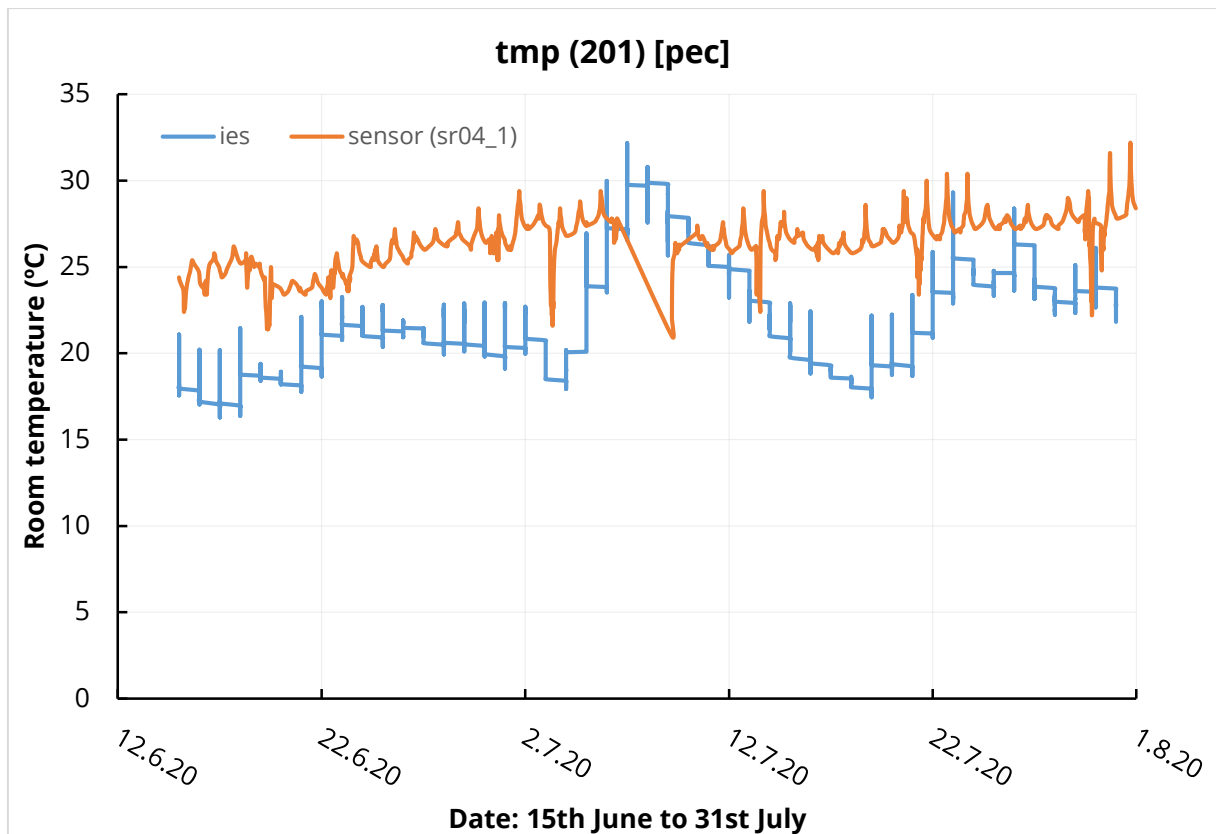


Figure 65: Temperature levels from the IES simulations and from the sensors in room 201.

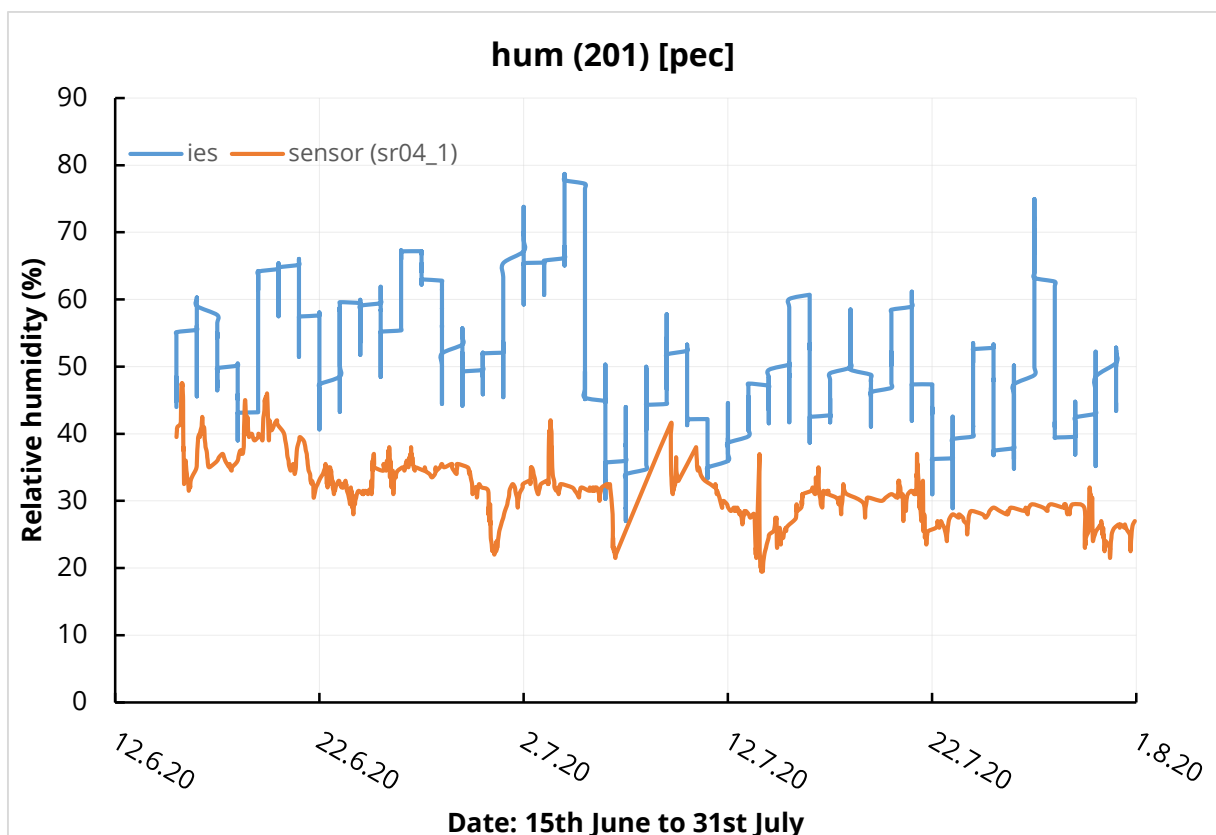


Figure 66: Relative humidity levels from the IES simulations and from the sensors in room 201.

4.2 Calibration 1.0 of the IES model

In the last section, the graphs for IES simulations and the room's sensors data were presented for the CO₂ concentration, temperature, and humidity levels. Subsequently, the existing IES model was calibrated on the actual environmental data collected from the sensors equipped in various rooms. The calibration is done keeping with the aim of bringing the IES simulation as close as possible to the real sensor data, with a focus on environmental data inside rooms such as CO₂, temperature, and humidity levels. This step is called as Calibration 1.0.

The original IES model had some discrepancies, which were rectified foremost to make the IES simulations more in the vicinity of the actual data collected by the sensors. Firstly, the external concrete wall was missing an insulation layer, thus an insulation layer was included in the external wall to for the calibration of the model. Secondly, the base external CO₂ concentration was set as 400 ppm which exactly the same for the room sensors. Additionally, the original IES model had an occupancy profile of 1 person for all the rooms, which was upgraded to 2 persons to match the actual CO₂ concentration measured. Temperature levels recorded from the outdoor weather station and the room sensor (sr04) are used as a reference to revise the maximum and minimum dry bulb temperature in the IES model from May to June. The temperatures were adjusted as follows for May (20°C and 23.6°C), June (23.4°C and 32.6°C), and July (25°C and 33.2°C) to match the real-time monitoring. In the case of relative humidity, before running the simulations the minimum and maximum saturation levels were set as 20% and 55% respectively for all the rooms. The values of 20% and 55% were obtained from the sr04 room sensors which record the relative humidity. All the calibration methodologies utilized in the original IES model can be referred through Appendix C.2.

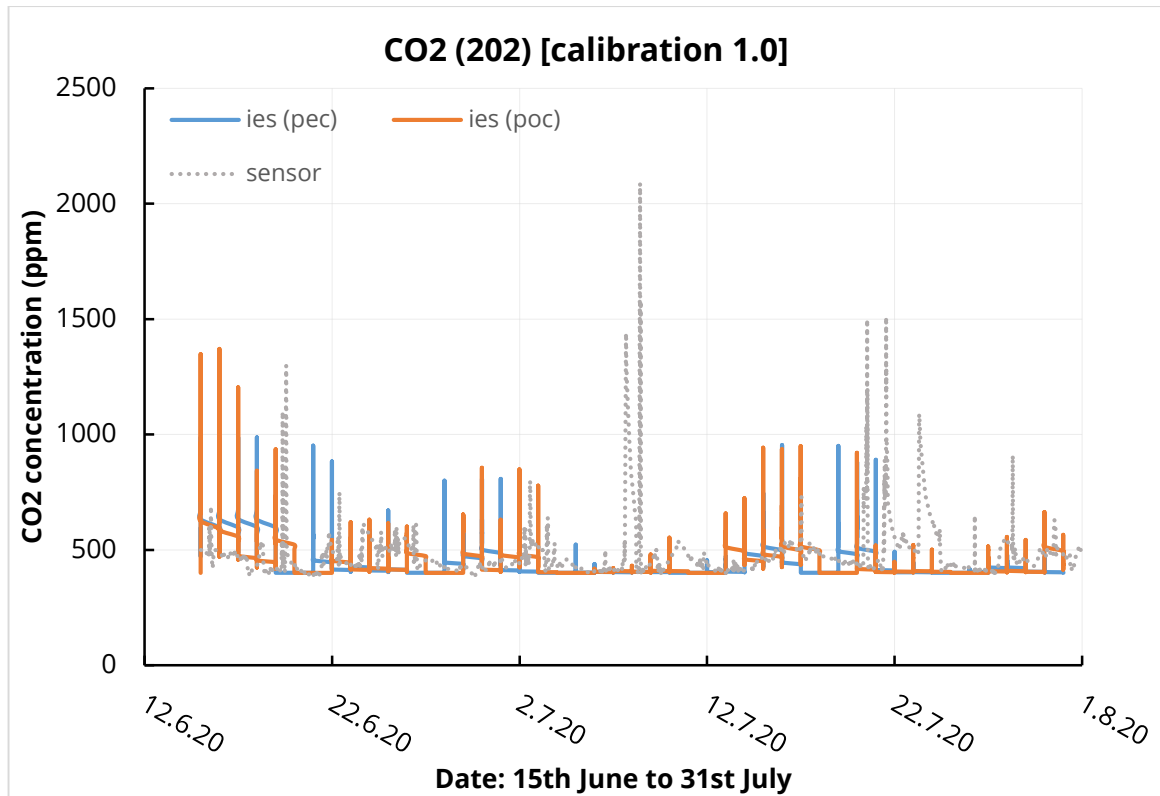


Figure 67: Calibration of CO₂ concentration levels in IES using data measured by the sensors as a reference for room 202.

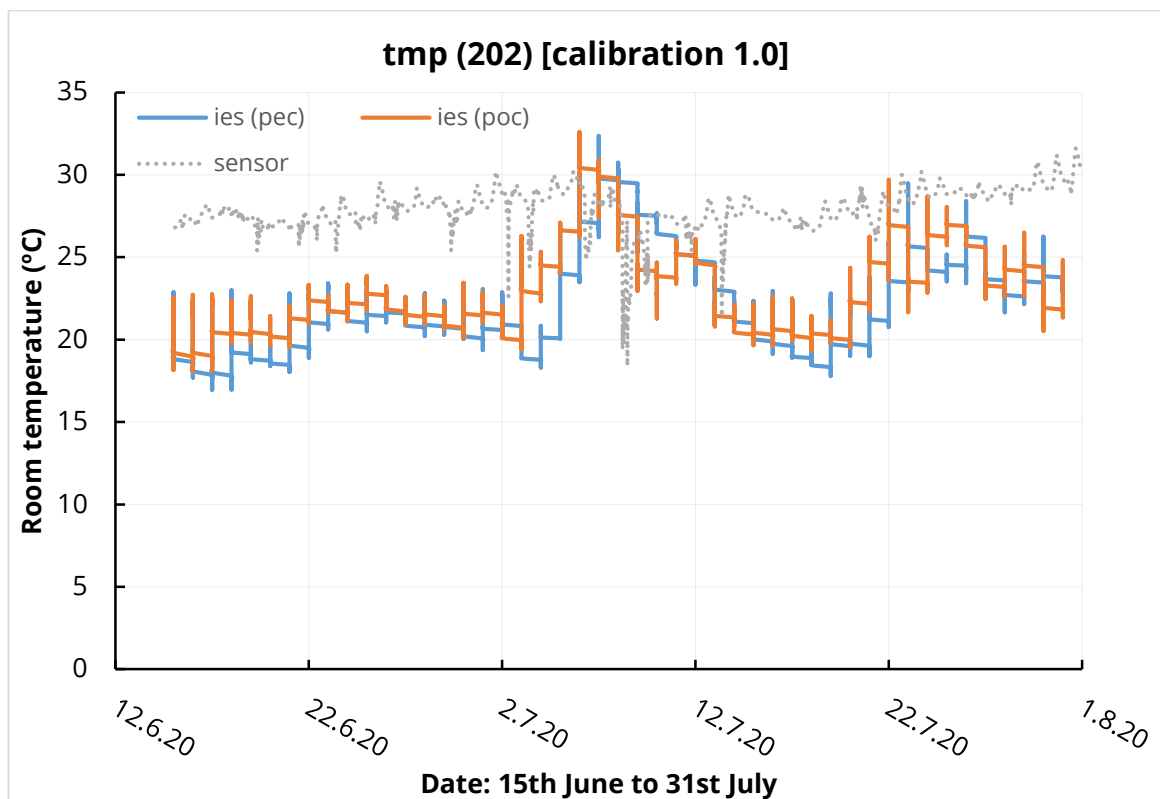


Figure 68: Calibration of temperature levels in IES using data measured by the sensors as a reference for room 202.

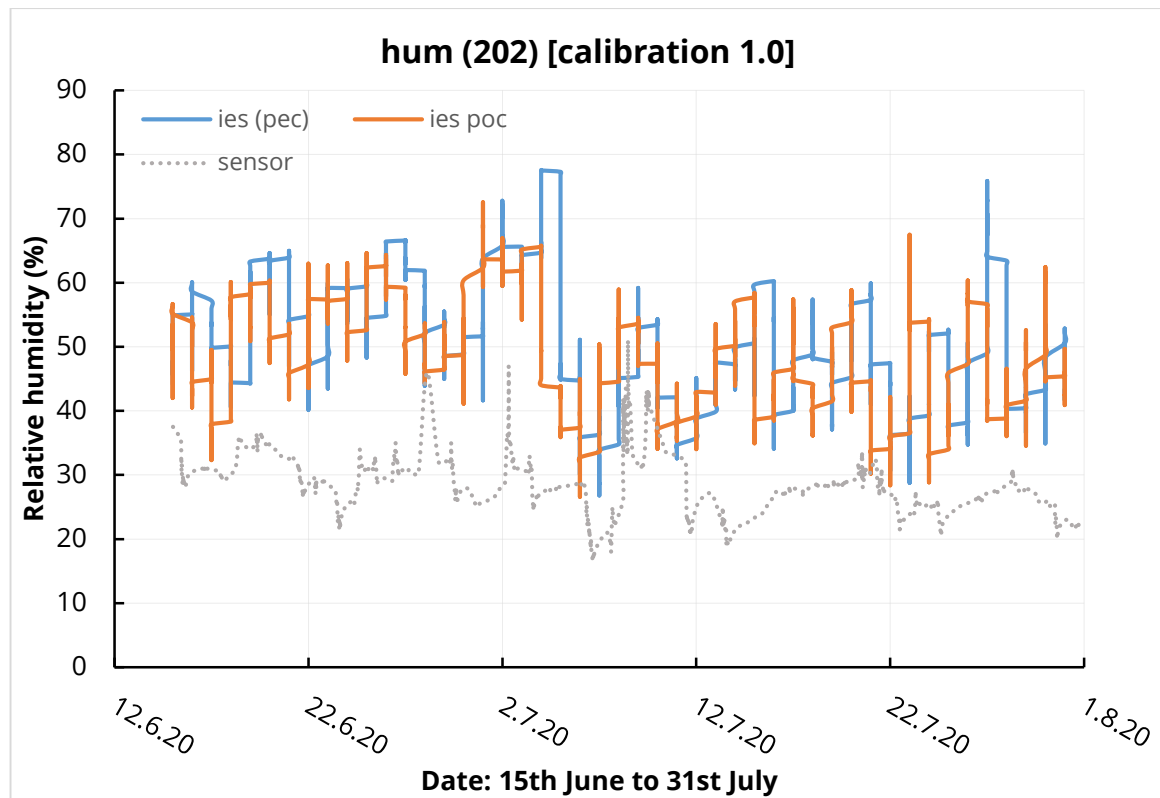


Figure 69: Calibration of relative humidity levels in IES using data measured by the sensors as a reference for room 202.

Figure 67 shows the calibration results for the CO₂ concentration for room 202. Post the calibration, CO₂ levels, improve significantly from around 1000 ppm to about 1500 ppm. The main reason behind this is the increasing occupancy profile, as the presence of people inside indoor spaces determines the changes in thermal conditions due to sensible and latent heat release. While Figure 68 depicts the effect of calibrating the temperature levels for room 202. Since in IES the maximum and minimum dry bulb temperature for any particular month can be set globally and not locally. Which means for instance in June the maximum and minimum 23.4°C and 32.6°C respectively is the same for the whole 30 days rather than changing for each particular day of the month which in actuality is recorded by the sensors, thus we observe large variations in temperature simulations of IES in comparison the sensor data which is more or less constant. In Figure 69 the calibration results of relative humidity levels are presented, where after the calibration the results are a bit closer to the real data sensed and measured by the sensors. But since relative humidity is correlated to temperature levels the IES simulation shows a similar type of variation as temperature levels. For the calibration results corresponding to room 201 refer to Appendix C.3.

4.3 Calibration 2.0 of the IES model

This section is a continuation of the work mentioned in the previous section and this version is categorized as Calibration 2.0 of the IES model. In this calibration, more real-time parameters were taken into consideration for enhanced calibration of the IES model. Firstly, the real weather data from the already installed weather station at the Institute is used. Secondly, profiles for air exchange were set according to the actual profile set for the operable windows. Lastly, the time profile (daily/weekly) is also set for the occupancy by approximating the number of persons from the sensed CO₂ concentration levels recorded by the room sensors. These give us much closer results to the actual data recorded by the sensors.

The data collected by the HomeMatic weather station is used as the source for editing the weather file. The weather file was edited by Elements developed by Big Ladder software which is a free, open-source, cross-platform software tool for creating and editing custom weather files for building energy modeling. The latitude, longitude, and elevation are adjusted for Dresden as a location. We get parameters such as dry bulb temperature, relative humidity, wind speed directly from the HomeMatic weather station itself. The atmospheric pressure and radiation are taken from the website for the weather station located at Dresden airport for the desired time period. The remaining parameters such as wet bulb temperature and dew point temperature are calculated using formulas consisting of the given parameters (air temperature, atmospheric pressure, and relative humidity). The time span for the edited weather data is from 15th June to 31st July, and a preconditioning period of 10 days prior to the simulation from 5th June is also considered. Refer to Appendix C.4 for a detailed description of the edited weather file for the IES simulations.

Figure 70 exhibits the temperature levels in room 201 after Calibration 2.0. What is quite evident is the shift of IES simulation results towards the sensor data. Although, we still observed spikes in the IES simulation which is due to the high variation of temperature levels during a whole day (about 5°C - 10°C). Also, a window opening profile is assigned to open the window for 20 minutes between the lectures during each day of the week for heat transfer by ventilation. These air exchanges may be sourced from the outside air. The rate of airflow is specified

before the simulation but may be made to vary with time by means of a profile which is our window opening profile.

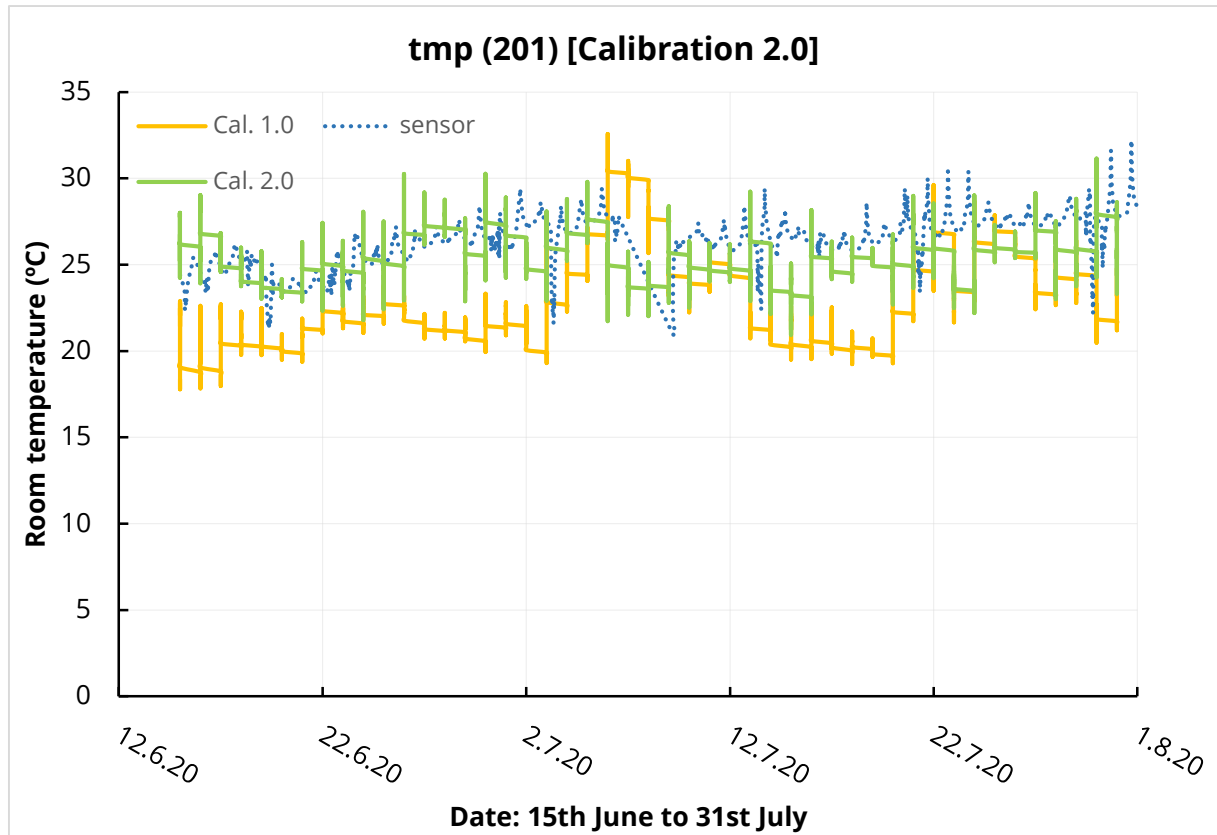


Figure 70: Calibration 2.0 of temperature levels on IES for room 201(library).

In Figure 71 the relative humidity levels are shown for the library room (201). Higher humidity is correlated to a lower temperature and vice versa. Although the overall change in humidity levels between cal. 1.0 and cal. 2.0 is not significant but still, the second calibrations are comparatively closer to the sensor's humidity levels. In IES the user cannot define the humidity (transpiration) of the humans and only heat gains by those persons can be defined. Furthermore, upon studying it is found that it is likely that IES doesn't take into account humidity gains (perspiration) by humans. With 10 bodies the temperature in the room increases and the air can take a higher rate of moisture through evaporation and this leads to the notable drop in relative humidity levels. Additionally, it is found the relative humidity recorded by two adjacent sensors in room 210 showed deviations and thus the sensors need calibration to detect anomalies in terms of deviations.

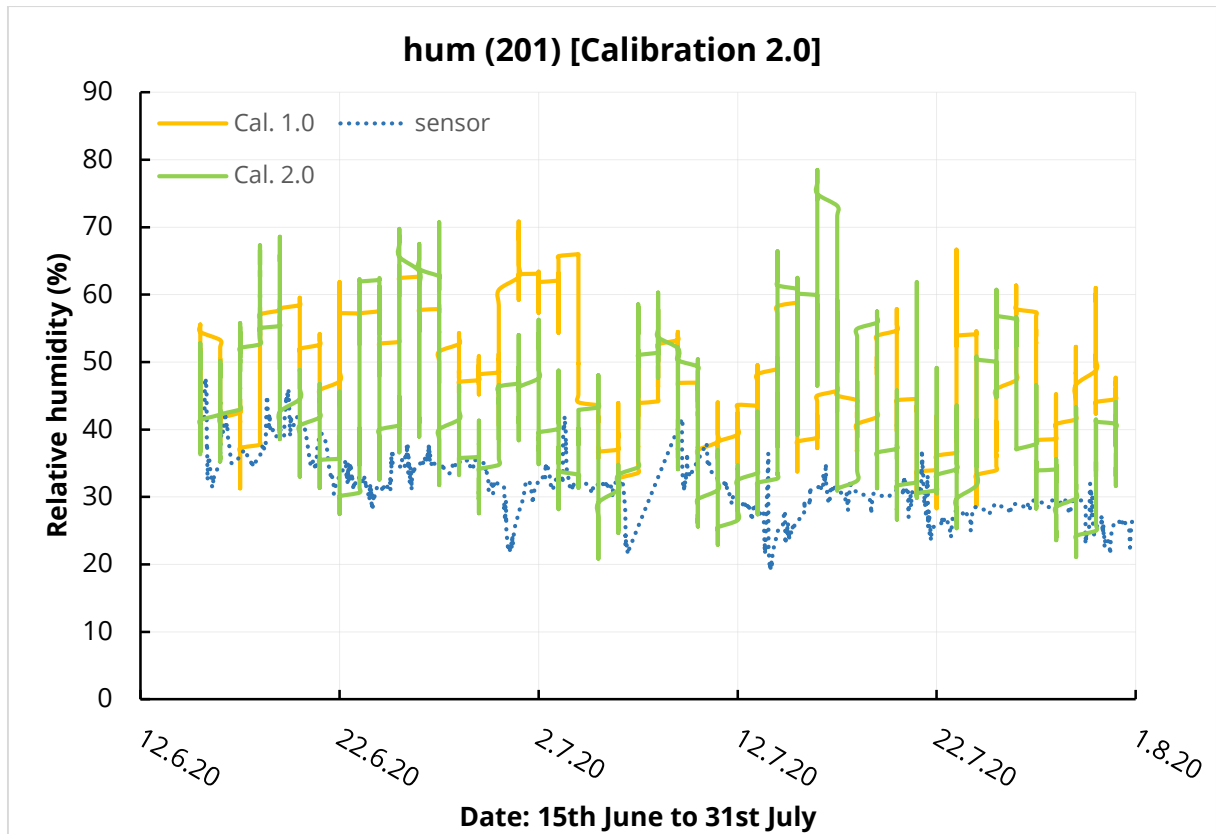


Figure 71: Calibration 2.0 of relative humidity levels on IES for room 201(library).

Figure 72 describes the CO₂ levels after Calibration 2.0, where we can see the “cal. 2.0” results are much closer to the sensor data in comparison to “cal. 1.0” results. The high values (above 1500 ppm) in some instances are because in our case the room sensors were placed on a desk, where people were very near to the desks and this could lead to very high sensed CO₂ concentration values along with the multiple persons presents in a room.

Table 12: Daily occupancy profile according to sensor data.

Day	Time	Occupancy value
Monday	11:00 – 13:00	1
Tuesday	11:00 – 13:00	3
Wednesday	11:00 – 13:00	2
Thursday	11:00 – 13:00	3
Friday	11:00 – 13:00	2

Table 12 shows the implemented occupancy profile for each working day of the week. The weekend is set at no CO₂ gains thus only showing a base value of 400

ppm from outdoor CO₂ in the graphical results. The occupancy values are approximated from the sr04_1 room sensor placed in room 201, assuming a single person produces about 400 ppm CO₂ in a room. Thus we get an approximate occupancy which is then assigned to the time during a day that recorded most CO₂ activity.

However, we approximated the occupancy with the number of persons to 10 in IES to bring it closer to the sensed data and the values from Table 12 are taken in a ratio of 10 persons by IES. But there are still uncertainties, as it is still not clear to us how IES distributes the persons in a room, hence we assume an even distribution across the room and not according to the arrangement of the furniture. And it is still not clear where and how IES determines the precision of the CO₂ measurements. Also, outdoor CO₂ concentration in IES is modeled in a simplistic manner with a constant value of 400 ppm. Considering a more advanced model of CO₂ levels would mean taking into account the natural seasonal and diurnal variations of this quantity due to photosynthesis phenomena, not to mention the global rise of atmospheric CO₂ levels on a larger timescale.

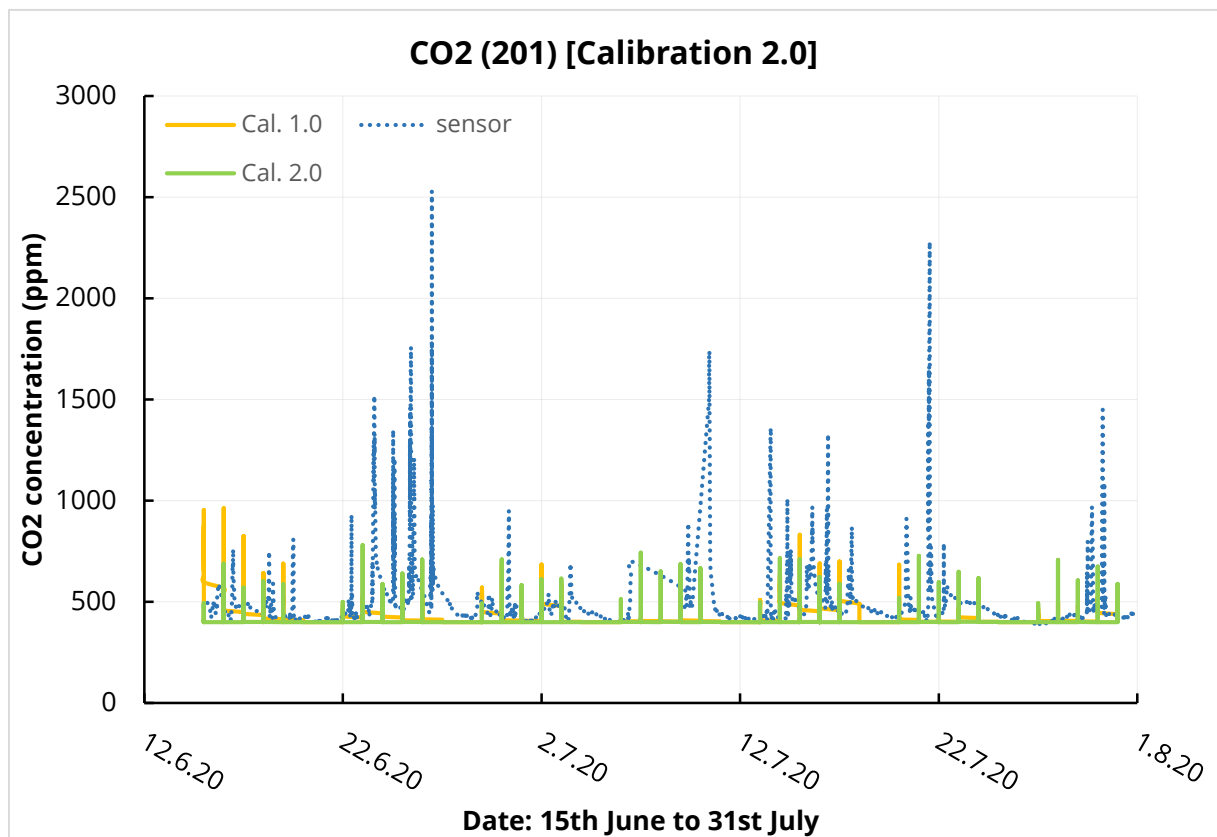


Figure 72: Calibration 2.0 of CO₂ concentration levels on IES for room 201(library).

4.4 Visualization of data

Architectural and urban design is always about the idea of visualization and materialization. The importance of BIM is although significant for this cause, but it has its limitations. When it comes to visualization of the 3D model, VR is the only technology that is capable of offering an immersive 1:1 scale present in the environment. With consumer VR headsets being easily accessible, room-scale tracked VR provides a realistic walk-through experience, enabling the users to move around the virtual environment. Apart, from providing a highly interactive experience the experience enables the user to virtually be in the building and observe all aspects of the project in finer details.

The concept of visualization in this research study is accomplished in two ways, firstly the visualization of the simulations obtained from the calibrated IES energy model is carried out. Subsequently, the visualization of the sensor data measured by the BAS installed at the Institute of Construction Informatics is done. Both these visualizations are carried out in the already existing Unity3D VR model of the Institute. The apparatus used for the visualization in Unity is the HTC VIVE Pro VR set, consisting of two base stations on either side, two wireless controllers mainly for navigating in the game environment, and the VR headset for a high-resolution immersive VR experience. The PC setup used for the VR visualization had specifications of Intel® Core i7-6700 CPU @ 4.00 GHz, a 32.0 GB RAM with a 64-Bit operating system, and AMD Radeon RX 580 graphics card.

The Unity3D model that is used for visualization was developed by a Bachelors's studies student for his bachelor thesis work (Schinkel, 2020). Subsequently, that model was improved upon for the visualization in this research study, in the course of which several hindrances were observed which will be explained in chapter 4.4.2. Also, a private GitHub repository is used for future version control in order to easily merge changes during code development and also maintain a backup of the unity project. A separate repository for the institute would allow multiple personnel to coordinate programming work among themselves and work as a team to improve the efficiency of the digital model of the Institute of Construction Informatics.

4.4.1 Visualization of simulation data

The visualization of the analysis obtained in the energy simulation model in IES software is carried out on Unity3D. Usually, the data received from the energy simulation analysis of a structure is represented in the form of graphs and tables of various parameters such as CO₂, relative humidity, comfort index, etc. Thus, a 3D immersive representation on the VR of the simulation results would enable the user to better understand energy performance and thermal comfort during the building's life cycle.

Visualization of MicroFlo CFD data

For the purpose of visualization, the MicroFlo application in IES software is chosen. MicroFlo tool predicts the internal airflow temperature, direction, and velocity along with external airflow direction and velocity. The generated results are accessed via graphical views of 2D slices at any grid line. For example, if the user selects a particular Z-grid (e.g. height) it will get a 2D X and Y-dimension display of the selected variable (e.g. temperature and velocity). The range, scale, and color of contours and vectors can be adjusted to improve results interpretation.

CFD is a branch of fluid mechanics used to analyze and solve problems involving fluid flows, which has begun to be applied in architectural, urban planning, and environmental engineering fields. Whereas, VR generates a 3D space in the virtual environment of a computer. In contrast, Augmented Reality (AR) superimposes real surrounding landscape, acquired through a video camera into 3D computer graphics. Figure 73 provides a flowchart for the implementation of CFD visualization in Unity3D. As explained by Berger and Cristie (2015) that there are buildings 3D model and the corresponding CFD results, which must then be post-processed into visuals that any user can interact with. The 3D models (.obj or .fbx format) can be imported into Unity3D as in this study it was done by importing the 3D REVIT model. For other software like ANSYS Fluent which is a commonly used engineering software for CFD simulations, whose results are then exported to text format (.txt or .csv) can be read by Unity3D. For temperature, humidity, and pressure data, however, we must pre-process it into 3D spatial data structures before handling it to the game engine such that it will be easier to process during interactive exploration. Unity3D will finally do the rendering to be shown in the display(s) and the user will be able to interact and navigate through the

environment by using a controller. Hence, this would be the most appropriate pathway to implement CFD visualizations in Unity3D using software like ANSYS Fluent.

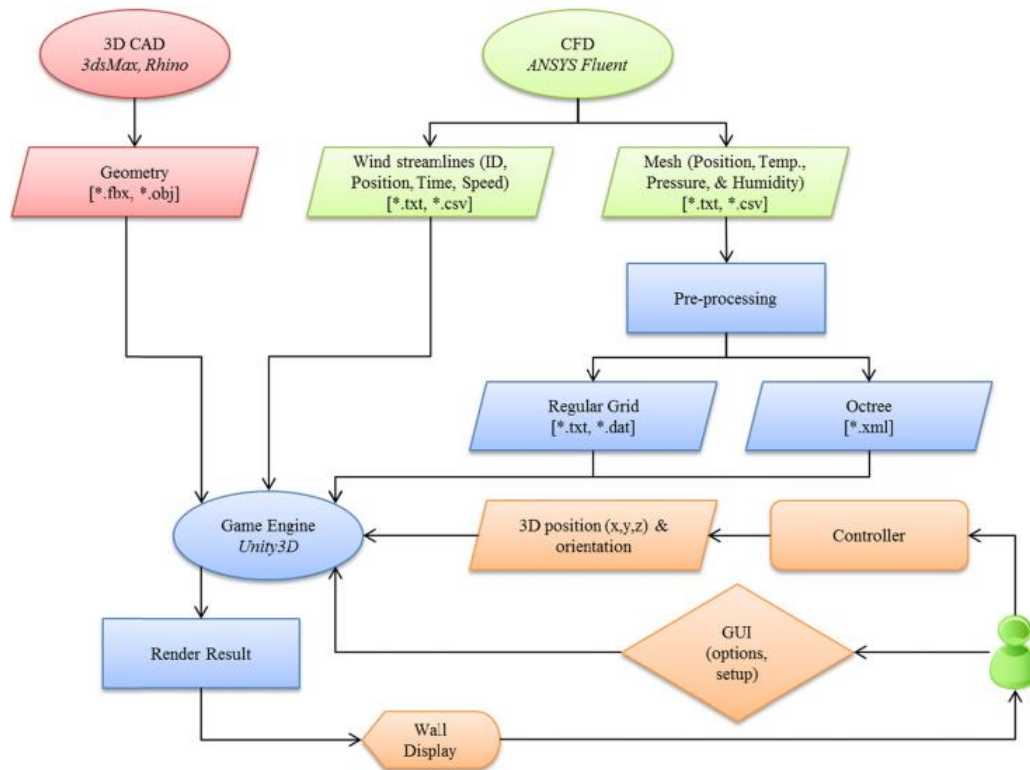


Figure 73: Flowchart of the CFD visualization (Berger and Cristie, 2015).

However, in this master thesis study, the CFD analysis was done on the IESVE software, which does not allow to present the output of CFD results over the whole CFD mesh as a text file (IESVE, 2020). There is only scope to get MicroFlo to dump the results out to a text file at a certain number of monitoring points which won't allow for a realistic visualization on Unity3D. Meanwhile, the problem is such that it is impossible to export the arrows and the color map information as vector data from the CFD simulation executed on IES software. Therefore, the images to be texture mapped were output as raster data in this study. Figure 74 illustrates the issue encountered for the visualization of CFD data in IESVE software. Wherein, the temperature key slices initiated at the two corners of the room are respectively for the X and Y-axis directions, and the slice on the floor of the room is in the Z-axis direction. Since we cannot obtain the Cartesian coordinate data for each slice of CFD moving across the room for an appropriate visualization VR, thus we had to think of a hack to do the CFD visualization. Wherein we take images as texture,

which is only possible for the Z-direction i.e. the floor of the room as for the rest of the axis directions (X and Y) the frame of the room obstructs our texture image which would spoil our visualization, so we try to keep a top 2D view of the room to do so.

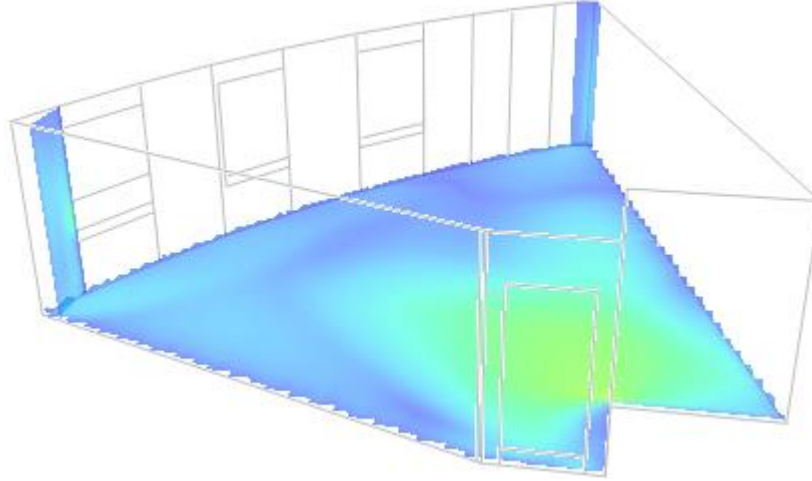


Figure 74: MicroFlo CFD viewer showing CFD grid all three Cartesian directions.

After obtaining the CFD analysis as raster images they are to be imported to Unity3D for visualization. Since many images of slices in the alignment from the floor to the roof of the room are taken, they are then edited using GIMP image manipulation software. Where we create a mask and assign it to all the images to extract the same floor area every time through which we get precise images in terms of measurement and shape of the multiple CFD slices in the Z-axis direction.

Afterwards in Unity 3D, four CFD slice images were imported at different heights of the room as materials. The heights were at floor level, 0.5 m above the floor, middle of the window panes, and then at the roof level. Then the 4 different CFD slice images are assigned as texture layers to a 3D plane covering the floor area of the relevant room and an algorithm is developed to move the CFDplane along different heights of the room showing the respective textures assigned to them. The two arrows shown in Figure 75 are allocated as buttons to allow the user to move the CFD visualization at different heights of the room. Figure 75 shows the initial CFD slice on the floor for room 201 appearing when we interact with the arrow button using a VR controller. Figure 76 depicts the changes in temperature as the CFD slice moves up in the library (201) room. This interactive and immersive 3D visualization of CFD simulation facilitates studying airflow patterns although in

a not so decisive Z-axis direction of the room it is the first step towards proper visualization of CFD in VR. In the near future with better CFD data sharing through the IESVE software or using an alternate CFD simulation software we can visualize room air characteristics (temperature and velocity) in the relevant X and Y-axis directions thus empowering the user to improve the buildings energy performance.

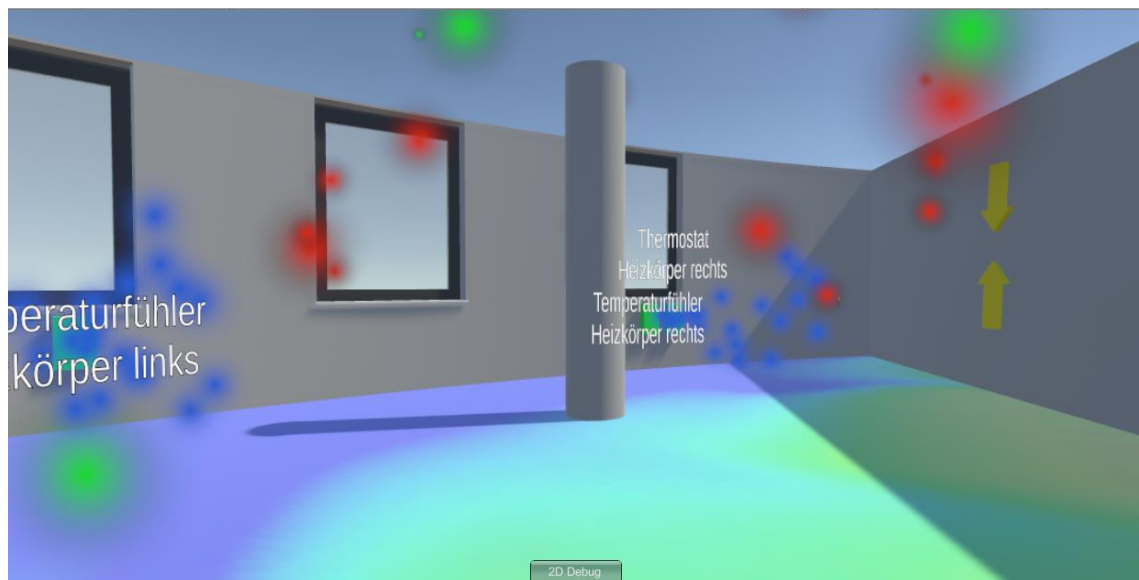


Figure 75: Results of CFD simulation visualized on VR in room 201.

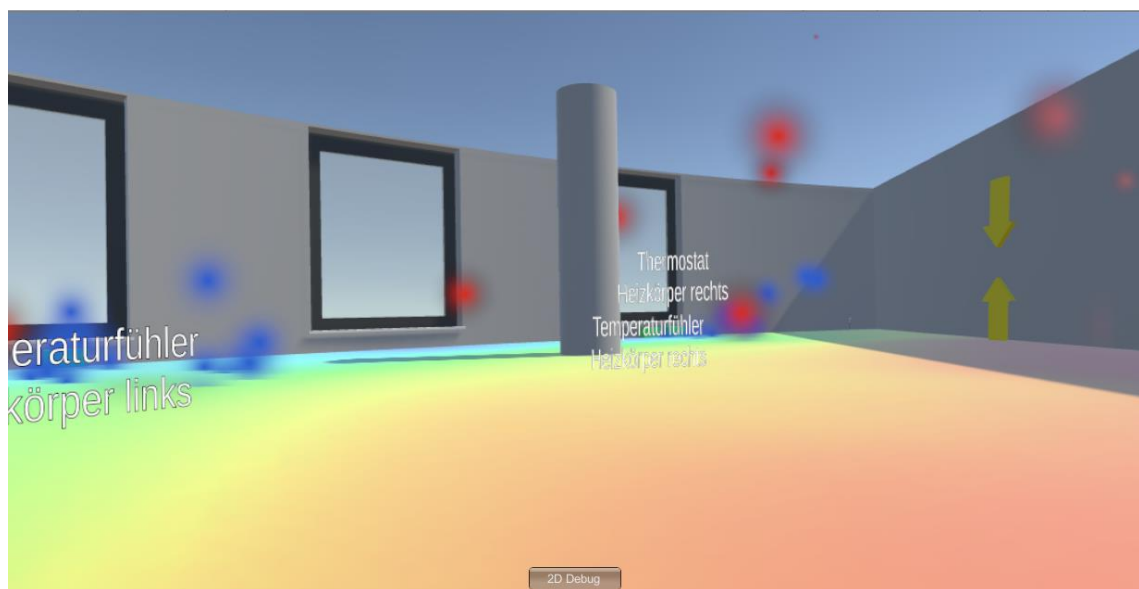


Figure 76: Results of CFD simulation moving in Z-axis direction visualized on VR in room 201.

Visualization of RadianceIES (Daylighting) analysis

For the purpose of energy simulation visualization the RadianceIES simulation tool of the IES software which predicts the daylight distribution in a room is chosen. The simulation takes into account the position of the building, sky conditions, material properties, and shading surfaces. Simulations can include detailed complex geometry and a wide variety of material types. Both luminance (what your eye sees) and surface or working plane illuminance (what the surface receives) can be analyzed.



Figure 77: Interactive 3D visualization of daylighting simulation of room 204 on VR.

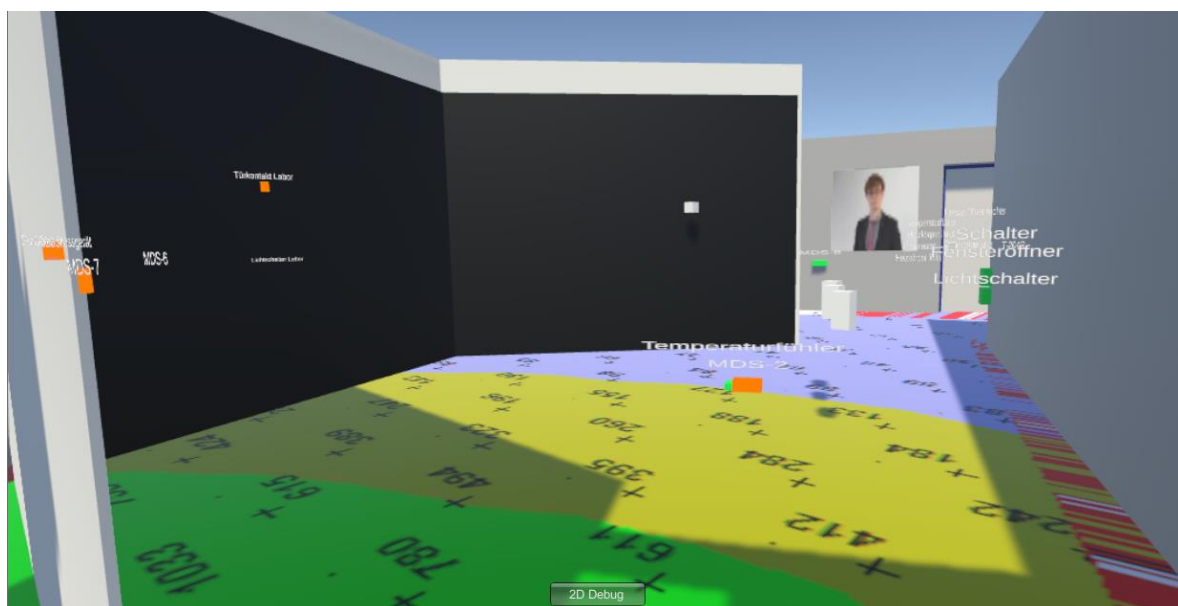


Figure 78: Interactive 3D visualization of daylighting simulation of room 213 (view 1) on VR.

Thus this simulation is visualized in Virtual Reality on Unity3D. Figure 77 and Figure 78 portray the daylighting RadianceIES simulation on the floor of rooms 204 and 213 respectively. The values illustrated on the floor of the room are the illuminance levels in Lux units across the room's floor area. The daylight simulation results from IESVE are imported as raster images to be assigned as textures on a 3D plane positioned at the floor of the room which gets activated by pushing down a cube-shaped button place in mid-air of the room to demonstrate the RadianceIES simulation on VR. Through this immersive tool, user can identify over-lit or under-lit areas through analysis of simulations results, users were able to teleport to the exact location and investigate what element had caused the underperformance from a closer, human-centric point of view.

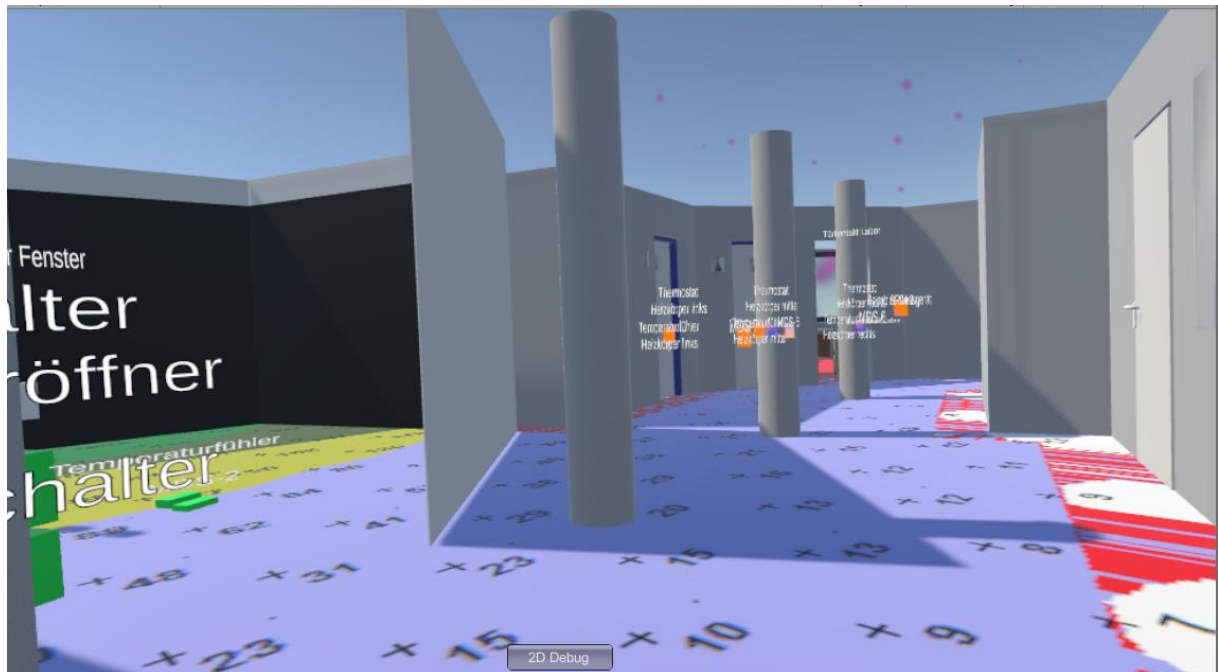


Figure 79: Interactive 3D visualization of daylighting simulation of room 213 (view 2) on VR.

Hence, this 3D visualization on VR would make it potentially useful as a layout planning tool and as an aid for a decision on the installment of an artificial lighting system. Besides, this tool could help in better identification of what building elements impact simulation results compared to the 2D display analysis tool.

4.4.2 Visualization of sensor data

The data accumulated by the sensors installed at the institute is analyzed from May to June and then subsequently visualized on VR. Since the sensed data is obtained through a database file from the Home Assistant WebUI, and in turn, Unity3D uses that database file for the visualization on Virtual Reality. Therefore, the database file used in this visualization study was from the period of 14th May 2020 to 09th July 2020, as the installed home automation system had some network issues and we couldn't a single database file for visualization for the duration of May to July. As a consequence of which difficulties were encountered on Unity3D to create an algorithm for visualization by combining two database files and thus first database file (14th May to 09th July) was applied.

Visualization of historical sensor data

The data collected by the sensors is of significant value when we can analyze graphs for the data collected over a certain time. Hence, the device (sensor) detail view consists of a canvas that is displayed in the virtual room when we select an IoT device that shows the data recorded by that sensor. Type-dependant device metadata such as location or the number of value counts (no. of data entries for each sensor) are also displayed. The size of the information display is static and rotates with the user's movement in order to keep the display text readable. The interaction button for all the devices has an appropriate size to be easily selectable using the controller. The exit is possible via a dedicated "Close Chart" button.

Room 202 is selected to test the visualization of historical graphical data. The two main sensors equipped in the room are the sr04-2 sensor (see Figure 80) that measures CO₂ concentration, temperature levels, and relative humidity in the room along with the mds-3 sensor (see Figure 81) that measures the illuminance levels in the room. The user when walking through the Unity3D model can view the graphical data by walking in room 202 and interacting with the sensor model by using a VR controller. The time period selected for visualization is of 1 month as the database consists of a vast amount of data values, and displaying the graphical data for more than 30 days will require more call back values from the database, hence requiring more GPU from the PC by Unity3d. The chart library used for the graphs in visualization was developed by (Schinkel, 2020), in which we observed few discrepancies which still remain in the existing model. The first issue

that was observed was in regards to the Y-axis values for the graphs displayed, although the shape of the graphs matched the actual sensor data plotted on excel separately, the values displayed on the Y-axis were very random, which means it was unrelated to the selected parameter (e.g. CO₂ concentration axis values were shown in the range of 2700 to 27,000). However, the actual values called by the algorithm in the Unity3D model precisely matched the values from the database. Whereas, while displaying it on the graph we see irregularities in the Y-axis value and range. Since we are unaware of the graph library used in the previous work (Schinkel, 2020) for the visualization no clear pathway was defined to get a suitable solution for this problem in the current study.

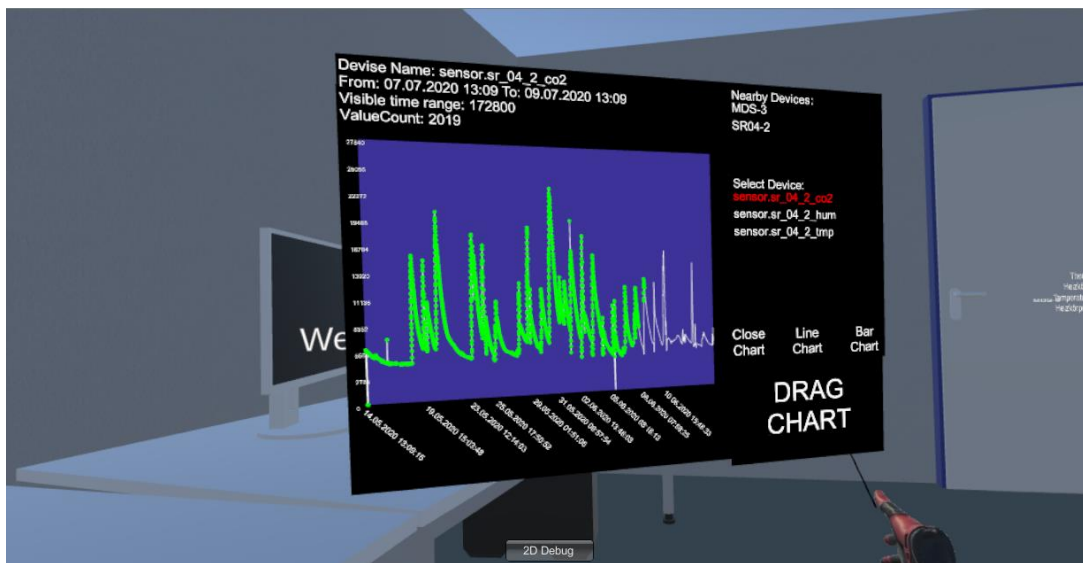


Figure 80: Display of device (sr04-2) information in room 202.

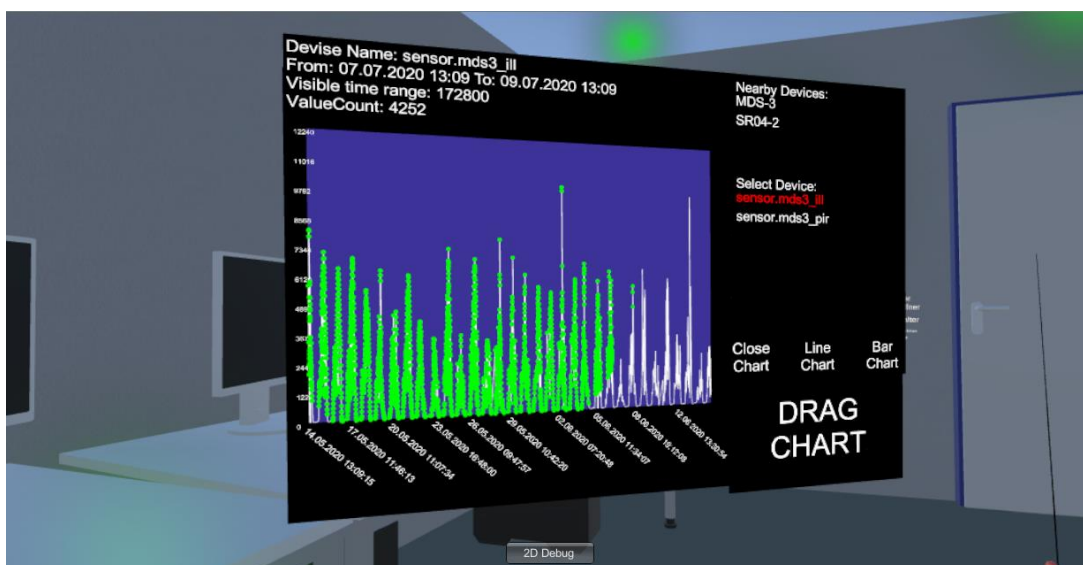


Figure 81: Display of device (mds-3) information in room 202.

Visualization of the room heating system

The BAS installed at the Institute of Construction Informatics is modelled on Unity3D. The heating system at the institute consists of standard room radiators powered by a gas heating system with a regulator. In the BAS the room radiators are further equipped with an automatic thermostat wired to the regulator of the radiator. This means that during winters when the room temperature is below the desired level the thermostat on the radiator will automatically regulate the heating levels to maintain occupant comfort. Since the thesis study was carried out during predominantly summer months i.e. May to July, actual temperatures recorded by the sensors were on an average above 18 °C, thus the room radiators were not turned on during these months. Due to this limitation, a threshold value of 25 °C was chosen in order to visualize the heat generated by the radiators in the rooms. Which can be then further altered to lower temperatures during the winter months which would be our primary requirement for any room heating system. The main idea is for the heating animation from the radiators to start when the value from the sensor database is below the threshold temperature (i.e. 25 °C). The particle system in the form of red-colored particles to represent the heated airflow emitting out from the room radiators.



Figure 82: Particle effect switched off when above the threshold temperature.

The visualization here is assigned to the room radiator in room 204, where it call-backs value from the database for the period of 20th June to 30th June. Where using the arrow buttons we get the temperature value and the respective time stamp and then can move along the database using those values between the assigned time period (20th June to 30th June). Figure 82 shows that the particle system assigned to the room radiator below the window of the room is switched off when the room temperature is above 25 °C, as we can see the actual temperature is 27 °C along with the timestamp on the left. While, Figure 83 depicts the switched on heating from the room radiator, where the actual temperature from the database is 25 °C or below 25 °C (i.e. 21.8 °C), thus giving us the concept of turning on the room radiators when the temperature is low in order to maintain the room comfort for the users. This visualization was done in room 204 due to the absence of room furniture so as to give us a clear view for implementing the visualization, thus this template can be implemented in the rest of the rooms as well.

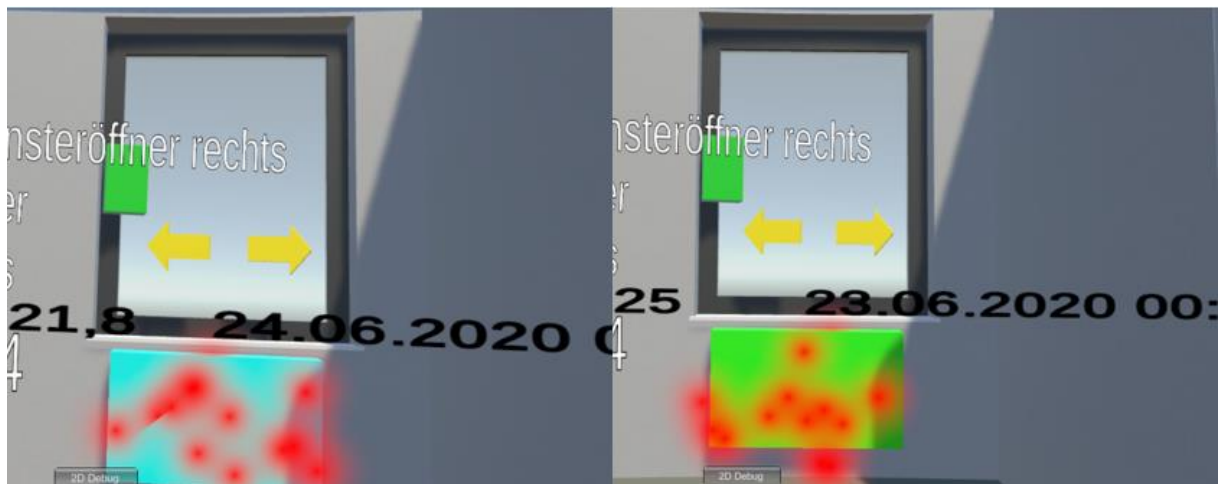


Figure 83: Particle effect switched on when below the threshold temperature.

Henceforth through this visualization on VR, the user can gain a first-hand experience of how the room heating system alters the atmosphere of the room, especially during winter months. By correlating the real heating to the virtual model would result in identifying better design alternatives that leads to the improvement of building energy performance.

Room temperature based color metamorphism

The BAS at the Institute consists of room sensors (sr04) that collect temperature, relative humidity, and CO₂ levels. These sensors and their measured values were

visualized on VR, wherein the modelled sensor in the room call-backs the required value from the database and then presents an interactive experience on VR. The visualization technique adopted here is based on the color metamorphism of the object (room sensor) based on the temperature value. An algorithm is developed where the color of the cube changes according to the temperature on that particular day. A spectrum of colors is assigned to the range of actual temperatures recorded from 14th May 2020 to 09th July 2020, based on that correlation the color of the cube changes. The lower and upper limits are set at 19 °C and 30 °C, which can be altered manually by the user on Unity3d depending on the temperature range. Table 13 shows the color spectrum assigned on the algorithm for the room temperature based color transformation.

Table 13: Color spectrum assigned for temperature based metamorphism.

Color	Range
Blue	0 – 0.25
Cyan	0.25 – 0.50
Green	0.50 – 0.75
Yellow	0.75 – 1.0
Red	≥1.0

Figure 84 and Figure 85 shows the various color transformation of the room sensor based on the sensor data. Alongside this, we can also see the temperature value on the left of the sensor and the respective time stamp on the right. When interacting with the arrow buttons we can move along a dataset of temperature value and observe color changes on the room sensor accordingly.

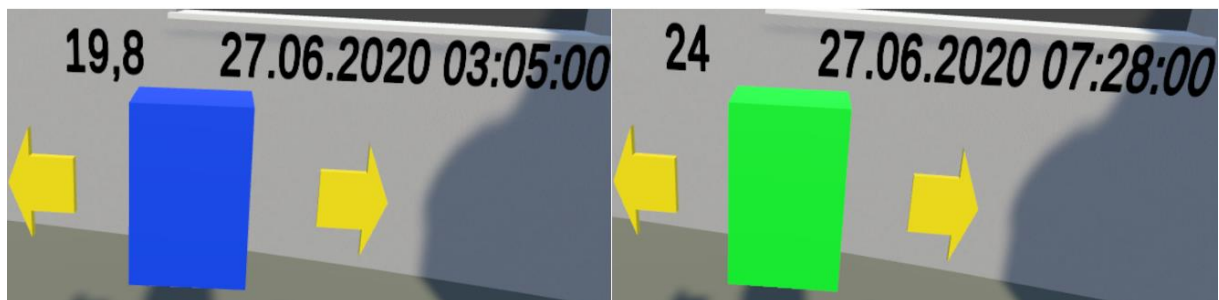


Figure 84: Color transformation (blue and green) based on temperature from room sensors.

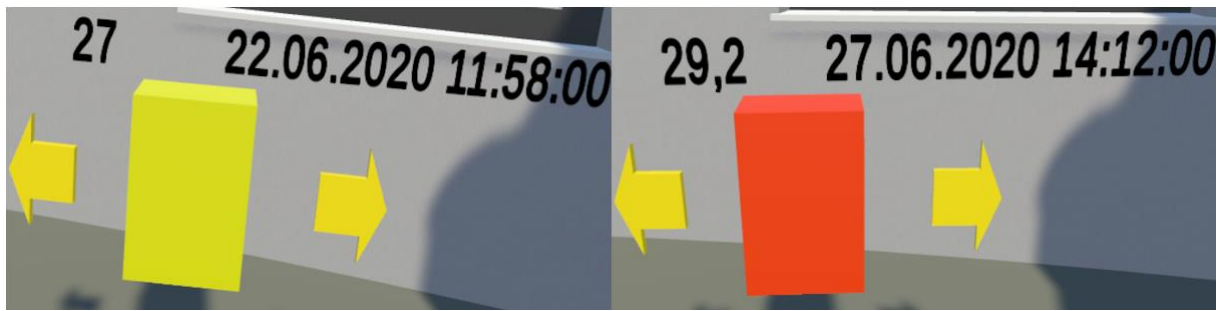


Figure 85: Color transformation (yellow and red) based on temperature from room sensors.

By means of this visualization, the user has the option of creating coordination among different sensors, for instance, if the room sensor attains a certain value/color based on which the operable windows can automatically open or close to enable air exchange. Thus, providing a basis for a Digital Twin environment based on which it can in return optimize the sensors to enhance energy efficiency.

Particle system as a visualization tool.

Unity3D provides a well performance particle system which is primarily used for effects such as smoke, fire, water droplets, or leaves. In the room heating system, we assign a particle effect system to visualize the airflow pattern and intensity. To distinguish the two parts, we set the room radiator airflow as blue and the normal room airflow as red, green, and pink respectively for rooms 201,202 and 210 of the institute respectively. Figure 86 illustrates the visualization for room 202, where blue colored particles represent the BAS and the green-colored particles the normal room atmosphere.

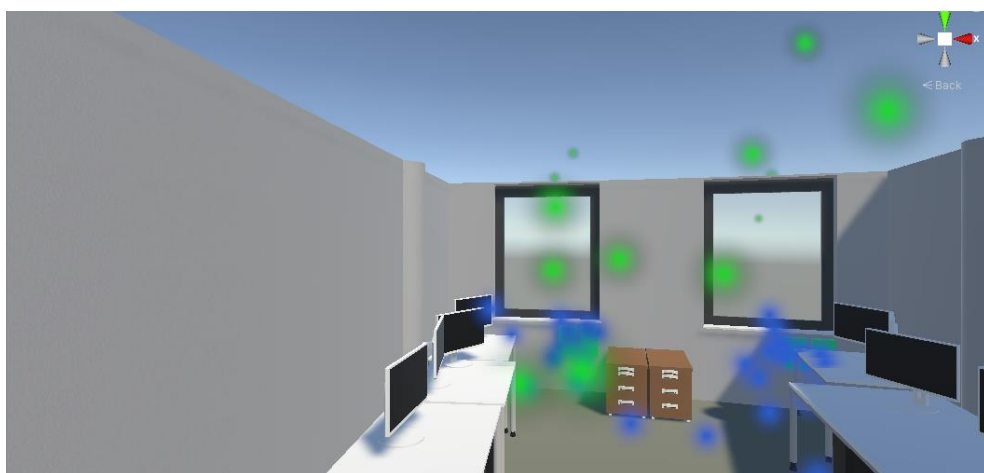


Figure 86: Particle system as visualization on VR for room 202.

Figure 87 shows the airflow direction for BAS (blue colored) and the normal room atmosphere (pink colored) in room 210. Where in the room the green-colored cubes emit the blue particle system where emission is in the shape of a cone and more or less along a plane of the cone's circumference and limited to a certain distance in the room to accurately mimic the actual effect of air from the room radiators. Whereas, the normal room atmosphere (pink-colored particle system) spreads through a cube-shaped emission and disperses along the whole volume of the room. Since currently, there is no HVAC system installed at the institute, for future purposes we can design the shape of it to be airflow objects in the supply and exhaust duct. Using the particle system, we can assign visualization such as what happens when two different colored particle systems collide and the subsequent changes resulting in the room's atmosphere thus providing a very immersive and interactive experience for the user through the medium of VR.

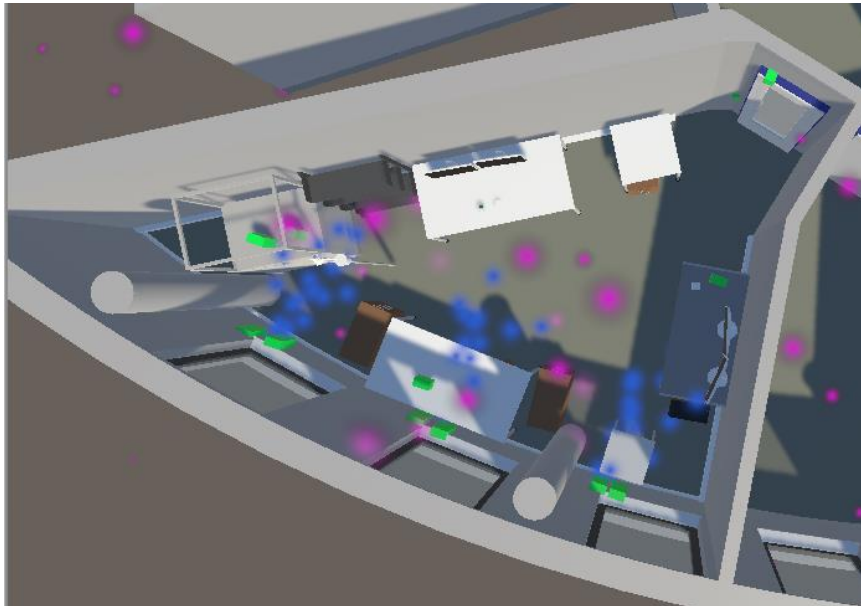


Figure 87: The airflow direction for both particle systems in room 210.

In order to make the animated airflow match the field-measured data, a pseudo correlation was used to correlate particle densities to the actual airflow values. This correlation was purely for illustration purposes and did not have any computational fluid dynamics (CFD) bases. However, this visualization tool is at a very basic level can be improved upon for showing airflow patterns and further interaction between the HVAC system along with the BAS with a normal room atmosphere.

4.5 Digital Twin environment

With all the data gathered from the simulations along with the sensed and measured data from the BAS, our aim is to establish a Digital Twin for the Institute of Construction Informatics. As per the research in (Nasaruddin, Ito and Tuan, 2018) the definition of a Digital Twin of a building would be “integration between the real-world building’s indoor environment and a digital yet realistic virtual representation model of a building environment, which yields the opportunity on real-time monitoring and data acquisition”. However, in this thesis only a “proof of concept” for a DT was achieved. The real-time data flow from the physical entity to the virtual representation and then the reverse communication which is the essence of a DT for the building's energy optimization still remains unachieved. However, we are able to create a framework with sensors installed at the Institute of Construction Informatics and the proper visualization of the building's energy performance possible with the scope of this master thesis. Whereas, in the near future this framework can be built upon to establish a function Digital Twin of the institute.

Digital Twin of a building entails with it several benefits, and one of them is building energy efficiency with regards to heating and lighting distribution when and where required. A Digital Twin can provide data concerning the building’s maintenance needs. Likewise, a DT can be used by various stakeholders such as the architects to improve the performance of future buildings. Also, we are able to provide a pathway to marry the real and the virtual world which is the essence of a DT by taking the sensor data and then optimizing the existing energy simulation model to replicate the prevailing conditions. We discuss a few possible applications in the context of this master thesis study in detail in this section.

An air conditioning system can source its air from a cooler part of a building rather than spend energy and recirculate the same air. This requires real-time monitoring of room air temperature and relative humidity of the whole building. The Digital Twin of a building with sensors measuring indoor air quality, temperature, and relative humidity can provide the required data for such a hybrid air-conditioning system for indoor spaces (Khajavi *et al.*, 2019). Thus the temperature and humidity sensors installed at the Institute could provide a basis for such a hypothesis.

Furthermore, an indoor measurement of the ambient light that is received from the outdoors allows for a fine adjustment of the lighting level inside the building. As a consequence, the energy consumption by the lighting system during the daytime can be drastically decreased. As an example, if operators are aware of the level of light reduction from the window glass, it would be viable for them to exercise the use of smart curtains to control the level of light on a real-time basis inside building spaces. In addition to this by applying smart motion detectors in such a scenario, the lights can be switched off when no user is in the room (Motlagh *et al.*, 2019). Henceforth, the RadianceIES simulation results from this thesis study could prove to be a vital tool along with operable windows of the BAS to establish this aspect of the Digital Twin of the Institute.

All the above-discussed prospects and the work achieved in this thesis gives us a framework and a possible workflow to establish a Digital Twin connecting the physical and the virtual asset with possible bi-directional information exchange with the aim of optimizing the building's efficiency.

5 Conclusions and Future work

5.1 Conclusions

In regards to the two main objectives of this research work, the investigation has been conducted based upon the concepts available previously and thus applying those in the context of this research study. In this research study, we set out to present a “proof of concept” for establishing a Digital Twin. For which the Institute of Construction Informatics at TU Dresden was considered as a testbed physical structure to establish a possible DT of the Institute.

Furthermore, the two vibrant case studies for a functioning DT in AEC are significant targets to be achieved by this research study.

- I. As mentioned in the previous chapters, the first objective of the research work is “To exploit sensor data from the existing BAS for calibration purposes of the existing IES energy simulation model.” Initially, the installed BAS is analyzed by studying all the relevant sensors in the duration of May to July. Additionally, the already existing IES energy simulation model is investigated with ApacheSim, RadianceIES, and MicroFlo CFD simulations. Subsequently, the calibration of that model is carried out using the sensor data as a reference. The calibration is done in two steps, namely Calibration 1.0 and Calibration 2.0, wherein first the IES model’s rectification of discrepancies and then utilization of actual environmental data from sensors is achieved. To demonstrate this task, the outcomes drawn are mentioned below:
 - Firstly, the database for the BAS is ill-structured thus taking additional time for analysis. Also, due to server issues of the BAS we were not able to obtain an appropriate single database file to work on.
 - In addition, the sensors were not accurately calibrated and we observed anomalies in terms of deviations and also large portions of missing data set values. The proper calibration must be achieved for improved results.
 - Since also in IES the building is not exactly modeled to real-life conditions thus this should also be taken into consideration for the difference in simulation results and the actual data recorded by the sensors. The

building in IES was modeled with just 3 floors while in actuality the building has 7 floors. Also, the adjacent buildings and the built environment is not modeled. Thus the data used in IES simulations are for a microclimate and not for the prevailing conditions.

- Moreover, the inbuilt restrictions in the IES software offered hindrances to the proper calibration. For instance, the setting of external CO₂ levels was very simplistic and doesn't take into account realistic parameters such as seasonal variations and precision of CO₂ levels measured in terms of location and persons for a particular room. Also, the transpiration gain by humans in terms of relative humidity cannot be taken into account.

II. The second objective of this research study is "To exploit sensor and simulation data for visualization purposes in VR, aiming to represent historical and current statuses of buildings." With relation to this task, the primary point of visualizing the simulation data with RadianceIES simulation (daylighting) and the CFD simulation was achieved. Also, the visualization of the sensor data is achieved through graphical representations, visualizing the room heating system, the room temperature variations during a day, and a particle system to show airflow in the room. The below-mentioned problems were encountered in this task:

- Concerning the visualization of simulation results, the main issue stumbled upon is the direct transfer of CFD results in Unity3D, which due to the use of IES software was not possible, and thus another indirect approach was adopted to visualize the CFD results on Virtual Reality.
- Additionally, the database developed by the sensors is improperly structured thus causing complications in data exchange with other software such as Unity. The database structure should be optimized considerably for proper workflow.
- Whereas, in relation to the visualization of sensor data the non-availability of an API documentation of the previous work (Schinkel, 2020) was the main obstacle. Issues observed were such as the discrepancies in axis values of the historical sensor data and the non-intractable value counts on the displayed graph. In conclusion, these

issues are solvable if provided with complete knowledge of the previous work. Furthermore, another issue is the call back of values from the sensor database cannot be achieved for a longer time period which means more data values as Unity requires a higher GPU to do this and thus an optimized solution can be found out for this in the future.

For the purpose of creating a Digital Twin environment of the Institute of Construction Informatics, we are able to aspect every available aspect. Foremost, the real-time data recorded by the sensors installed is analyzed, based on which we optimize the existing energy simulation model in IES to match prevailing conditions. Subsequently, all these parameters are visualized on VR through Unity3D giving us an interactive and immersive experience to study the building's energy performance more astutely.

Ultimately we were able to establish a data flow model from the real to the virtual world, which can be used as a reference for establishing a functioning DT of the building. Henceforth, it can be concluded that the necessary tasks for the fulfillment of this master thesis study were accomplished and further tuning of the processes can be performed to attain efficient results for creating a Digital Twin.

5.2 Future work

Within the scope of this research work, there were mainly two objectives (i) Calibration of the existing IESVE energy simulation model based on the actual data collected by the sensors installed at the Institute of Construction Informatics at TU Dresden and (ii) Visualization of the simulation results and sensor data in VR through the Unity3D model of the institute. Henceforth, this research work can be improved and extended along the following possible aspects mentioned below:

1. Further inclusion of internal gains such as artificial lighting, and electrical appliances in the IES model. Thus improving the accuracy of simulation results.
2. Explore the possibility of real-time data integration into the Digital Twin of the Institute of Construction Informatics. Wherein the real-time sensor data from the Home Assistant database is automatically updated to a DT dashboard.
3. Development of a dashboard for the Digital Twin of the Institute of Construction Informatics which can be used on a user interface (UI) webpage or be installed at the institute's entrance. Thus providing an interactive interface for informed decision-making, building efficiency, and comfort enhancement.
4. Optimize the sensor configuration based on the usability of the building system as well as from a cost perspective. Sensor replacement in case of damage and loss, connectivity maintenance for both wired and wireless connections, as well as gateway and software maintenance and updates should be made for efficient for maintenance of a DT of the institute.
5. Deployment of different types of sensors along with the environmental sensors such as human count sensors to measure occupancy in multi-personnel rooms, AI cameras, and emotional analysis devices to study human behavior with a focus on the office environment.
6. The application of Augmented Reality technology will enhance real environments with digital contents through the use of a head-mounted mobile device. Augmented Reality enables users to interact with both real and virtual objects by overlaying digital information and 3D objects on real objects.

Bibliography

- Alam, K. M. and El Saddik, A. (2017) 'C2PS: A digital twin architecture reference model for the cloud-based cyber-physical systems', *IEEE Access*. IEEE, 5, pp. 2050–2062. doi: 10.1109/ACCESS.2017.2657006.
- Anthopoulos, L. (2017) 'Smart utopia VS smart reality: Learning by experience from 10 smart city cases', *Cities*. Elsevier Ltd, 63, pp. 128–148. doi: 10.1016/j.cities.2016.10.005.
- ARUP (2019) 'Digital twin: towards a meaningful framework', p. 160. Available at: <https://www.arup.com/perspectives/publications/research/section/digital-twin-towards-a-meaningful-framework>.
- Azhar, S., Khalfan, M. and Maqsood, T. (2012) 'Building information modeling (BIM): Now and beyond', *Australasian Journal of Construction Economics and Building*, 12(4), pp. 15–28. doi: 10.5130/ajceb.v12i4.3032.
- Berger, M. and Cristie, V. (2015) 'CFD post-processing in Unity3D', *Procedia Computer Science*, 51(December), pp. 2913–2922. doi: 10.1016/j.procs.2015.05.476.
- Bode, G. *et al.* (2019) 'Cloud, wireless technology, internet of things: The next generation of building automation systems?', *Journal of Physics: Conference Series*, 1343(1), pp. 0–6. doi: 10.1088/1742-6596/1343/1/012059.
- Boje, C. *et al.* (2020) 'Towards a semantic Construction Digital Twin: Directions for future research', *Automation in Construction*. Elsevier, 114(January), p. 103179. doi: 10.1016/j.autcon.2020.103179.
- Dresden, T. (2020) <https://tu-dresden.de/bu/bauingenieurwesen/cib>.
- Editorial, M. (2019) *Rotterdam's Digital Twin Redefines Our Physical, Digital, & Social Worlds*. Available at: <https://eu-smartcities.eu/news/rotterdams-digital-twin-redefines-our-physical-digital-social-worlds>.
- Fabi, V., Spigliantini, G. and Corgnati, S. P. (2017) 'Insights on Smart Home Concept and Occupants' Interaction with Building Controls', in *Energy Procedia*. Elsevier Ltd, pp. 759–769. doi: 10.1016/j.egypro.2017.03.238.
- Fuller, A. *et al.* (2020) 'Digital Twin: Enabling Technologies, Challenges and Open Research', *IEEE Access*, 8, pp. 108952–108971. doi: 10.1109/ACCESS.2020.2998358.
- Ghaffarianhoseini, Ali *et al.* (2017) 'Building Information Modelling (BIM) uptake: Clear benefits, understanding its implementation, risks and challenges', *Renewable and Sustainable Energy Reviews*. Elsevier Ltd, pp. 1046–1053. doi: 10.1016/j.rser.2016.11.083.
- Grieves, M. (2014) 'Digital Twin : Manufacturing Excellence through Virtual Factory

Replication This paper introduces the concept of a A Whitepaper by Dr . Michael Grieves', *White Paper*, (March). Available at: https://www.researchgate.net/publication/275211047_Digital_Twin_Manufacturing_Excellence_through_Virtual_Factory_Replication.

IESVE (2014) *CFD : MicroFlo User Guide*.

IESVE (2020) *CFD as text file*. Available at: https://www.iesve.com/support/ve/knowledgebase_faq/faq/1550 (Accessed: 14 November 2020).

Jones, B. (2017) *Microsoft shows how AI can make a construction site safer at Build 2017*. Available at: <https://www.digitaltrends.com/computing/microsoft-build-2017-ai-workplace/> (Accessed: 12 July 2020).

Kastner, W. *et al.* (2005) 'Communication systems for building automation and control', *Proceedings of the IEEE*, 93(6), pp. 1178–1203. doi: 10.1109/JPROC.2005.849726.

Khajavi, S. H. *et al.* (2019) 'Digital Twin: Vision, benefits, boundaries, and creation for buildings', *IEEE Access*, 7, pp. 147406–147419. doi: 10.1109/ACCESS.2019.2946515.

Li, J. and Zhang, Y. (2013) 'Intelligent building automation and control based on IndasIBMS', *Proceedings of International Conference on Service Science, ICSS*, pp. 266–270. doi: 10.1109/ICSS.2013.51.

Liu, Q. *et al.* (2019) 'Digital twin-driven rapid individualised designing of automated flow-shop manufacturing system', *International Journal of Production Research*. Taylor & Francis, 57(12), pp. 3903–3919. doi: 10.1080/00207543.2018.1471243.

Maile, T., Fischer, M. and Bazjanac, V. (2007) 'Building Energy Performance Simulation Tools - a Life-Cycle and Interoperable Perspective', *Center for integrated facility engineering*, (December), pp. 1–49. Available at: cife.stanford.edu/sites/default/files/WP107.pdf.

Martynova, O. (2020) *Digital Twins in Facility Management: The Clear Path Forward for Intelligent Buildings*. Available at: <https://www.intellias.com/digital-twins-in-facility-management-the-clear-path-forward-for-intelligent-buildings/> (Accessed: 21 June 2020).

Menzel, K. (2018) 'Module VEL-LE-03 : Heat Transfer in Building Elements & Spaces', in *BIM-based Virtual Engineering Lab TU Dresden*.

Mohammadi, N. and Taylor, J. E. (2018) 'Smart city digital twins', *2017 IEEE Symposium Series on Computational Intelligence, SSCI 2017 - Proceedings*, 2018-Janua, pp. 1–5. doi: 10.1109/SSCI.2017.8285439.

Motlagh, N. H. *et al.* (2019) 'An IoT-based automation system for older homes: A

use case for lighting system', *Proceedings - IEEE 11th International Conference on Service-Oriented Computing and Applications, SOCA 2018*, 2019-Janua, pp. 247–252. doi: 10.1109/SOCA.2018.8645771.

Nasaruddin, A. N., Ito, T. and Tuan, T. B. (2018) 'Digital Twin Approach to Building Information Management', *The Proceedings of Manufacturing Systems Division Conference*, 2018(0), p. 304. doi: 10.1299/jsmemsd.2018.304.

Qi, Q. and Tao, F. (2018) 'Digital Twin and Big Data Towards Smart Manufacturing and Industry 4.0: 360 Degree Comparison', *IEEE Access*. IEEE, 6, pp. 3585–3593. doi: 10.1109/ACCESS.2018.2793265.

Rwamamara, R. *et al.* (2010) 'Using visualization technologies for design and planning of a healthy construction workplace', *Construction Innovation*, 10(3), pp. 248–266. doi: 10.1108/14714171011060060.

Sacks, R. *et al.* (2018) *BIM Handbook*, *BIM Handbook*. John Wiley & Sons, Inc. doi: 10.1002/9781119287568.

Schachinger, D. and Kastner, W. (2016) 'Semantics for smart control of building automation'. IEEE, pp. 1073–1078.

Schinkel, F. (2020) *Visualisierung von IoT-Systemen zur Gebäudeautomation in VR*. Technische Universität Dresden.

Tao, F. *et al.* (2019) 'Digital Twin in Industry: State-of-the-Art', *IEEE Transactions on Industrial Informatics*. IEEE, 15(4), pp. 2405–2415. doi: 10.1109/TII.2018.2873186.

Tetik, M. *et al.* (2019) 'Direct digital construction: Technology-based operations management practice for continuous improvement of construction industry performance', *Automation in Construction*. Elsevier, 107(September), p. 102910. doi: 10.1016/j.autcon.2019.102910.

Wasmi, T. and Salih, M. (2019) 'Insulation Materials', (January 2016). doi: 10.13140/RG.2.2.36009.03681.

Woods, E. and Freas, B. (2019) 'Creating Zero Carbon Communities: The Role of Digital Twins Commissioned by Integrated Environmental Solutions (IES) Eric Woods', *White Paper*.

Appendices

Appendix A: Sensor data from BAS

A.1: Brightness sensor data for respective rooms

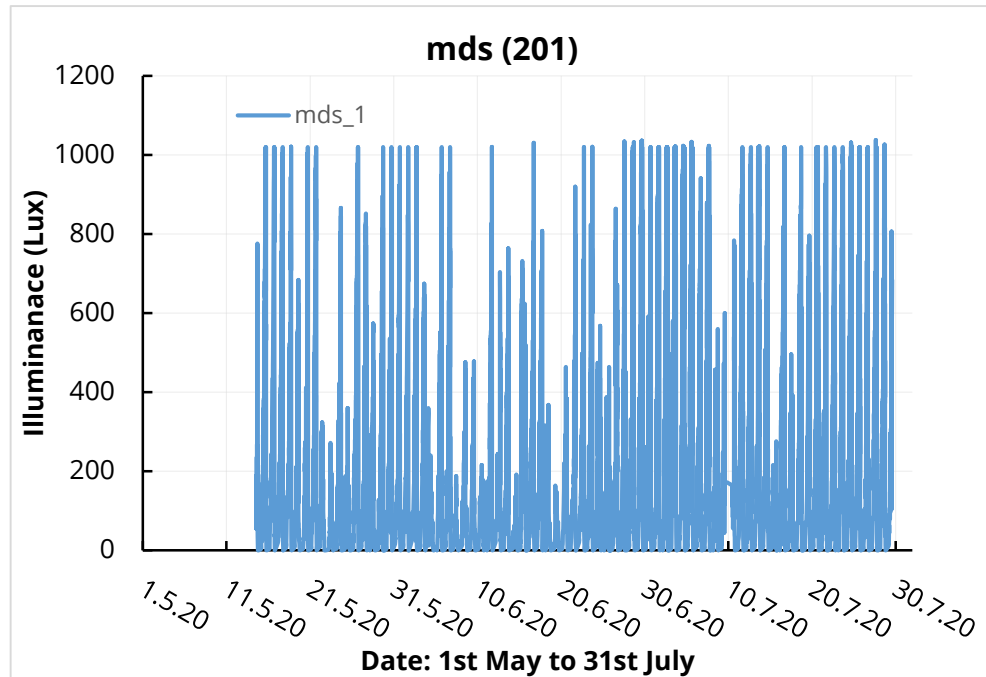


Figure 88: Illuminance (brightness) levels measured by mds-sensor in room 201.

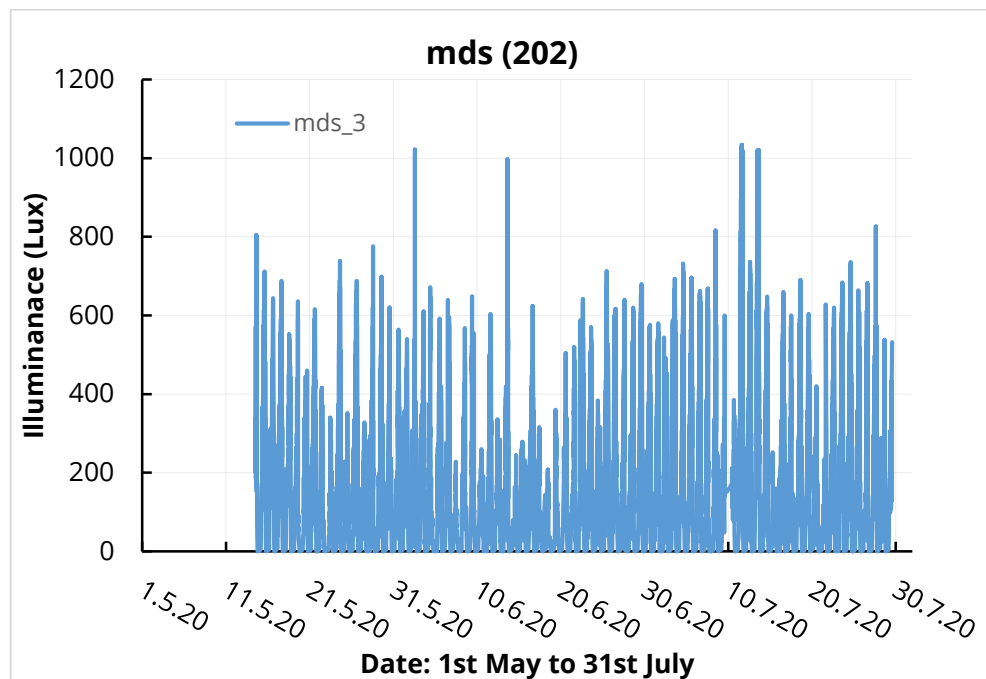


Figure 89: Illuminance (brightness) levels measured by mds-sensor in room 202.

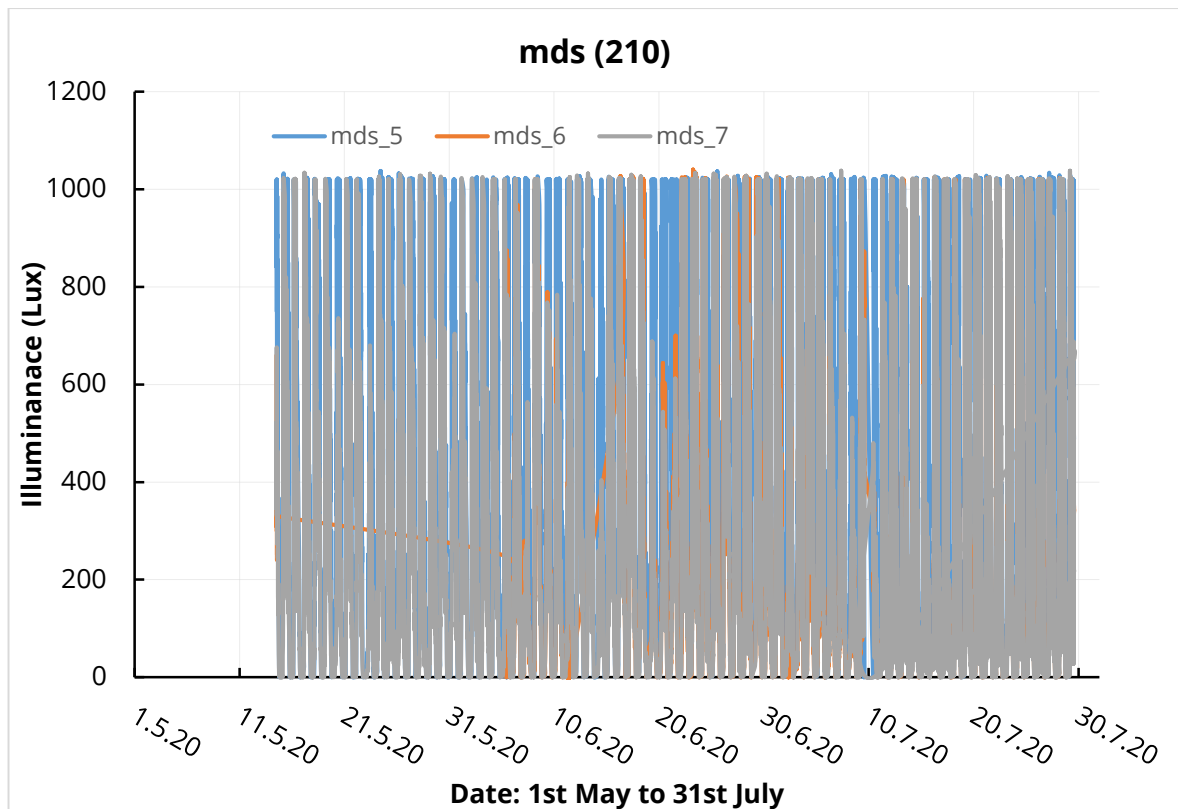


Figure 90: Illuminance (brightness) levels measured by mds-sensors in room 210.

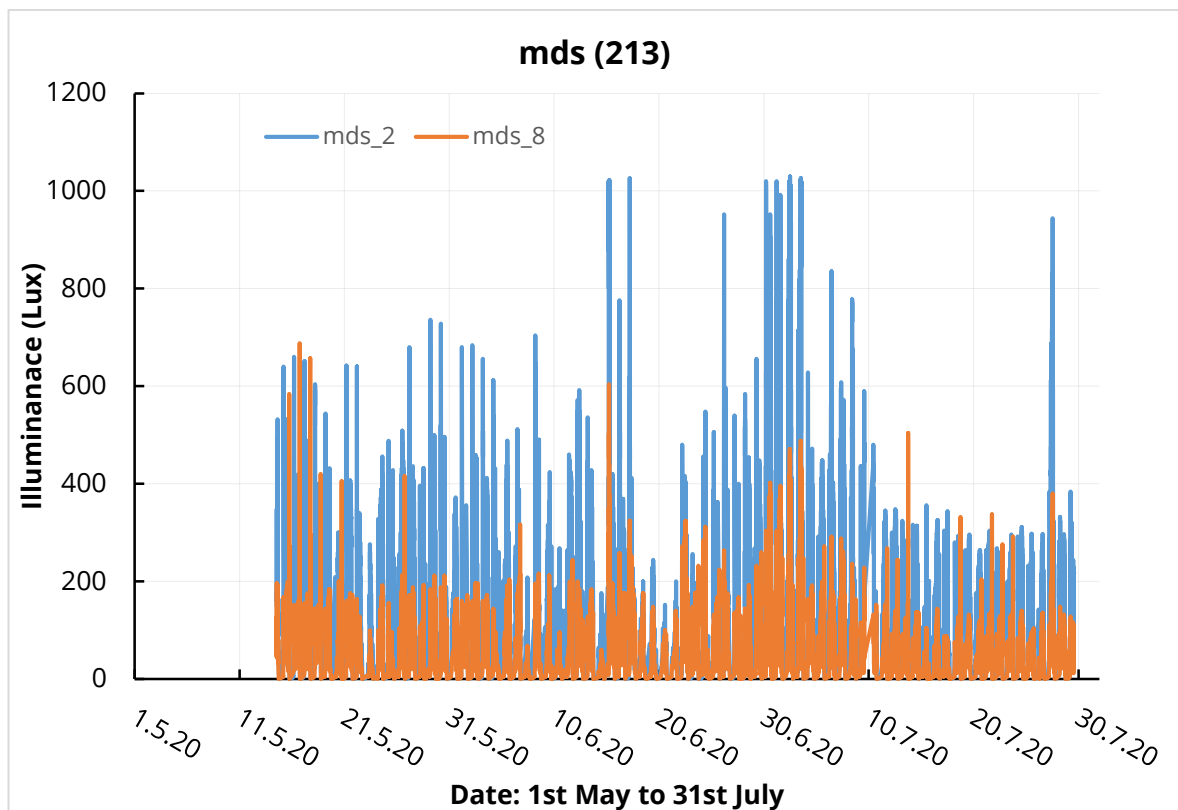


Figure 91: Illuminance (brightness) levels measured by mds-sensors in room 213.

Appendix B: Existing IES VE model

B.1: Construction details

Ground floor:

Material	Thickness mm	Conductivity W/(m·K)	Density kg/m ³	Specific Heat Capacity J/(kg·K)	Resistance m ² K/W	Vapour Resistivity GN·s/(kg·m)	Category
[STD_PH1] Insulation	98.2	0.0250	700.0	1000.0	3.9280	-	Insulating Materials
[STD_CC2] Reinforced Concrete	100.0	2.3000	2300.0	1000.0	0.0435	-	Concretes
Cavity	50.0	-	-	-	0.2100	-	-
[STD_FBA] Chipboard Flooring	20.0	0.1300	500.0	1600.0	0.1538	-	Boards, Sheets & Decking

Figure 92: Ground floor construction details (U-value: 0.2200 W/m²K).

Internal floor/Ceiling:

Material	Thickness mm	Conductivity W/(m·K)	Density kg/m ³	Specific Heat Capacity J/(kg·K)	Resistance m ² K/W	Vapour Resistivity GN·s/(kg·m)	Category
[BASEC03] SYNTHETIC CARPET	20.0	0.0600	160.0	2500.0	0.3333	200.000	Carpets
[USCB0000] LW CONCRETE BLOCK - HF-C2	280.0	0.3800	609.0	837.0	0.7368	83.000	Concretes

Figure 93: Internal 300 mm floor construction details (U-value: 0.7873 W/m²K).

Material	Thickness mm	Conductivity W/(m·K)	Density kg/m ³	Specific Heat Capacity J/(kg·K)	Resistance m ² K/W	Vapour Resistivity GN·s/(kg·m)	Category
[STD_CHF] Chipboard Flooring	20.0	0.1300	500.0	1600.0	0.1538	-	Boards, Sheets & Decking
Cavity	50.0	-	-	-	0.2100	-	-
[STD_SC1] SCREED	50.0	1.1500	1800.0	1000.0	0.0435	-	Screeds & Renders
[STD_CC2] Reinforced Concrete	100.0	2.3000	2300.0	1000.0	0.0435	-	Concretes
Cavity	50.0	-	-	-	0.2100	-	-
[STD_US4] Plasterboard	12.5	0.2100	700.0	1000.0	0.0595	0.000	Plaster

Figure 94: Internal 282.5 mm floor construction details (U-value: 1.0866 W/m²K).

Exterior wall:

Material	Thickness mm	Conductivity W/(m·K)	Density kg/m ³	Specific Heat Capacity J/(kg·K)	Resistance m ² K/W	Vapour Resistivity GN·s/(kg·m)	Category
[ALM] ALUMINIUM	1.0	160.0000	2800.0	896.0	0.0000	3000000.000	Metals

Figure 95: External 1 mm aluminium wall construction details (U-value: 5.8821 W/m²K).

Material	Thickness mm	Conductivity W/(m·K)	Density kg/m ³	Specific Heat Capacity J/(kg·K)	Resistance m ² K/W	Vapour Resistivity GN·s/(kg·m)	Category
[STD_SM1] Rainscreen	3.0	50.0000	7800.0	450.0	0.0001	-	Metals
Cavity	50.0	-	-	-	0.1300	-	-
[STD_EPS] Insulation	81.4	0.0250	20.0	1030.0	3.2560	-	Insulating Materials
[STD_USP] Cement bonded particle board	12.0	0.2300	1100.0	1000.0	0.0522	0.000	Boards, Sheets & Decking
Cavity	50.0	-	-	-	0.1800	-	-
[STD_US1] Plasterboard	12.5	0.2100	700.0	1000.0	0.0595	0.000	Plaster

Figure 96: External 208.9 mm wall construction details (U-value: 0.2599 W/m²K).

Material	Thickness mm	Conductivity W/(m·K)	Density kg/m³	Specific Heat Capacity J/(kg·K)	Resistance m²K/W	Vapour Resistivity GN's/(kg·m)	Category
[SM] STEEL	1.0	50.0000	7800.0	480.0	0.0000	3000000.000	Metals

Figure 97: External 1 mm steel wall construction details (U-value: 5.8817 W/m²K).

Material	Thickness mm	Conductivity W/(m·K)	Density kg/m³	Specific Heat Capacity J/(kg·K)	Resistance m²K/W	Vapour Resistivity GN's/(kg·m)	Category
[PLL] PLASTER (LIGHTWEIGHT)	20.0	0.1600	600.0	1000.0	0.1250	45.000	Plaster
[CCD] CAST CONCRETE (MEDIUM)	300.0	1.4000	2100.0	840.0	0.2143	500.000	Concretes
[PLL] PLASTER (LIGHTWEIGHT)	20.0	0.1600	600.0	1000.0	0.1250	45.000	Plaster

Figure 98: External 340 mm wall construction details (U-value: 1.5766 W/m²K).

Interior wall/Partition:

Material	Thickness mm	Conductivity W/(m·K)	Density kg/m³	Specific Heat Capacity J/(kg·K)	Resistance m²K/W	Vapour Resistivity GN's/(kg·m)	Category
[STD_US2] Plasterboard	15.0	0.2100	700.0	1000.0	0.0714	0.000	Plaster
Cavity	125.0	-	-	-	0.1800	-	-
[STD_US3] Plasterboard	15.0	0.2100	700.0	1000.0	0.0714	0.000	Plaster

Figure 99: Internal 155 mm wall construction details (U-value: 1.7157 W/m²K).

Material	Thickness mm	Conductivity W/(m·K)	Density kg/m³	Specific Heat Capacity J/(kg·K)	Resistance m²K/W	Vapour Resistivity GN's/(kg·m)	Category
[STD_US2] Plasterboard	12.5	0.2100	700.0	1000.0	0.0595	0.000	Plaster
Cavity	50.0	-	-	-	0.1800	-	-
[STD_US3] Plasterboard	12.5	0.2100	700.0	1000.0	0.0595	0.000	Plaster

Figure 100: External 75 mm wall construction details (U-value: 1.7888 W/m²K).

Door:

Material	Thickness mm	Conductivity W/(m·K)	Density kg/m³	Specific Heat Capacity J/(kg·K)	Resistance m²K/W	Vapour Resistivity GN's/(kg·m)	Category
[STDCRM21] Plywood- 30 mm	37.0	0.1300	500.0	1500.0	0.2846	-	Timber

Figure 101: Door construction details (U-value: 2.1977 W/m²K).

Window/Glazing:

Material	Thickness mm	Conductivity W/(m·K)	Angular Dependence	Gas	Convection Coefficient W/m²·K	Resistance m²K/W	Transmittance	Outside Reflectance	Inside Reflectance	Refractive Index	Outside Emissivity	Inside Emissivity	Visible Light Specified
[STD_EXW] Outer Pane	6.0	1.0600	Fresnel	-	-	0.0057	0.409	0.289	0.414	1.526	0.837	0.042	No
Cavity	12.0	-	-	Argon	1.4033	0.6183	-	-	-	-	-	-	-
[STD_INW] Inner Pane	6.0	1.0600	Fresnel	-	-	0.0057	0.783	0.072	0.072	1.526	0.837	0.837	No

Figure 102: Window construction details (U-value: 1.600 W/m²K).

Material	Thickness mm	Conductivity W/(m·K)	Angular Dependence	Gas	Convection Coefficient W/m ² ·K	Resistance m ² ·K/W	Transmittance	Outside Reflectance	Inside Reflectance	Refractive Index	Outside Emissivity	Inside Emissivity	Visible Light Specified
[STD_EXW] Outer Pane	6.0	1.0600	Fresnel	-	-	0.0057	0.409	0.289	0.414	1.526	0.837	0.042	No
Cavity	12.0	-	-	Argon	1.4033	0.6183	-	-	-	-	-	-	-
[STD_INW] Inner Pane	6.0	1.0600	Fresnel	-	-	0.0057	0.783	0.072	0.072	1.526	0.837	0.837	No

Figure 103: Window construction details (U-value: 1.600 W/m²K).

Material	Thickness mm	Conductivity W/(m·K)	Angular Dependence	Gas	Convection Coefficient W/m ² ·K	Resistance m ² ·K/W	Transmittance	Outside Reflectance	Inside Reflectance	Refractive Index	Outside Emissivity	Inside Emissivity	Visible Light Specified
[STDGBM09] 0 mm clear glass (for	0.0	1.0000	Fresnel	-	-	0.0000	0.816	0.074	0.074	1.526	0.840	0.840	No

Figure 104: Window construction details (U-value: 3.8462 W/m²K).

Material	Thickness mm	Conductivity W/(m·K)	Angular Dependence	Gas	Convection Coefficient W/m ² ·K	Resistance m ² ·K/W	Transmittance	Outside Reflectance	Inside Reflectance	Refractive Index	Outside Emissivity	Inside Emissivity	Visible Light Specified
[STD_RF0] Outer Pane	6.0	1.0600	Fresnel	-	-	0.0057	0.580	0.186	0.227	1.526	0.837	0.209	No
Cavity	12.0	-	-	Argon	2.2396	0.3056	-	-	-	-	-	-	-
[STD_RF1] Inner Pane	6.0	1.0600	Fresnel	-	-	0.0057	0.783	0.072	0.072	1.526	0.837	0.837	No

Figure 105: Window construction details (U-value: 2.300 W/m²K).

Roof:

Material	Thickness mm	Conductivity W/(m·K)	Density kg/m ³	Specific Heat Capacity J/(kg·K)	Resistance m ² ·K/W	Vapour Resistivity GN·s/(kg·m)	Category
[STD_CC2] Reinforced Concrete	300.0	2.3000	2300.0	1000.0	0.1304	-	Concretes

Figure 106: Roof 300 mm construction details (U-value: 3.6977 W/m²K).

Material	Thickness mm	Conductivity W/(m·K)	Density kg/m ³	Specific Heat Capacity J/(kg·K)	Resistance m ² ·K/W	Vapour Resistivity GN·s/(kg·m)	Category
[STD_PHF] Insulation	154.4	0.0300	40.0	1450.0	5.1467	-	Insulating Materials
[STD_MEM] Membrane	0.1	1.0000	1100.0	1000.0	0.0001	-	Asphalts & Other Roofing
[STD_CC1] Concrete Deck	100.0	2.0000	2400.0	1000.0	0.0500	-	Concretes
Cavity	50.0	-	-	-	0.1600	-	-
[STD_US5] Plasterboard	12.5	0.2100	700.0	1000.0	0.0595	0.000	Plaster

Figure 107: Roof 317 mm construction details (U-value: 1.1800 W/m²K).

B.2: Location and weather file details

The screenshot shows the 'ApLocate - institute' software interface with the 'Location & Site Data' tab selected. The 'Location Data' section shows 'Dresden, Germany' as the location, with latitude 51.03° N, longitude 13.72° E, elevation 230.1 m, and time zone 1 (hours ahead of GMT). The 'Daylight saving time' section shows a time adjustment of 1 hour, from April to October. The 'Site Data' section shows ground reflectance of 0.20 for summer and winter, terrain type 'Suburbs', and reference air density of 1.200 kg/m³. The 'Design Weather Data' section shows the 'Selection Wizard...' button and 'Add to custom database' button. The 'Simulation Weather Data' section shows the 'Design Weather Data Source and Statistics' table.

	Min Tdb (°C)	Max Tdb (°C)	Twb at Max Tdb (°C)
Jan	7.60	12.30	9.10
Feb	9.80	15.40	10.30
Mar	11.30	18.00	10.80
Apr	14.20	22.60	13.00
May	16.80	26.30	16.60
Jun	21.40	30.30	18.50
Jul	22.60	32.30	20.20
Aug	23.50	32.90	20.10
Sep	19.20	27.10	17.80
Oct	16.80	23.80	16.90
Nov	9.30	14.20	10.80
Dec	9.40	13.70	9.50

Figure 108: Location selection and corresponding weather parameters.

The screenshot shows the 'Location & Weather Data Wizard' (Page 4 of 4) in the 'ApLocate - institute' software. The 'ApacheSim' section shows the file 'BerlinIWEV.fwt' selected. The 'UK Building Regulations' section shows 'City: None' selected. The 'Simulation Weather File' section shows 'None' selected. A 'Climate Data Files...' dialog box is open, showing a list of nearest weather files. The file '111km: PragueIWEV.fwt' is selected.

Distance	File Name
111km	PragueIWEV.fwt
113km	BerlinIWEV.fwt
354km	MunichIWEV.fwt
452km	InnsbruckIWEV.fwt
465km	GrazIWEV.fwt
519km	WarsawIWEV.fwt
519km	CopenhagenIWEV.fwt
597km	StHubertIWEV.fwt
597km	NancyIWEV.fwt
623km	VeniceIWEV.fwt
623km	VicenzaIGDG.fwt
633km	AmsterdamIWEV.fwt
643km	BrusselsIWEV.fwt
705km	MilanIWEV.fwt
758km	OostendeIWEV.fwt
759km	TorinoIWEV.fwt
845km	NorwichIWEV.fwt
849km	ParisOrlyIWEV.fwt
854km	PisaIWEV.fwt
867km	FRA_Lyon_074810_IWEV.fwt
978km	KewIWEV.fwt
978km	KEW.FWT
978km	Hrow9697.fwt

Figure 109: Nearest to site weather file.

B.3: Thermal templates

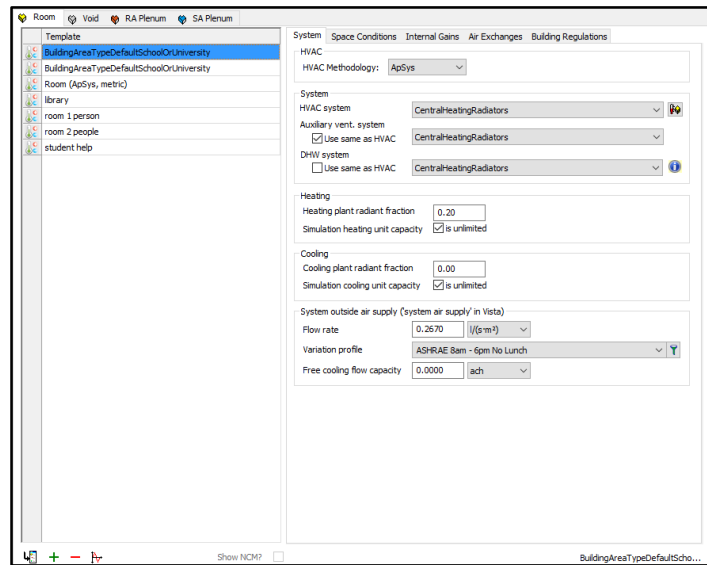


Figure 110: Thermal template for various space systems.

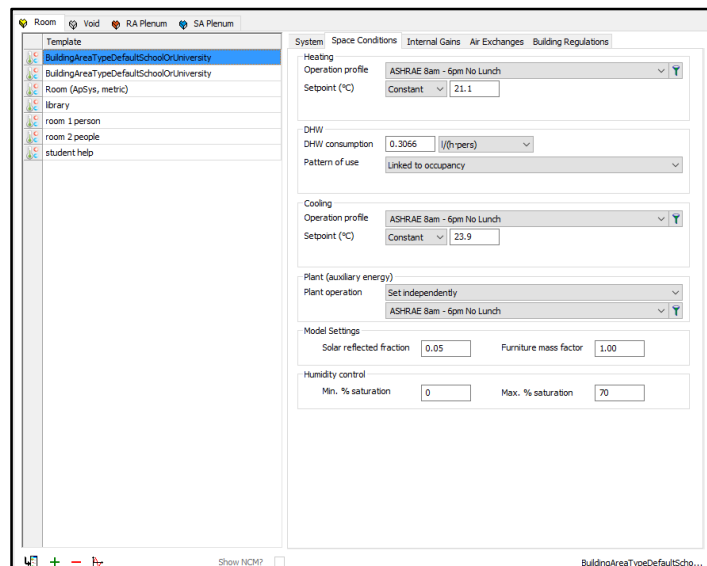


Figure 111: Thermal template for space conditions.

Type	Gain Reference	Maximum Sensible	Maximum Latent G	Occupancy	Max Power C	Radiant Fracto	Meter	Variation	Dimming	Add To Tem
People	1 person	90,000 W/person	60,000 W/person	1,000 people	-	-	-	Biuniform	-	-
People	2 People	90,000 W/person	60,000 W/person	2,000 people	-	-	-	Biuniform	-	-
Fluorescent Lighting	1.2 - 8 W/ft	12,917 W/ft	-	-	12,917 W/ft	0.45	Electricity: Meter	Biuniform	on contr	T
Miscellaneous	0.5 - 8 W/ft	5,382 W/ft	0,000 W/ft	-	5,382 W/ft	0.22	Electricity: Meter	Biuniform	-	T
People	250 - 8 W/ft - 157	73,358 W/person	58,614 W/person	15,515 m ² /pe	-	-	-	Biuniform	-	T

+ Add Internal Gain
 - Remove Internal Gain
 Select All
Deselect All

Type: People
 Reference: 1 person

Occupancy units: People

Variation Profile: Sainformatik Week

Maximum Sensible Gain (W/P): 90,000

Maximum Latent Gain (W/P): 60,000

Number of people: 1,000

Diversity factor: 1

% of convective gain to RA plenum: 0.00 %

☒ Allow profile to saturate for loads analysis?

OK
Cancel

Figure 112: Thermal template for space internal gains.

B.4: VistaPro

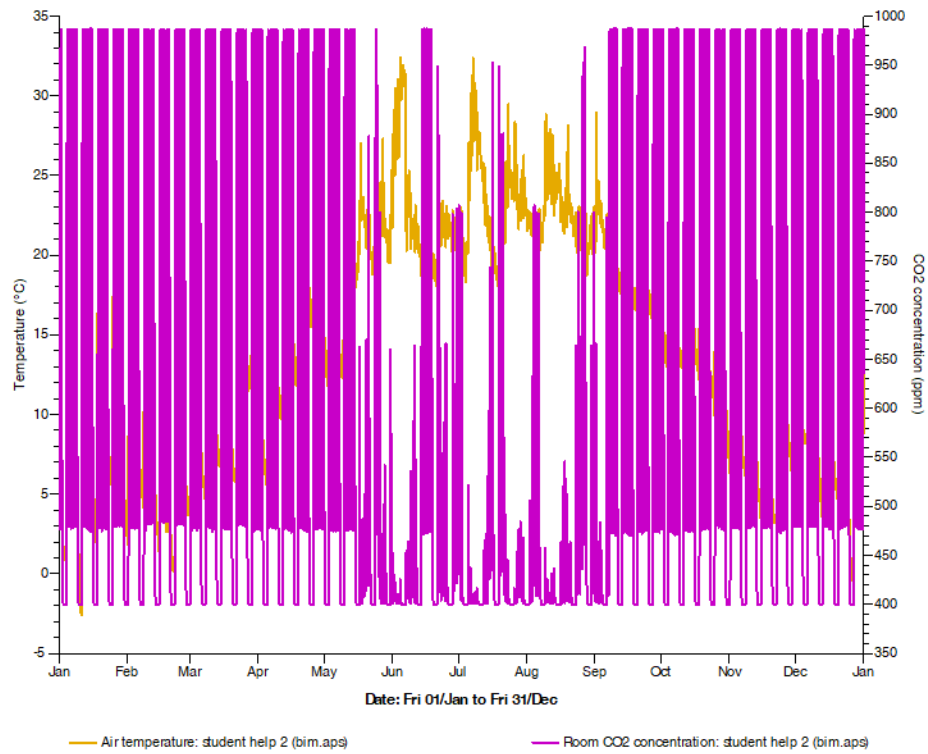


Figure 113: Correlation between air temperature and CO2 concentration (student help).

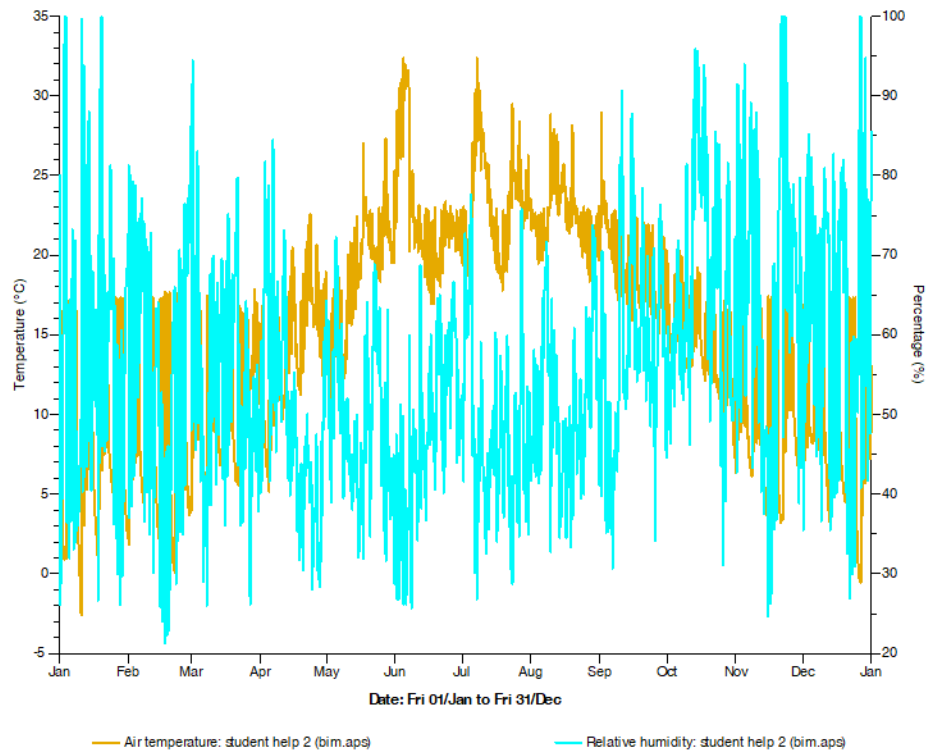


Figure 114: Correlation between air temperature and relative humidity (student help).

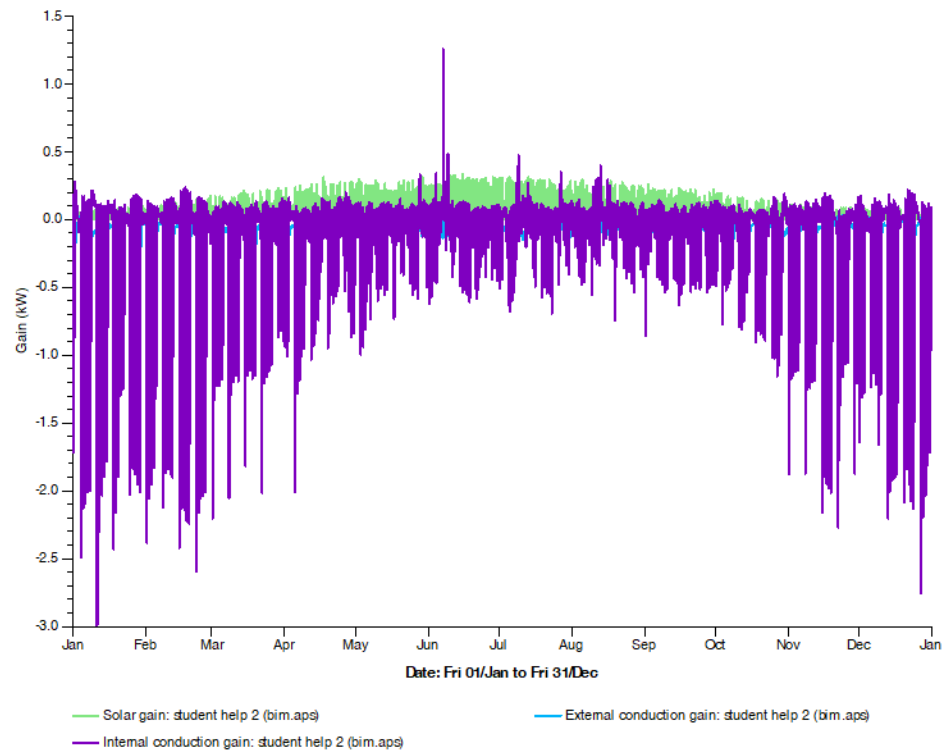


Figure 115: Correlation between solar gain and conduction gain (external and internal) (student help).

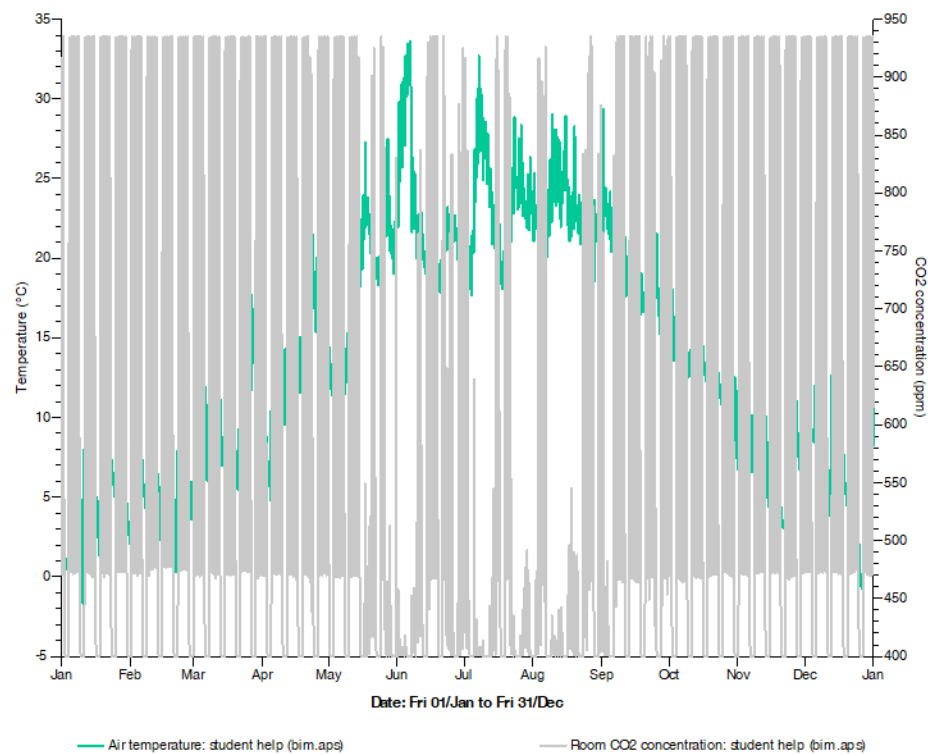


Figure 116: Correlation between air temperature and CO2 concentration (laboratory).

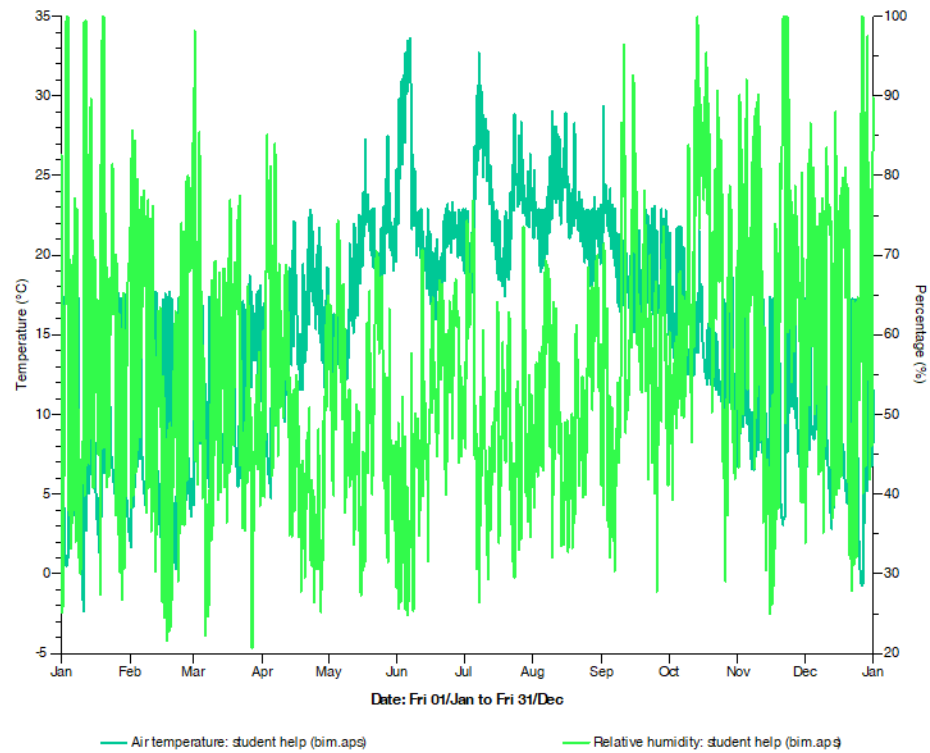


Figure 117: Correlation between air temperature and relative humidity (laboratory).

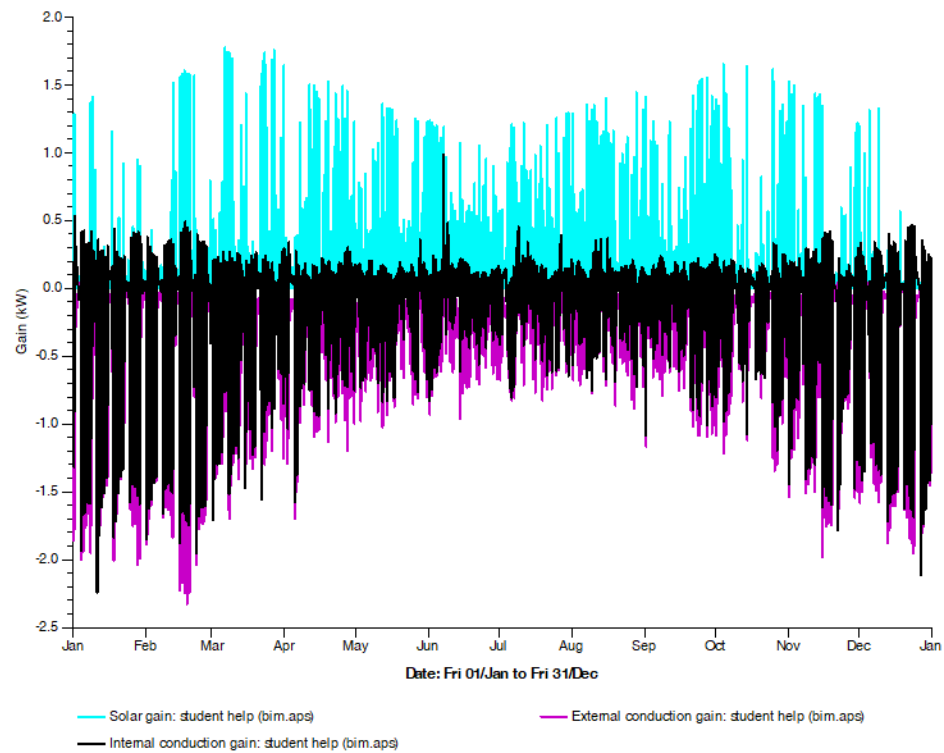


Figure 118: Correlation between solar gain and conduction gain (external and internal) (laboratory).

B.5.1: Radiance IES templates

Simulate View Images Sky/Eye Surface Properties Component Settings Luminaire Settings Sensor Settings Dynamic Results WP Grid AOI VSC

Type

- ☐ Luminance
- ☐ Illuminance
- ☐ Sensors
- ☒ Advanced

Options

Quality:

WP height (m)

WP grid (m)

Show Summary ☐

Overture (pre-sim) ☒

Simulation

Figure 119: Selected Annual Sunlight Exposure (ASE) for the daylighting simulation.

Simulate View Images Sky/Eye Surface Properties Component Settings Luminaire Settings Sensor Settings Dynamic Results WP Grid AOI VSC

Results

- 1_000001.ase
- 1_000001.awp
- 1_000001.sda
- 1_000001_Jul17@15-59-34.sda

Room ID/Name:

Post Processing

☒ AWP ☒ ASE ☒ sDA ☒ Backups ☒ Select

Figure 120: Generated dynamic results for ASE simulation.

Process Annual WP data

Analysis Period

Start Time Finish Time

☐ Use data roughening

Filter

☐ Remove Weekends

☐ Remove Holidays

☒ ASE

Target Lux for Hours

☐ Useful Daylight Illuminance (UDI)

☐ Threshold

☐ ALE

File Options

☐ Append Data to File ☐ Apply to ALL

Figure 121: The target of 750 Lux for 50 hours in the ASE simulation.

Simulation Options

Ground Reflectance	Window Frames	Sky Resolution
Working Plane	Maintenance Factor	AOI Shrinkage

Working Plane

The Working Plane (WP) is a virtual plane which is set at a given height above the floor of the zone.

Plane height (m):

Grid Size

Grid size is the pitch of a grid of points across the WP, which is used for "WP Data" and "Dynamic" simulations.

Grid Size (m):

☐ **Customise Maintenance Factors**

The Maintenance Factor is used to take account of a reduction in the reflectivity of surfaces (or for glass – the transmissivity) due to dirt on the surface.

Surface Maint. Factor (%):

Glazing Maint. Factor (%):

Figure 122: Template for the Radiance IES simulation.

Simulation Options

Ground Reflectance	Window Frames	Sky Resolution
Working Plane	Maintenance Factor	AOI Shrinkage

Area Of Interest (AOI) - Shrinkage

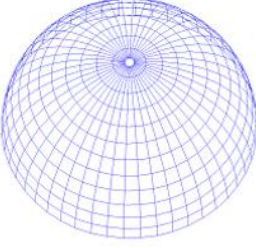
The Area of Interest (AOI) is created by subtracting this distance from the outer boundary of the zone.

Shrinkage (m)

☒ Automatically Create AOI files

Sky Resolution

The Sky Resolution is the number of patches the sky hemisphere is divided into for the calculation of the Daylight Coefficients used in the Dynamic Daylighting Simulations.



☐ 145 Patches

☒ 577 Patches

☐ 2305 Patche

Figure 123: Template parameters selected for Radiance IES simulation.

B.5.2: Radiance IES simulations

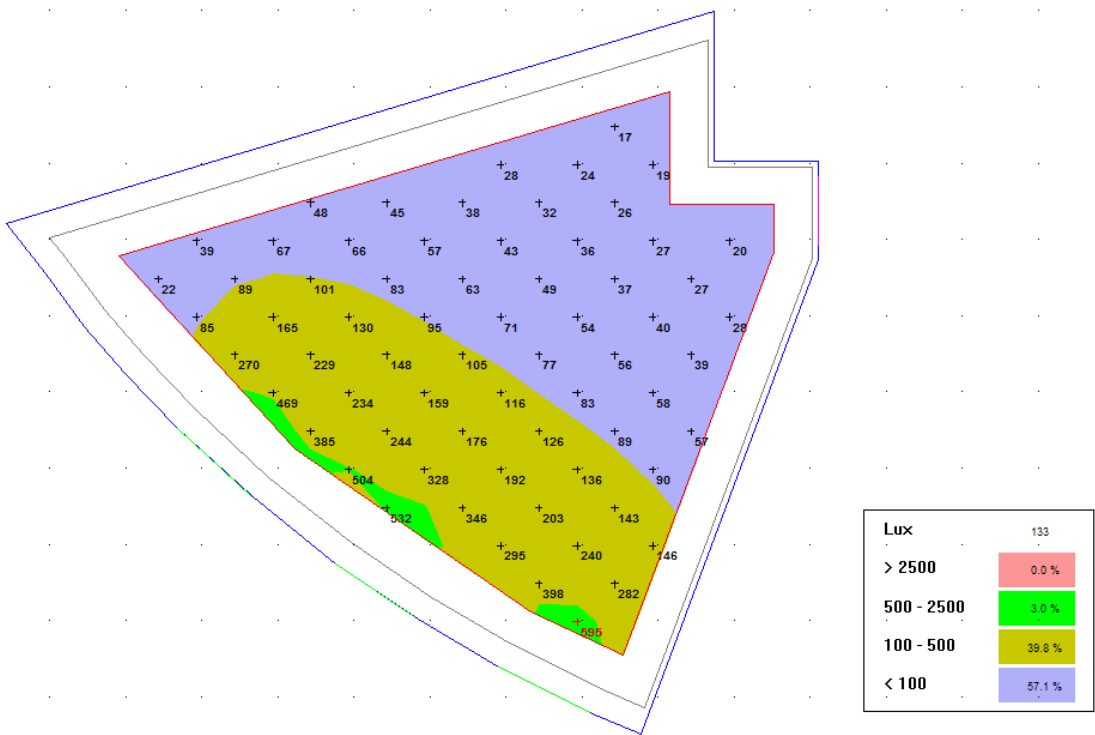


Figure 124: Illuminance in room 201 (library).

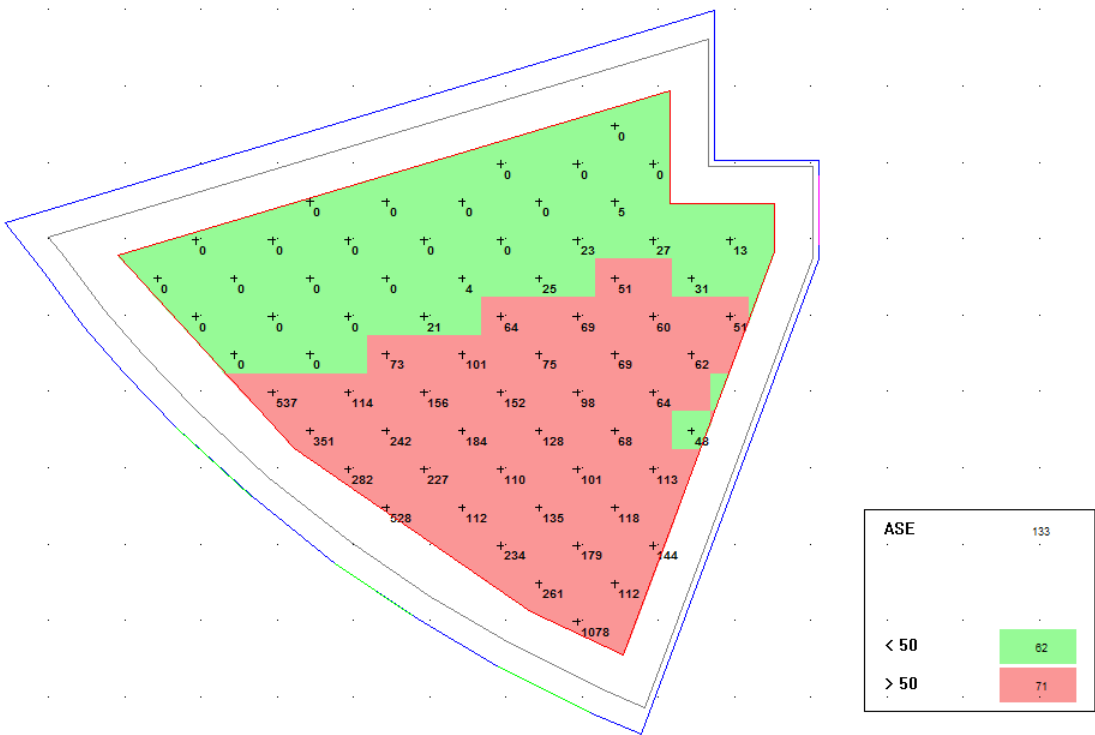


Figure 125: The ASE simulation with a target of 750 Lux for at least 50 hours in room 201 (library)

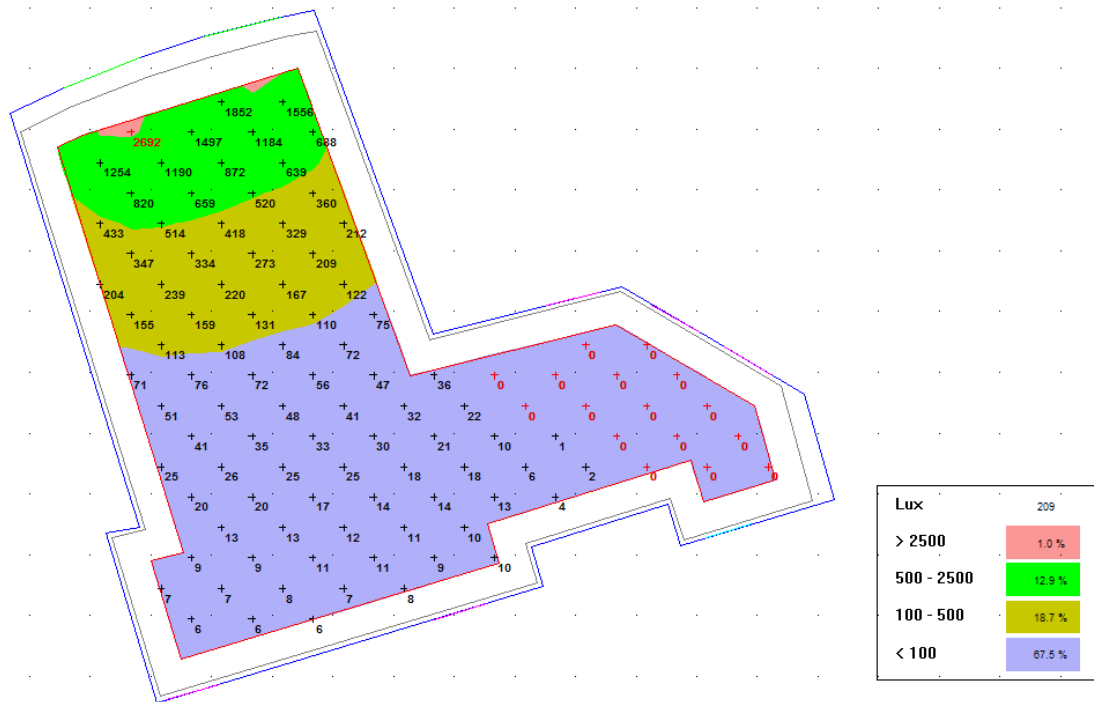


Figure 126: Illuminance in room 213 (VR cave).

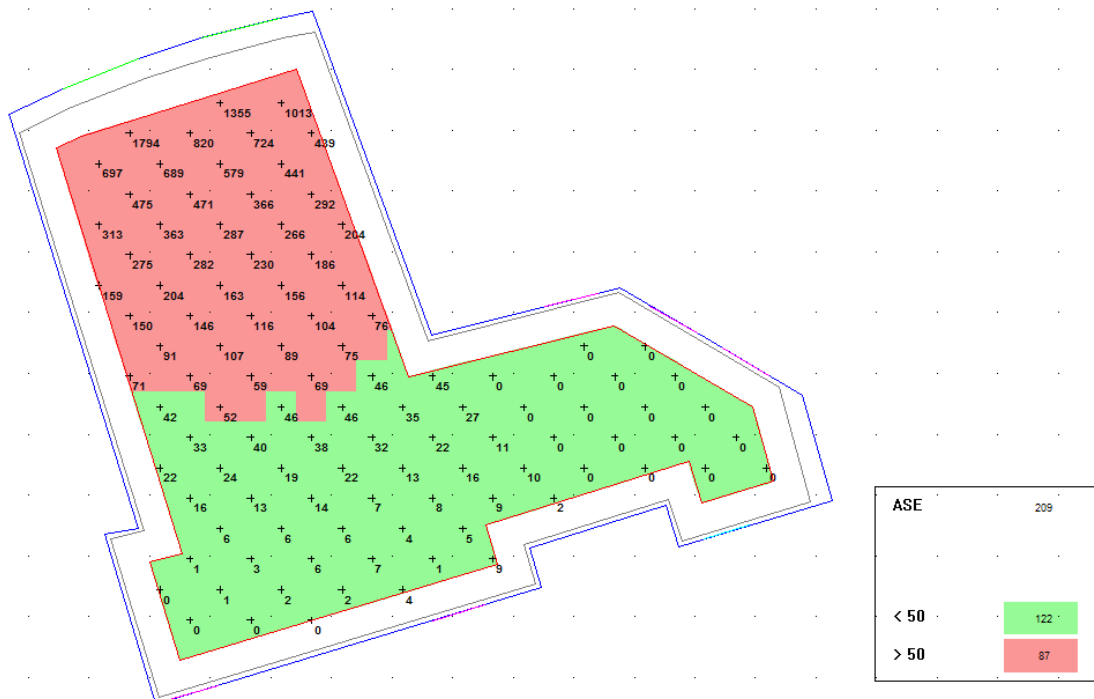


Figure 127: The ASE simulation with a target of 750 Lux for at least 50 hours in room 213 (VR cave).

B.6.1: MicroFlo (CFD) templates

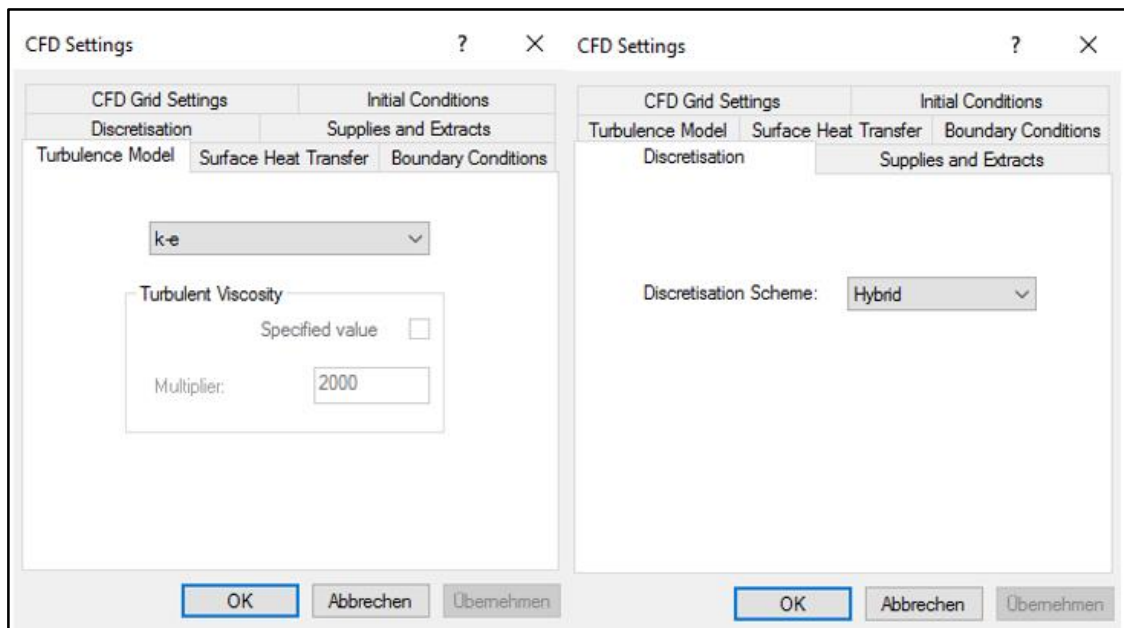


Figure 128: Template for running a CFD analysis.

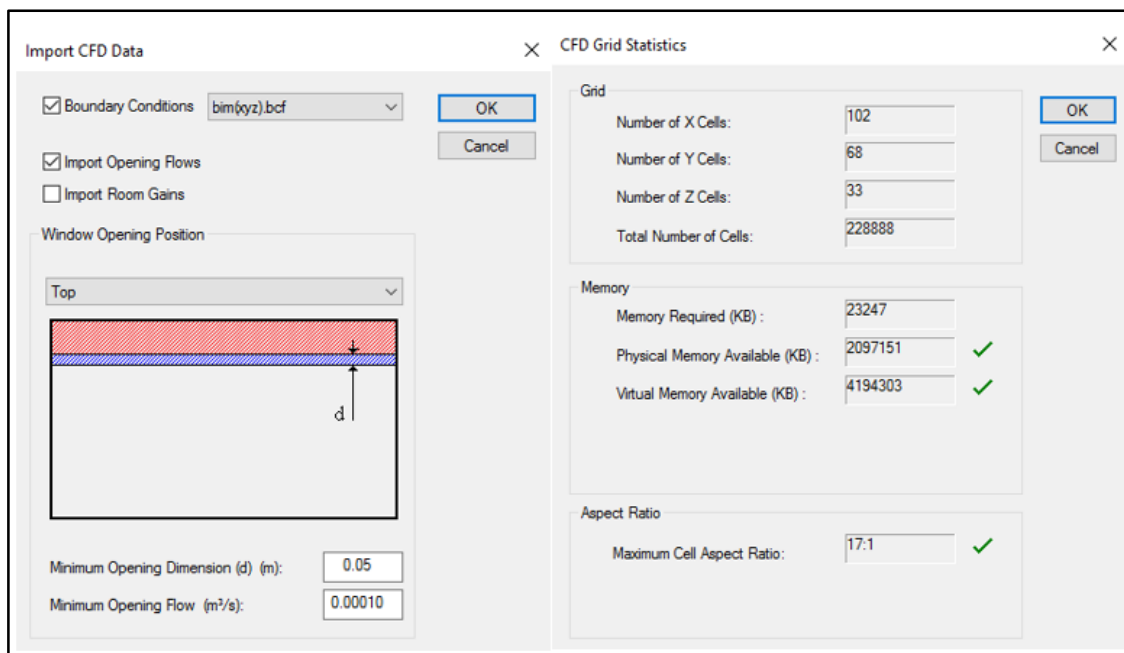


Figure 129: Template for importing boundary conditions to run a MicroFlo (CFD) analysis at a particular instance of time.

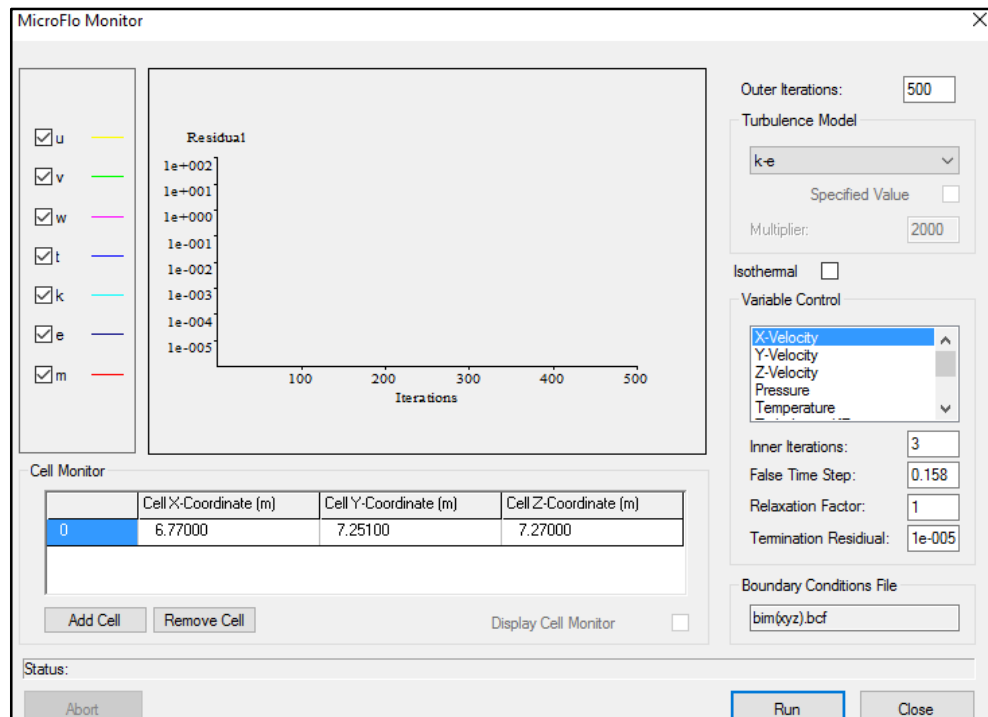


Figure 130: Defining the iteration level (500 iterations) for CFD analysis.

B.6.2: MicroFlo (CFD) simulation

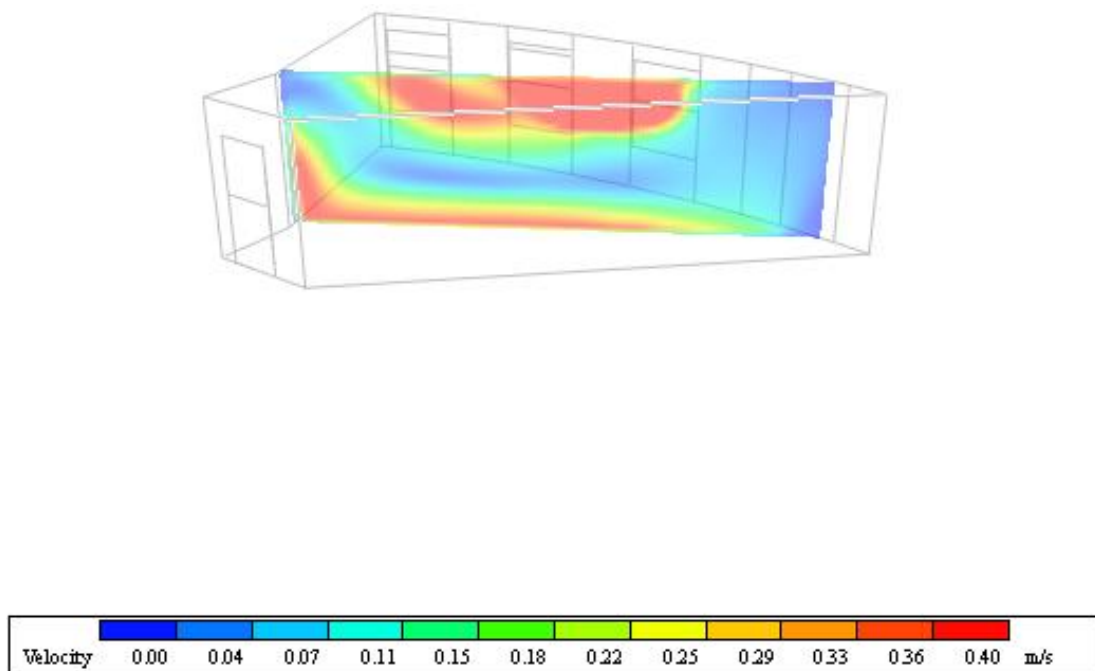


Figure 131: CFD (velocity filled contour) in the 210 room.

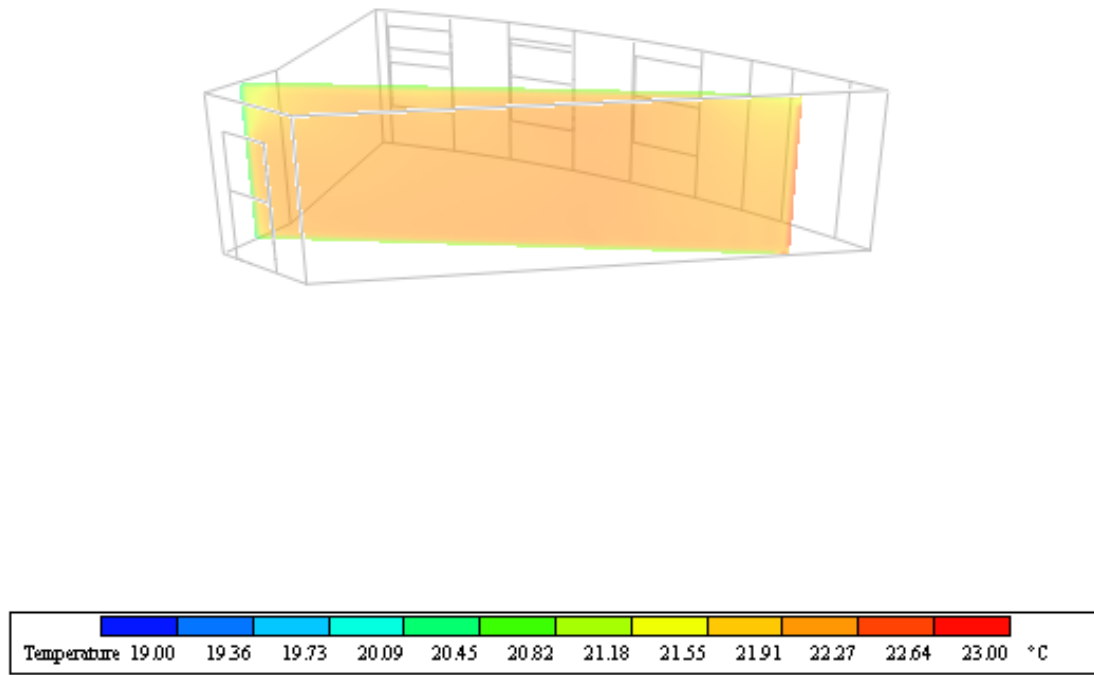


Figure 132: CFD (temperature filled contour) in the 210 room.

Appendix C: Calibration of simulation and sensor data

C.1: Pre-calibration IES simulation and sensor data

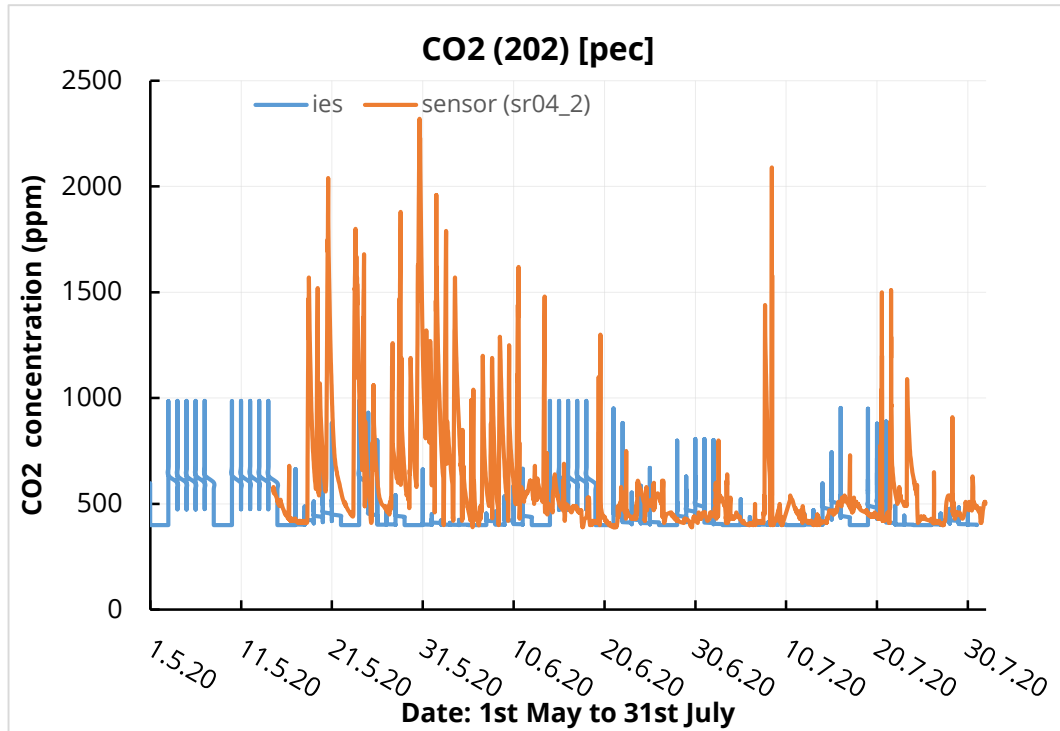


Figure 133: CO₂ concentration levels from the IES simulations and from the sensors in room 202.

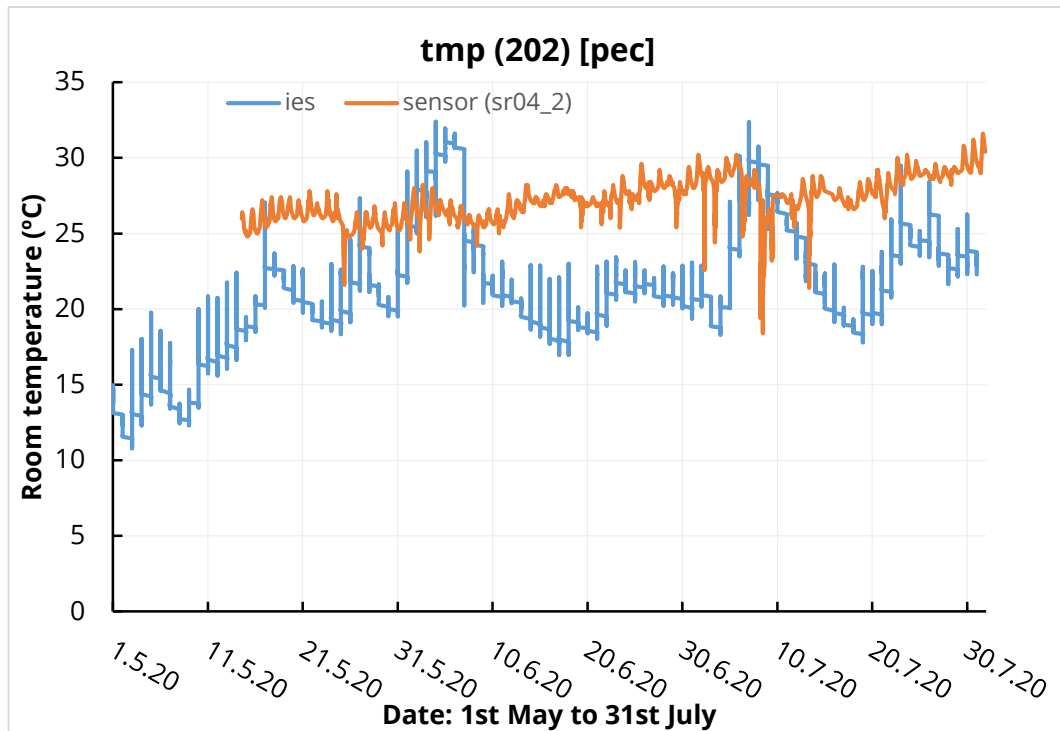


Figure 134: Temperature levels from the IES simulations and the sensors in room 202.

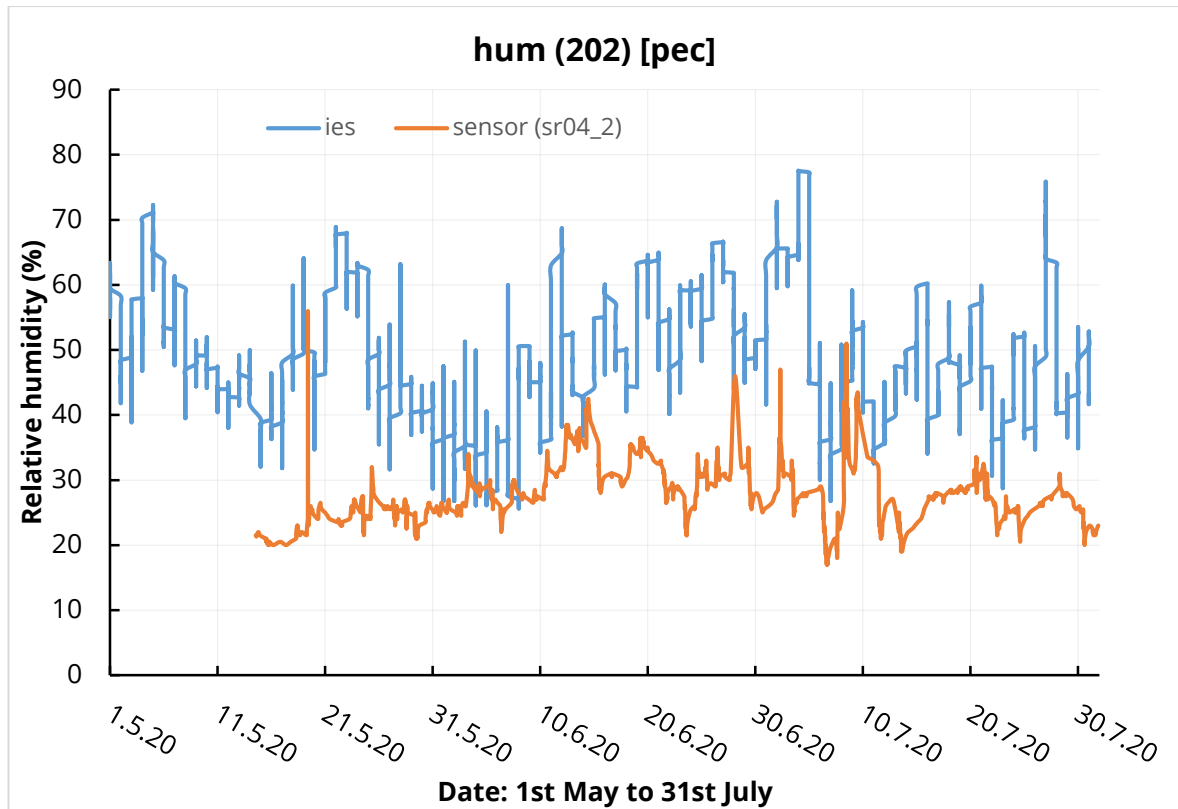


Figure 135: Relative humidity levels from the IES simulations and the sensors in room 202.

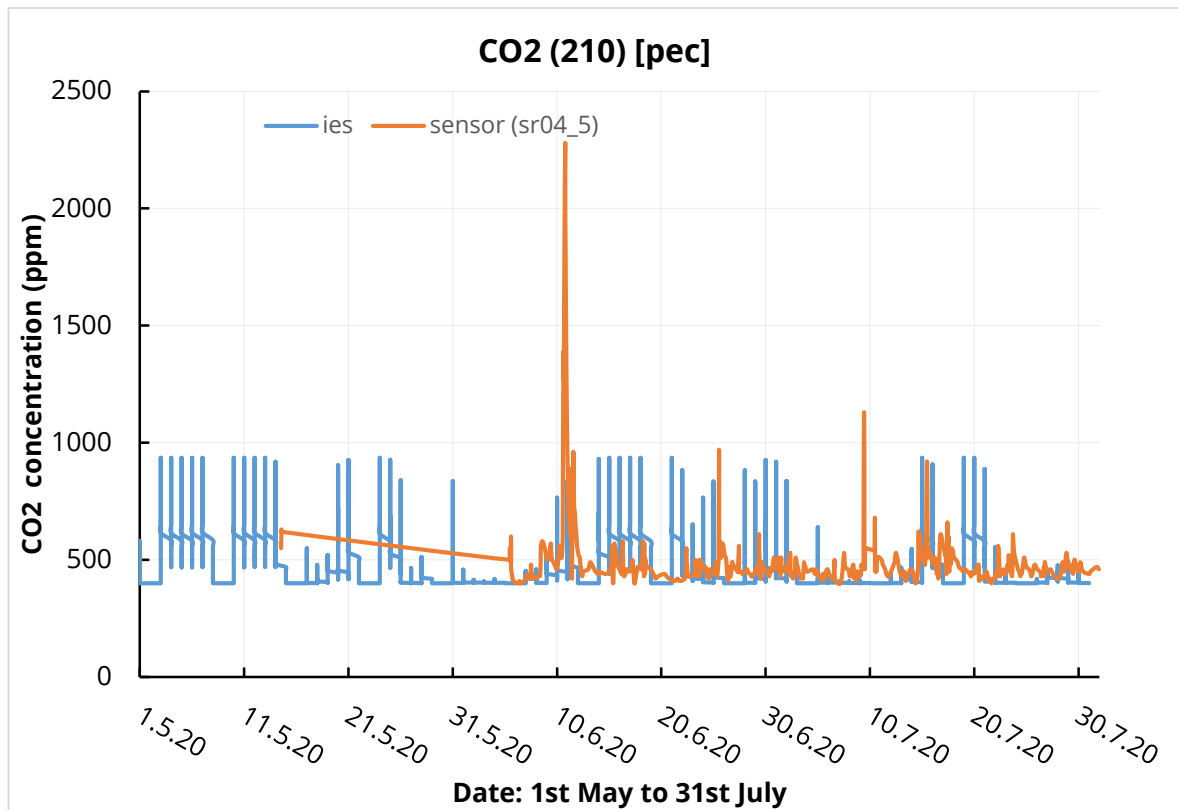


Figure 136: CO₂ concentration levels from the IES simulations and the sensors in room 210.

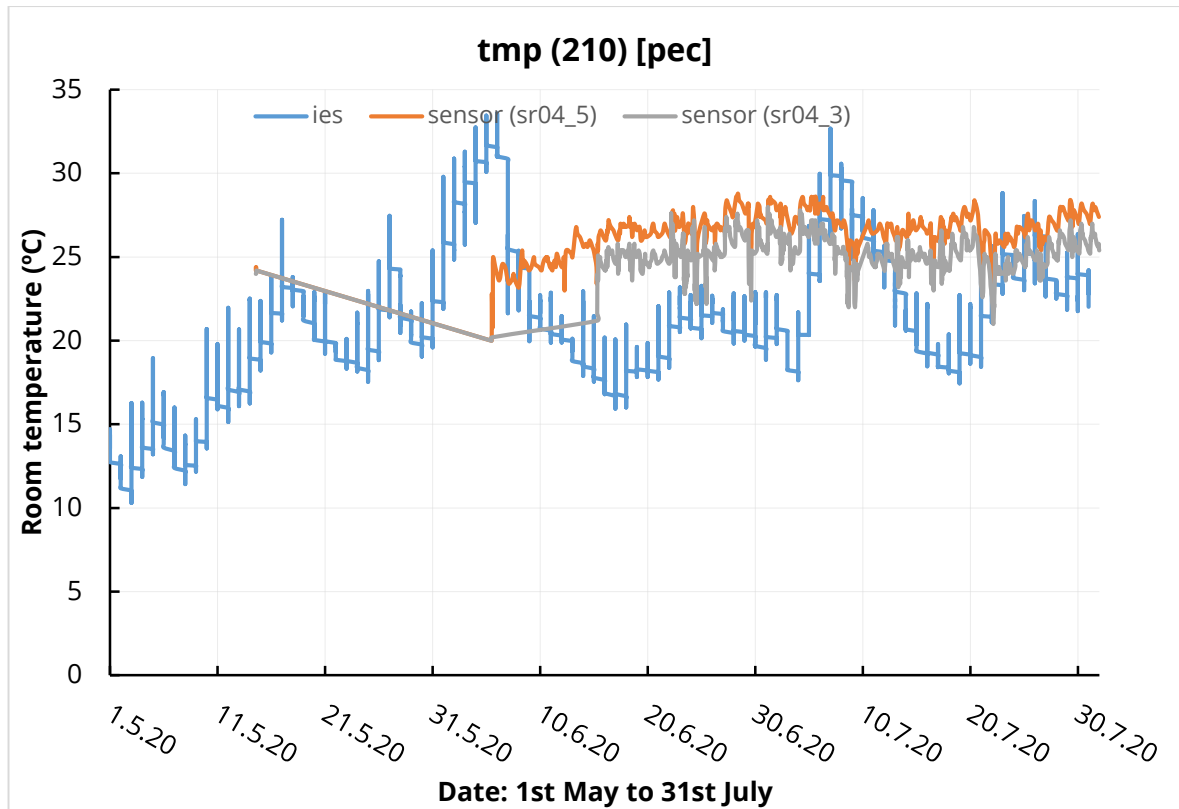


Figure 137: Temperature levels from the IES simulations and the sensors in room 210.

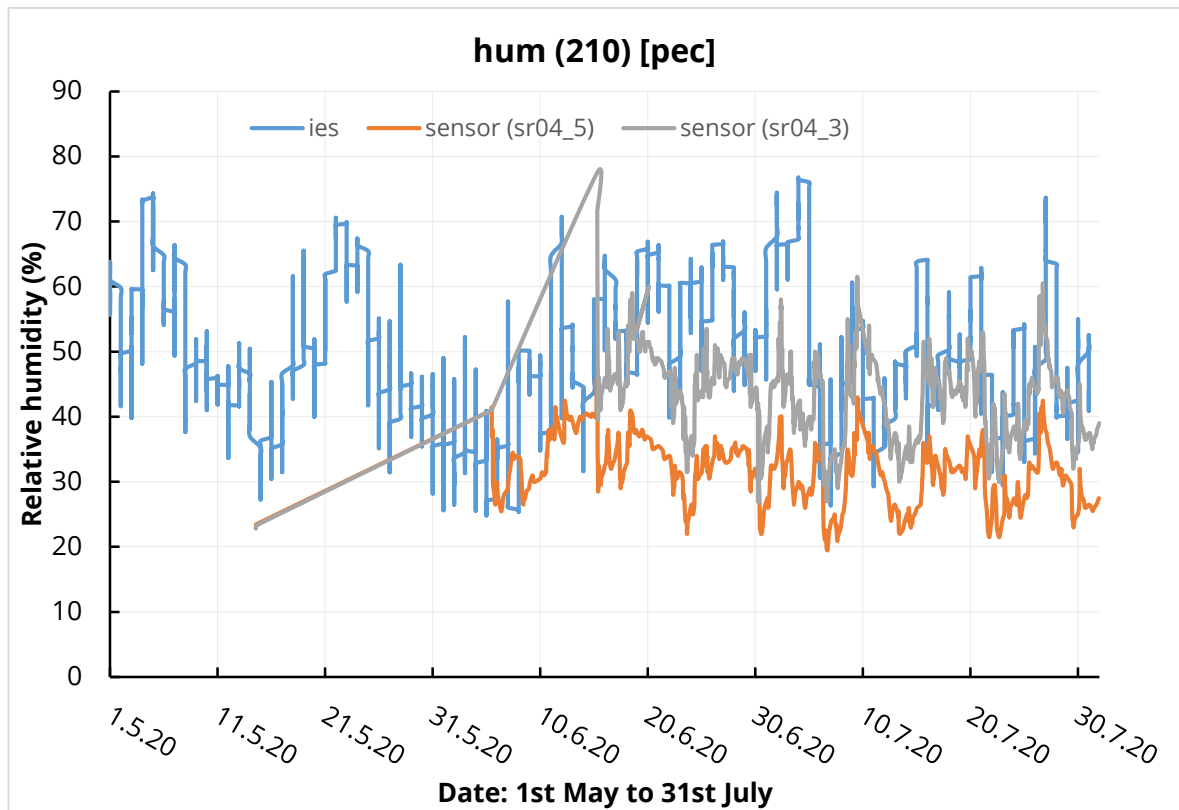


Figure 138: Relative humidity levels from the IES simulations and the sensors in room 210.

C.2: Tools for Calibration 1.0 on the existing IES model

ApLocate - institute

Location & Site Data | Design Weather Data | Simulation Weather Data | Simulation Calendar

Selection Wizard... | Add to custom database

Design Weather Data Source and Statistics

Source of design weather: ASHRAE design weather database v6.0
 ASHRAE weather location: Dresden, Germany
 Monthly percentile for Heating Loads design weather (%): 99.60
 Monthly percentile for Cooling Loads design weather (%): 0.40

Heating Loads Weather Data

Outdoor Winter Design Temperature (°C): -13.30

Cooling Loads Weather Data

Adjust max. outside temps (°C)... Display: ☒ ASHRAE / ☐ CIBSE

Dry-bulb 33.10 Apply Hourly temp. variation: ☐ Sinusoidal / ☒ ASHRAE standard

Wet-bulb 27.00 Plot design day: Graphs Tables

	Min Tdb (°C)	Max Tdb (°C)	Twb at Max Tdb (°C)	Solar Radiation
Jan	7.60	12.30	9.10	
Feb	9.80	15.40	10.30	
Mar	11.30	18.00	10.80	
Apr	14.20	22.60	13.00	
May	20.00	23.60	21.20	
Jun	23.40	32.60	26.90	
Jul	25.00	33.20	27.00	
Aug	23.50	32.90	20.10	
Sep	19.20	27.10	17.80	
Oct	16.80	23.80	16.90	
Nov	9.30	14.20	10.80	
Dec	9.40	13.70	9.50	

Figure 139: Calibrating dry-bulb temperature according to data from sensors.

Building Template Manager

General | Constructions | MacroFlo | Thermal | LightPro | Radiance

Room | Void | RA Plenum | SA Plenum

Template

- BuildingAreaTypeDefaultSchoolOrUniversity
- BuildingAreaTypeDefaultSchoolOrUniversity
- Room (ApSys, metric)
- Room (ApSys, metric)
- Library
- room 1 person
- room 2 people
- student help

System | Space Conditions | Internal Gains | Air Exchanges | Building Regulations

Heating

Operation profile: Bauinformatik Heating Week

Setpoint (°C): Constant 21.1

DHW

DHW consumption: 0.3066 l/(h·pers)

Pattern of use: Linked to occupancy

Cooling

Operation profile: ASHRAE 8am - 6pm No Lunch

Setpoint (°C): Constant 23.9

Plant (auxiliary energy)

Plant operation: Set to heating profile

Bauinformatik Heating Week

Model Settings

Solar reflected fraction: 0.05 Furniture mass factor: 1.00

Humidity control

Min. % saturation: 20 Max. % saturation: 55

Figure 140: Setting the minimum and maximum saturation levels according to data from sensors.

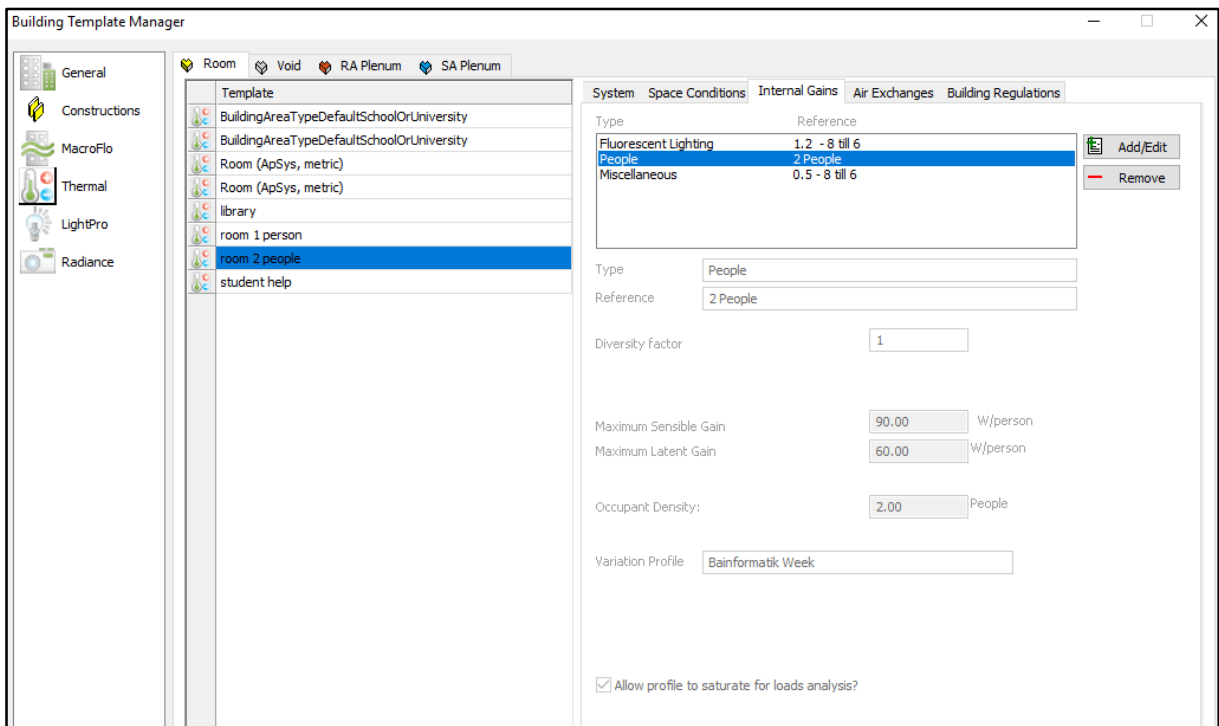


Figure 141: Enhancement of occupancy profile.

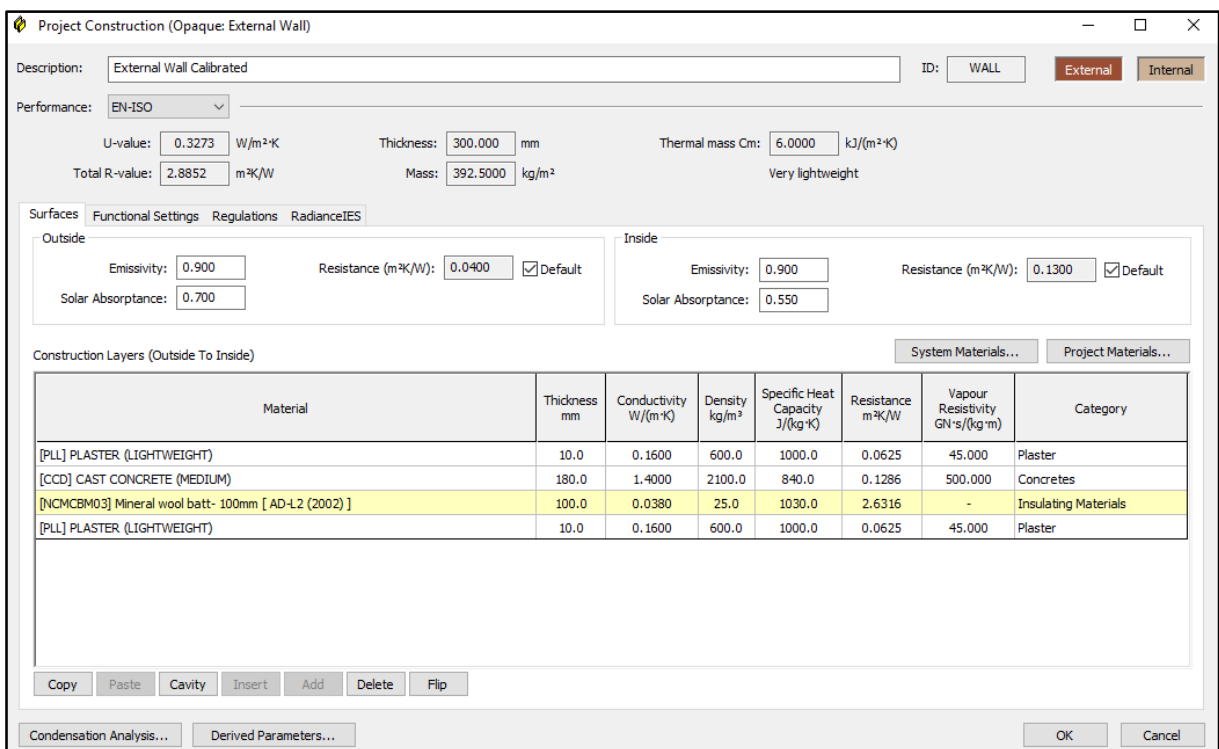


Figure 142: Addition of missing insulation layer in the external wall.

C.3: Post-calibration (1.0) of existing IES model

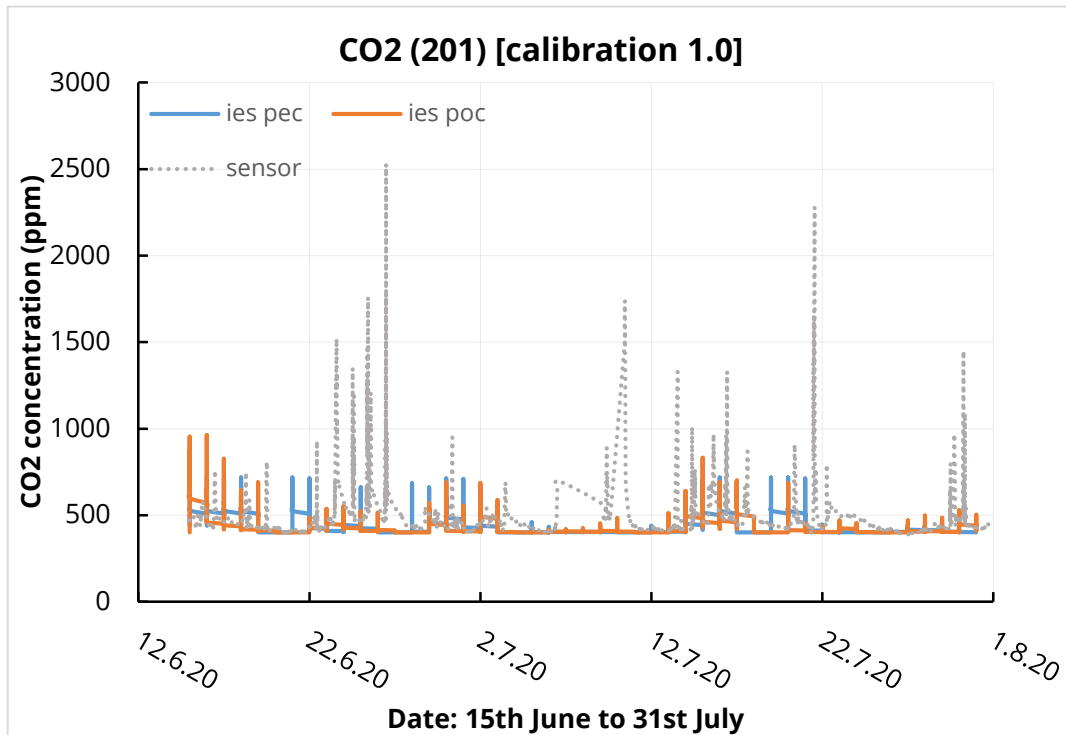


Figure 143: Calibration of CO2 concentration levels in IES using data measured by the sensors as a reference for room 201.

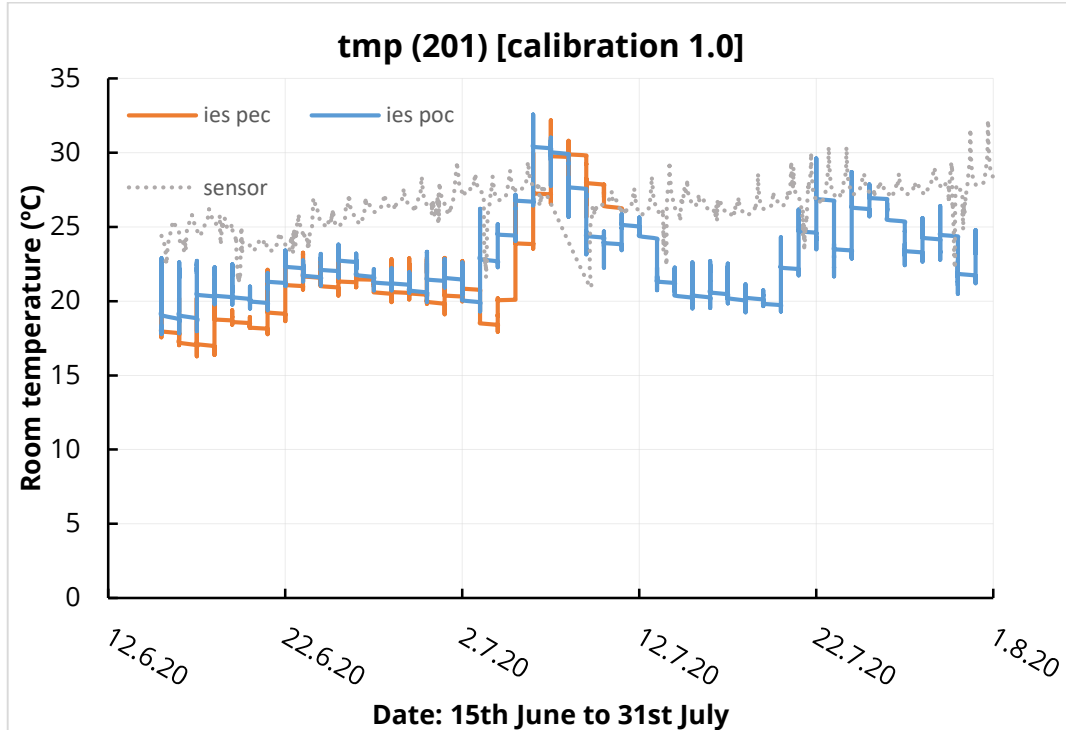


Figure 144: Calibration of temperature levels in IES using data measured by the sensors as a reference for room 201.

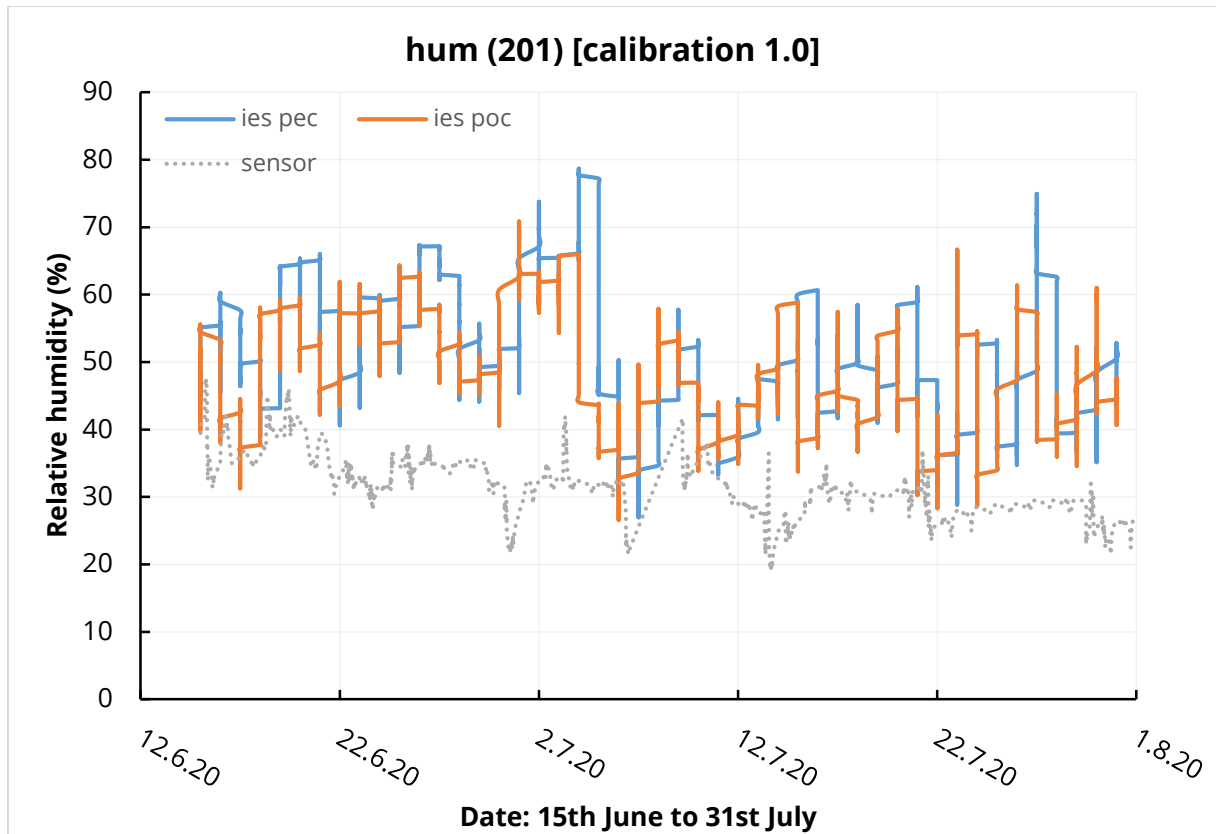


Figure 145: Calibration of relative humidity levels in IES using data measured by the sensors as a reference for room 201.

C.4: Edited weather file for Calibration 2.0

DEU_Dresden.103840_IWEC.epw - Elements

File Edit Tools View Window Help

Site Name: DRESDEN
 Latitude [degrees]: 51.03 Longitude [degrees]: 13.72
 Time Zone: 1 Elevation [m]: 115

Tools:

Variables to Hold Constant: Wet Bulb Temperature, Dry Bulb Temperature

Date/Time	Dry Bulb Temperature [C]	Wet Bulb Temperature [C]	Atmospheric Pressure [kPa]	Relative Humidity %	Dew Point Temperature [C]	Global Solar [Wh/m2]	Normal Solar [Wh/m2]	Diffuse Solar [Wh/m2]	Wind Speed [m/s]
2020/06/04 @ 22:00:00	24.1	17.46	101.3	52	13.67	0	0	0	3.6
2020/06/04 @ 23:00:00	23.3	17.1	101.3	54	13.51	0	0	0	3.1
2020/06/05 @ 00:00:00	15.3	14.19	99.4	89	13.53	0	0	0	3
2020/06/05 @ 01:00:00	14.7	13.61	99.4	89	12.94	0	0	0	1.3
2020/06/05 @ 02:00:00	14.4	13.32	99.4	89	12.64	0	0	0	0.2
2020/06/05 @ 03:00:00	14.3	13.12	99.4	88	12.37	0	0	0	0.3
2020/06/05 @ 04:00:00	13.9	12.84	99.4	89	12.15	20	0	20	1.2
2020/06/05 @ 05:00:00	12.5	11.58	99.4	90	10.94	110.99	159	77	5.2
2020/06/05 @ 06:00:00	12.8	11.58	99.5	87	10.72	254.63	336	132	1.8
2020/06/05 @ 07:00:00	13.8	11.84	99.5	80	10.44	419.46	556	135	1.4
2020/06/05 @ 08:00:00	14.3	11.48	99.5	72	9.36	576.23	659	152	5.7
2020/06/05 @ 09:00:00	14.1	11.19	99.7	71	8.96	708.85	780	122	3.9
2020/06/05 @ 10:00:00	14.4	11.36	99.7	70	9.03	812.43	792	155	2.2
2020/06/05 @ 11:00:00	14.6	11.21	99.7	67	8.58	842.58	751	188	5.7

Columns:

Units: ☒ SI ☐ IP

Figure 146: Edited weather file for Dresden using Elements software.